

THE ROLE OF COLONIC ANTIMICROBIAL
PEPTIDES IN HUMAN *BLASTOCYSTIS* INFECTIONS

JOHN ANTHONY D. YASON
(*B.S. Public Health, University of the Philippines;*
M.Sc. Microbiology, University of the Philippines)

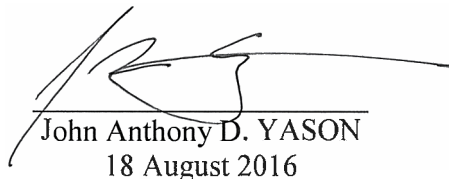
A THESIS SUBMITTED

FOR THE DEGREE OF DOCTOR OF PHILOSOPHY
DEPARTMENT OF MICROBIOLOGY
AND IMMUNOLOGY
YONG LOO LIN SCHOOL OF MEDICINE
NATIONAL UNIVERSITY OF SINGAPORE

2016

DECLARATION

I hereby declare that the thesis is my original work and
it has been written by me in its entirety.
I have duly acknowledged all the sources of information
which have been used in the thesis.
This thesis has also not been submitted for any degree
in any university previously.



John Anthony D. YASON
18 August 2016

ACKNOWLEDGEMENTS

First, my sincere gratitude to my supervisor, A/Prof. Kevin Tan. He was a firm and encouraging guide in the pursuit of my PhD degree, from start to finish. He gave me freedom and necessary resources to pursue different directions in my project. His insights were invaluable and I appreciate the example he showed to all of us in the lab.

My thanks also to the members of my TAC: A/Prof. Vincent Chow and Dr. Stephan Gasser. I have incorporated their suggestions in my research and my thesis became better for it.

I also appreciate the help and support of my seniors in the lab: Wendy, Joshua and Sitara. Wendy and Joshua were patient in helping me get started in *Blastocystis* work. They were also a source of isolates, reagents and other materials when I lacked them. Sitara's animal work is also included in this thesis.

My gratitude also to the other members of the lab: Jun Hong, Wan Ni, Yan Quan, Chiew Yee, Chuu Ling and Jie Xin. I treasure their camaraderie in and outside the lab. They were a source of support and encouragement.

I would not be able to do many technical work in my experiments without the expertise of these people: Geok Choo, Josephine, Guo Hui and Dr. Paul Hutchinson. Geok Choo in particular helped me in many details it would be impossible to list them.

TABLE OF CONTENTS

ACKNOWLEDGEMENTS	i
TABLE OF CONTENTS	ii
SUMMARY	vii
LIST OF TABLES AND FIGURES	ix
LIST OF ABBREVIATIONS	xi
LIST OF PUBLICATIONS ARISING FROM THESIS	xiv
CHAPTER 1 INTRODUCTION	1
1.1 Historical background	2
1.2 Classification of <i>Blastocystis</i>	2
1.3 Biology and life cycle of <i>Blastocystis</i>	4
1.4 Clinical relevance of human <i>Blastocystis</i> infections	6
1.5 Distribution of <i>Blastocystis</i> spp.	7
1.6 Antimicrobial peptides	8
1.7 AMPs of the human gut	10
1.8 AMPs and parasites	17
1.9 Study objectives	18
CHAPTER 2 SUSCEPTIBILITY OF <i>BLASTOCYSTITIS</i> TO ANTIMICROBIAL PEPTIDES	21
2.1 Introduction	22
2.2 Materials and Methods	23
2.2.1 Parasite cultivation and ethical approval	23
2.2.2 Subtyping of <i>Blastocystis</i> isolates	24

2.2.3 AMP susceptibility screening	24
2.2.4 Determination of IC ₅₀	25
2.2.5 Statistical analyses	25
2.3 Results	26
2.3.1 <i>Blastocystis</i> isolates subtyping	26
2.3.2 Susceptibility of <i>Blastocystis</i> to AMPs and determination of IC ₅₀ Values	28
2.4 Discussion	31
CHAPTER 3 CELLULAR EFFECT OF LL-37 ON <i>BLASTOCYSTIS</i> SUBTYPES PART A: MICROSCOPY AND ULTRASTRUCTURE	34
3.1 Introduction	35
3.2 Materials and Methods	37
3.2.1 Parasite cultivation	37
3.2.2 Viability staining and flow cytometry	37
3.2.3 Time-lapse microscopic imaging	37
3.2.4 Scanning electron microscopy	37
3.3 Results	38
3.3.1 LL-37 disrupts <i>Blastocystis</i> cell membrane	38
3.3.2 Time-lapse images of LL-37-induced lysis of <i>Blastocystis</i>	40
3.3.3 Scanning electron micrographs of LL-37-treated <i>Blastocystis</i>	42
3.4 Discussion	44
CHAPTER 4 CELLULAR EFFECT OF LL-37 ON <i>BLASTOCYSTIS</i> SUBTYPES PART B: IMAGING FLOW CYTOMETRY	46

4.1 Introduction	47
4.2 Materials and Methods	49
4.2.1 Parasite Cultivation	49
4.2.2 Fluorescence staining and imaging flow cytometry	49
4.2.3 LL-37 treatment of <i>Blastocystis</i>	52
4.2.4 Localization of LL-37 bound on the <i>Blastocystis</i> surface	52
4.3 Results	53
4.3.1 Round and irregularly-shaped cells found in <i>Blastocystis</i> STs	53
4.3.2. Profile of <i>Blastocystis</i> cells according to Hoechst staining and circularity	56
4.3.3 Profile of <i>Blastocystis</i> cells according to granularity	58
4.3.4 Profile of viable <i>Blastocystis</i> cells according to granularity and Hoechst staining	60
4.3.5 Size range of <i>Blastocystis</i> isolates	62
4.3.6 Imaging of <i>Blastocystis</i> showing classical morphological forms	64
4.3.7 Imaging of rare <i>Blastocystis</i> multinucleated cells	66
4.3.8 Application of imaging flow cytometry to <i>Blastocystis</i> treated with LL-37	68
4.3.9 Localization of LL-37 to <i>Blastocystis</i> surface	70
4.4 Discussion	72
CHAPTER 5 RESISTANCE MECHANISMS OF <i>BLASTOCYSTIS</i> ISOLATE B AGAINST LL-37	77
5.1 Introduction	78
5.2 Materials and Methods	79

5.2.1 Parasite cultivation (see Chapter 2)	79
5.2.2 LL-37 degradation and viability assay	79
5.2.3 pH adjustment of <i>Blastocystis</i> culture medium	80
5.2.4 Transmission electron microscopy	80
5.3 Results	81
5.3.1 <i>Blastocystis</i> ST7-B secretes proteases that can degrade LL-37	81
5.3.2 <i>Blastocystis</i> ST7-B lowers the pH in culture and attenuates LL-37 activity	83
5.3.3 Surface coat of <i>Blastocystis</i>	85
5.4 Discussion	87
CHAPTER 6 <i>BLASTOCYSTITIS</i> -MEDIATED MODULATION OF LL-37 EXPRESSION IN INTESTINAL EPITHELIAL CELLS	90
6.1 Introduction	91
6.2 Materials and Methods	92
6.2.1 Mouse intestinal explants exposure to <i>Blastocystis</i>	92
6.2.2 Co-culture of <i>Blastocystis</i> with HT-29 intestinal epithelial cells	93
6.2.3 Quantitative real-time PCR (qRT-PCR)	94
6.2.4 LL-37 secretion assay	95
6.2.5 Fluorescence microscopy	96
6.3 Results	97
6.3.1 <i>Blastocystis</i> induces cathelicidin expression and secretion	97
6.4 Discussion	102

CHAPTER 7 GENERAL DISCUSSION AND CONCLUSIONS	104
7.1 General Discussions	105
7.2 Future directions	113
7.2 Conclusions	115
REFERENCES	119

SUMMARY

Blastocystis is one of the most common eukaryotic organisms found in the human gut. Several reports have identified its role in gastrointestinal disorders, although its pathogenicity still needs to be elucidated. The study explores the roles of antimicrobial peptides expressed in the colon when *Blastocystis* infect humans. Antimicrobial peptides (AMPs) are elements of the innate immunity and contribute in the protection of the intestinal mucosa from microbial invasion. These AMPs are cationic which makes them bind to negatively-charged membrane surfaces. AMPs then disrupt the membrane and may cause cytoplasmic leakage and kill the cell. Aside from this direct killing, AMPs have also been reported to modulate downstream host immune responses. This study therefore investigates human colonic AMPs in the context of host-pathogen interactions occurring between the human host and *Blastocystis*. A modified drug screening assay was used to identify the susceptibility of *Blastocystis* to three colonic AMPs (cathelicidin, human beta-defensin 1 and human beta-defensin 2). LL-37, a fragment of cathelicidin antimicrobial peptide (CAMP), was found to have broad activity on various *Blastocystis* isolates in terms of growth inhibition. Its membrane disruptive effect on representative isolates was also revealed using conventional and imaging flow cytometry as well as electron microscopy. However, *Blastocystis* subtype (ST) 7 isolates showed relative resistance against the peptide. This is due to the ST's ability to secrete proteases that can degrade LL-37 and alter the surrounding pH that in turn attenuate the peptide's activity. The thicker surface coat of ST7 isolates may also confer resistance against LL-37 killing. Co-culture experiments between intestinal epithelial cells and *Blastocystis* revealed that the parasite can induce

LL-37 gene expression both in HT-29 cells and in mouse intestinal explants. LL-37 was also found to be secreted in the cell culture supernatant when the co-cultured with *Blastocystis*. Results in this study suggest a significant role for AMPs, particularly LL-37, in human *Blastocystis* infections. The data could also be relevant in clarifying how the parasite achieves colonization and other pathogenic events in the human gut. Lastly, this study points toward the many possible applications of AMPs particularly in parasitic infections.

LIST OF TABLES AND FIGURES

Figure 2.1	Structures of human β -defensin 1 and 2 dimers	12
Figure 1.2	Structure of LL-37	15
Table 1.1	Antimicrobial peptides in the gastrointestinal tract	16
Figure 1.3	Framework of the study exploring the roles of endogenous colonic AMPs in <i>Blastocystis</i> infections	20
Figure 2.1	Agarose gel showing amplified MLO gene fragments from various <i>Blastocystis</i> isolates and phylogenetic tree based on MLO gene sequences	27
Figure 2.2	Representative graphs showing fluorescence units of <i>Blastocystis</i> isolates ST1-NUH9 treated with different concentrations of AMPs	29
Table 2.1	Half maximal inhibitory concentration of hBD-1, hBD-2 and LL-37 on <i>Blastocystis</i> STs	30
Figure 3.1	LL-37 causes disruption of <i>Blastocystis</i> cell membrane	39
Figure 3.2	Time-lapse images of <i>Blastocystis</i> ST7-B cells treated with LL-37 and control	41
Figure 3.3	<i>Blastocystis</i> membrane exhibits pores of various sizes when treated with LL-37	43
Figure 4.1	Initial gating strategy to analyze <i>Blastocystis</i> cells.	51
Figure 4.2	Gating for round and irregular shapes of <i>Blastocystis</i>	54
Figure 4.3	<i>Blastocystis</i> STs display various shapes from both viable and non-viable populations	55
Figure 4.4	Round <i>Blastocystis</i> have higher DNA content	57
Figure 4.5	Analysis of <i>Blastocystis</i> based on granularity	59
Figure 4.6	Viable <i>Blastocystis</i> cells with high granularity have higher DNA content	61

Table 4.1	<i>Blastocystis</i> size profiles indicated by cell diameter range and average diameter	63
Figure 4.7	Image gallery of <i>Blastocystis</i> showing classical morphological forms at varying sizes in the viable populations	65
Figure 4.8	Image gallery of rare <i>Blastocystis</i> multinucleated cells	67
Figure 4.9	LL-37 causes morphological changes in <i>Blastocystis</i> isolates	69
Figure 4.10	LL-37 binds to the cell surface of <i>Blastocystis</i>	71
Figure 5.1	<i>Blastocystis</i> ST7-B isolate excreted-secreted products degrade LL-37	82
Figure 5.2	pH affects the activity of LL-37 on <i>Blastocystis</i>	84
Figure 5.3	<i>Blastocystis</i> ST7-B isolates have thicker and denser surface coats compared to ST4-WR1	86
Figure 6.1	<i>Blastocystis</i> induces LL-37 expression in mouse distal colon explants and HT-29 colonic epithelial cells	98
Figure 6.2	Trypan-blue exclusion assay determination of viability of HT-29 cells after co-incubation with <i>Blastocystis</i>	99
Figure 6.3	Flow cytometry demonstrates the specificity of anti-LL-37 antibody	100
Figure 6.4	Confluent HT-29 cells in monolayer increase production of cathelicidin after incubation with <i>Blastocystis</i>	101
Figure 7.1	The interactions between <i>Blastocystis</i> subtypes and LL-37	118

LIST OF ABBREVIATIONS

ABTS	2,2'-Azinobis [3-ethylbenzothiazoline-6-sulfonic acid]
ANOVA	analysis of variance
AMP	antimicrobial peptide
bp	base pair
BSA	bovine serum albumin
BF	brightfield
CFSE	carboxyfluorescein succinimidyl ester
CAMP	cathelicidin antimicrobial peptide
CRAMP	cathelicidin-related antimicrobial peptide
CCR6	CC-chemokine receptor 6
DEFB4A	defensin B4- α
DEFA	defensin- α
DNA	deoxyribonucleic acid
DMEM	Dulbecco's modified Eagle's medium
ELISA	enzyme-linked immunosorbent assay
ESP	excretory-secretory products
EDF	extended depth of field
FITC	fluorescein isothiocyanate
GAPdH	glyceraldehyde 3-phosphate dehydrogenase
GM-CSF	granulocyte macrophage colony-stimulating factor
IC ₅₀	Half maximal inhibitory concentration
HD	human defensin
HNP	human neutrophil peptide

hBD	human β -defensin
Ig	immunoglobulin
IRB	Institutional Review Board
IFN γ	interferon gamma
IL	interleukin
IBS	irritable bowel syndrome
IMDM	Iscove's modified Dulbecco's medium
kDA	kilo Dalton
LPS	lipopolysaccharide
MLO	mitochondria-like organelle
MOI	multiplicity of infection
NCBI	National Center for Biotechnology Information
NUS	National University of Singapore
NF- κ B	nuclear factor kappa-light-chain-enhancer of activated B cells
PBS-T	PBS-Tween 20
PBS	phosphate-buffered saline
PCR	polymerase chain reaction
PI	propidium iodide
PDB	Protein Data Bank
qRT-PCR	Quantitative real-time PCR
RCSB	Research Collaboratory for Structural Bioinformatics
RNA	ribonucleic acid
rRNA	ribosomal ribonucleic acid
SEM	scanning electron microscopy
SSU	small sub-unit

ST	subtype
TEM	transmission electron microscopy
TNF- α	tumor necrosis factor alpha
WHO	World Health Organization

LIST OF PUBLICATIONS ARISING FROM THESIS

1. **Yason, J. A.**, Ajjampur, S. S. R. & Tan, K. S. W. *Blastocystis* Isolate B Exhibits Multiple Modes of Resistance against Antimicrobial Peptide LL-37. *Infect. Immun.* **84**, 2220–2232 (2016).
2. **Yason, J. A.** & Tan, K. S. W. Seeing the Whole Elephant: Imaging Flow Cytometry Reveals Extensive Morphological Diversity within *Blastocystis* Isolates. *PLoS ONE* **10**, e0143974 (2015).

Blastocystis Isolate B Exhibits Multiple Modes of Resistance against Antimicrobial Peptide LL-37

John Anthony Yason, Sitara Swarna Rao Ajampur, Kevin Shyong Wei Tan

Laboratory of Cellular and Molecular Parasitology, Department of Microbiology and Immunology, Yong Loo Lin School of Medicine, National University of Singapore, Singapore

Blastocystis is one of the most common eukaryotic organisms found in humans and many types of animals. Several reports have identified its role in gastrointestinal disorders, although its pathogenicity is yet to be clarified. *Blastocystis* is transmitted via the fecal-to-oral route and colonizes the large intestines. Epithelial cells lining the intestine secrete antimicrobial peptides (AMPs), including beta-defensins and cathelicidin, as a response to infection. This study explores the effects of host colonic antimicrobial peptides, particularly LL-37, a fragment of cathelicidin, on different *Blastocystis* subtypes. *Blastocystis* is composed of several subtypes that have genetic, metabolic, and biological differences. These subtypes also have various outcomes in terms of drug treatment and immune response. In this study, *Blastocystis* isolates from three different subtypes were found to induce intestinal epithelial cells to secrete LL-37. We also show that among the antimicrobial peptides tested, only LL-37 has broad activity on all the subtypes. LL-37 causes membrane disruption and causes *Blastocystis* to change shape. *Blastocystis* subtype 7 (ST7), however, showed relative resistance to LL-37. An isolate, ST7 isolate B (ST7-B), from this subtype releases proteases that can degrade the peptide. It also makes the environment acidic, which causes attenuation of LL-37 activity. The *Blastocystis* ST7-B isolate was also observed to have a thicker surface coat, which may protect the parasite from direct killing by LL-37. This study determined the effects of LL-37 on different *Blastocystis* isolates and indicates that AMPs have significant roles in *Blastocystis* infections.

Blastocystis is an intestinal protistan parasite commonly detected in humans and many types of animals (1, 2). This organism is classified under the stramenopiles, although it lacks chloroplasts or structures for locomotion, which are common features of many members of this group. *Blastocystis* is widely distributed throughout the world. Parasitological surveys usually place *Blastocystis* as the most common eukaryotic parasite detected (3, 4). This organism has a global distribution and has numerous animal hosts. There is little host specificity for this organism, and there are reports indicating the zoonotic potential of *Blastocystis* (5). This organism, in its cyst form, is transmitted via the fecal-oral route. It then colonizes the large intestine and is excreted to its various forms. These forms may appear vacuolar, multivacuolar, avacuolar, or granular under a light microscope. *Blastocystis* has been implicated in a number of intestinal disorders, although its pathogenesis is yet to be elucidated. There are few reports associating it with gastrointestinal disease, the most common symptoms of which are diarrhea, vomiting, nausea, and urticaria (1, 5–7). *Blastocystis* is a species complex that is comprised of up to 19 subtypes (STs), with ST1 to ST9 having been isolated from humans (8). Recently, a report found that ST12 and another possible novel ST also infect humans (9). *Blastocystis* STs may differ in size range, nuclear arrangement, growth rate, and morphology (8). There have been reports on the differences in host range, protease activity, and characteristics of the immune response triggered (10–12). There are also variations in drug sensitivities (13, 14). Some researchers have suggested that symptomatology is dictated by ST identity (15).

LL-37 is a 37-amino-acid fragment of human cathelicidin antimicrobial peptide (CAMP), which has a direct killing effect on prokaryotic and fungal organisms (16, 17). Because of its positive charge, it can bind to negatively charged surfaces, which is a feature of prokaryotic membranes (18). It can cause the formation of pores on the cell membrane and subsequently effect cell lysis.

LL-37 is also a modulator of downstream immune responses such as the recruitment of other immune cells and the release of cytokines (19). Cathelicidin is produced by epithelial cells, including those lining the small and large intestines. It is processed by proteases, which results in the LL-37 fragment. There is basal secretion of LL-37 in the intestinal lumen. During infection, LL-37 becomes highly expressed, along with other antimicrobial peptides (AMPs). This leads to other immune responses such as the recruitment of inflammatory cells and the production of cytokines (20).

In this study, we explore the possible interactions between *Blastocystis* and human intestinal AMPs, particularly LL-37. We determined if the parasite can induce intestinal epithelial cells to secrete LL-37 using *in vitro* cell culture and a mouse model. We also tested several isolates of *Blastocystis* from three STs for susceptibility to three colonic AMPs, including LL-37. AMPs had variable effects on *Blastocystis*, and their effects on different *Blastocystis* STs were also not uniform. We identified possible parasite factors by which *Blastocystis* can possibly attenuate LL-37 activity.

Received 25 April 2016 Accepted 14 May 2016

Accepted manuscript posted online 23 May 2016

Citation Yason JA, Ajampur SSR, Tan KSW. 2016. *Blastocystis* isolate B exhibits multiple modes of resistance against antimicrobial peptide LL-37. *Infect Immun* 84:2220–2232. doi:10.1128/IAI.00339-16.

Editor: J. H. Adams, University of South Florida

Address correspondence to Kevin Shyong Wei Tan, kevin_tan@nuhs.edu.sg.

Supplemental material for this article may be found at <http://dx.doi.org/10.1128/IAI.00339-16>.

Copyright © 2016, American Society for Microbiology. All Rights Reserved.

RESEARCH ARTICLE

Seeing the Whole Elephant: Imaging Flow Cytometry Reveals Extensive Morphological Diversity within *Blastocystis* Isolates

John Anthony Yason, Kevin Shyong Wei Tan*

Department of Microbiology, Yong Loo Lin School of Medicine, National University of Singapore, Singapore, Singapore

* kevin_tan@nuhs.edu.sg



OPEN ACCESS

Citation: Yason JA, Tan KSW (2015) Seeing the Whole Elephant: Imaging Flow Cytometry Reveals Extensive Morphological Diversity within *Blastocystis* Isolates. PLoS ONE 10(11): e0143974. doi:10.1371/journal.pone.0143974

Editor: Nikolas Nikolaidis, California State University Fullerton, UNITED STATES

Received: August 11, 2015

Accepted: November 11, 2015

Published: November 30, 2015

Copyright: © 2015 Yason, Tan. This is an open access article distributed under the terms of the [Creative Commons Attribution License](https://creativecommons.org/licenses/by/4.0/), which permits unrestricted use, distribution, and reproduction in any medium, provided the original author and source are credited.

Data Availability Statement: Data are from the *Blastocystis* ImageStream study may be assessed at: <http://dx.doi.org/10.5281/zenodo.32605>.

Funding: The work was generously funded by a grant from the National University of Singapore (R-182-000-710-733). The funders had no role in study design, data collection and analysis, decision to publish, or preparation of the manuscript. JAY acknowledges the generous research scholarship from the National University of Singapore.

Competing Interests: The authors have declared that no competing interests exist.

Abstract

Blastocystis is a common protist isolated in humans and many animals. The parasite is a species complex composed of 19 subtypes, 9 of which have been found in humans. There are biological and molecular differences between *Blastocystis* subtypes although microscopy alone is unable to distinguish between these subtypes. *Blastocystis* isolates also display various morphological forms. Several of these forms, however, have not been properly evaluated on whether or not these play significant functions in the organism's biology. In this study, we used imaging flow cytometry to analyze morphological features of *Blastocystis* isolates representing 3 subtypes (ST1, ST4 and ST7). We also employed fluorescence dyes to discover new cellular features. The profiles from each of the subtypes exhibit considerable differences with the others in terms of shape, size and granularity. We confirmed that the classical vacuolar form comprises the majority in all three subtypes. We have also evaluated other morphotypes on whether these represent distinct life stages in the parasite. Irregularly-shaped cells were identified but all of them were found to be dying cells in one isolate. Granular forms were present as a continuum in both viable and non-viable populations, with non-viable forms displaying higher granularity. By analyzing the images, rare morphotypes such as multinucleated cells could be easily observed and quantified. These cells had low granularity and lower DNA content. Small structures containing nucleic acid were also identified. We discuss the possible biological implications of these unusual forms.

Introduction

Blastocystis spp. are protistan parasites found in humans and many types of animals. It is the most commonly isolated eukaryote in humans [1,2]. *Blastocystis* is a species complex comprising 19 subtypes (STs). ST1-9 have been found in humans and, with the exception of ST9, in other animal hosts as well. *Blastocystis* ST1 and ST3 are most frequently isolated, but there is geographical diversity in global distribution. For example, ST4 is common in Europe but not in the rest of the world [3]. ST2 and ST6 had a higher occurrence than ST3 in a study in Colombia

Chapter 1

Introduction

1.1 Historical background

The name '*Blastocystis*' first appeared in scientific literature at the beginning of the 20th century. Although several investigators described an organism they believed to be the parasite in the middle of the 1800's, it was only in 1911 when the requirements for nomenclature of *Blastocystis* was fulfilled. In the following year, Brumpt gave the name '*Blastocystis hominis*' to the organisms he found in humans. This name then became widely used to refer to a gut eukaryote which has a round shape and semi-hollow appearance (Clark et al., 2013; Zierdt, 1973, 1991). Throughout the 20th century, more isolates have been found, not just in humans but also in animals and insects. There were controversies regarding its status and some investigators argued that *Blastocystis* were just degenerate or cysts forms of other known intestinal protozoans. There was also a suggestion that it was a yeast. Cultural and morphological characteristics however showed that it was suitable to classify it under protozoa (Zierdt, 1991). Nucleic acid-based approaches have definitively separated *Blastocystis* from yeasts. Analyses of partial and full SSU rRNA gene sequences of various isolates showed that *Blastocystis* do not form a cluster with fungi (Tan et al., 2002).

1.2 Classification of *Blastocystis*

Establishing *Blastocystis*' taxonomic status was not straightforward. It was partly due to the lack of unique and apparent characteristics that could distinguish it from other unicellular eukaryotes, and therefore also rooted in the complexity of the protistan group itself. The classification of unicellular

eukaryotes underwent several revisions (Adl et al., 2012; Cavalier-Smith, 1993, 1998; Levine et al., 1980). A 1998 classification placed *Blastocystis* under Kingdom Chromista, Subkingdom Chromobiota, Infrakingdom, Heterokonta, Subphylum Opalinata and Class Blastocystea (Cavalier-Smith, 1998; Tan et al., 2002). *Blastocystis*, therefore, does not belong to protozoa but to another Kingdom (Chromista). It is thus more accurate to refer to *Blastocystis* as a protist rather than a protozoan. Small sub-unit ribosomal RNA (SSU rRNA) gene sequence analysis clustered *Blastocystis* spp. along with the group Stramenopiles. The most recent grouping placed the group *Blastocystis* at the same level with Opalinata under Stramenopiles, which belongs to the clade Sar (Adl et al., 2012). The organism however exhibits characteristics which are unusual to the other members of the group. For example, *Blastocystis* lacks cilia, possesses no plastids and therefore not photosynthetic (Clark et al., 2013; Silberman et al., 1996; Tan, 2008). *Blastocystis* isolates are highly polymorphic both in morphology and genetics (Clark, 1997; Yoshikawa et al., 2016). Previously, the naming of isolates was based on host origin, morphological features and *in vitro* culture characteristics and/or electrophoretic karyotypes (Yoshikawa et al., 2016). The problem that arose with this approach was that there were genetically dissimilar isolates isolated in one type of host (e.g. humans); and also, an isolate could be found in many different types of hosts. In short, the lack of apparent host specificity renders the approach of naming an isolate based on host origin and other factors untenable. A consensus was made in 2007 and classified human *Blastocystis* isolates into 9 subtypes (STs) based on complete SSU rRNA gene sequences (Stensvold et al., 2007). The term '*Blastocystis hominis*' was dropped as a collective name for these isolates

because reptilian and amphibian isolates may also fall into these STs. These isolates were then classified simply as *Blastocystis* spp. At present, seventeen different *Blastocystis* STs mainly from mammalian and avian hosts have been proposed. Isolates from humans are designated as STs 1-9 (Yoshikawa et al., 2016). Subtypes of *Blastocystis* can be determined by genetic analyses, but STs also exhibit differences in size, morphology, growth in culture, host range, drug resistance, host immune response, adhesion to host cells and protease activities (Mirza et al., 2011a; Roberts et al., 2014a; Tan, 2008; Teo et al., 2014; Wu et al., 2014). Studies have also indicated that ST identity may determine symptomatology and pathogenic potential (Casero et al., 2015; Roberts et al., 2014b) although other studies did not find a strong basis for this (Nagel et al., 2012; Souppart et al., 2010).

1.3 Biology and life cycle of *Blastocystis*

A typical *Blastocystis* cell has a spherical shape. Under the microscope, *Blastocystis* appear round with a prominent central vacuole. In the vacuolar form of the parasite, the cytoplasm is usually located at the edge where the nucleus (or several nuclei) and other organelles can be found. Granular forms can also be observed and some multi-vacuolar forms have been reported (Tan, 2008; Zhang et al., 2012, 2012). Irregularly-shaped cells are also seen and these have been labelled as amoeboid forms in some studies (Rajamanikam and Govind, 2013; Tan, 2008; Zhang et al., 2012). Investigators have also identified multinucleated and avacuolar forms but the vacuolar forms constitute much of cells found in any type of samples. Cultivation of the parasite requires anaerobic

conditions. The proposed life cycle of the organism commences when the environmentally-resistant cyst forms are ingested through contaminated food and water. There is excystment when *Blastocystis* reaches the intestines which by then develops into vegetative forms. The parasite then undergoes colonization in the large intestines. Some of the forms may develop into cysts which are passed on the feces. *Blastocystis* in fecal specimens and in cultures assumes different forms. *Blastocystis* reproduces by binary fission although some researchers proposed alternative reproductive modes for the parasite (Clark et al., 2013; Jeremiah and Parija, 2013; Tan, 2004, 2008). Images of plasmotomy or budding have been supposedly demonstrated (Yamada and Yoshikawa, 2012) but these could just have been asymmetrical binary fission (Tan and Stenzel, 2003). Under light microscopy, various forms have been described and interpreted as representing alternative modes of reproduction. However, these have not been supported by other methods (Tan, 2004; Yamada and Yoshikawa, 2012). Schizogony has also been put forward as a mode of reproduction in *Blastocystis* (Govind et al., 2002). This involves multiple fission that results in the production of more cells in one event compared to binary fission. This developmental event has been suggested to occur in *Blastocystis* as an attempt to explain the proliferative nature of the parasite in-vivo and in-vitro (Govind et al., 2002). Solid evidence for these alternative modes have not been achieved as yet. And at present, binary fission is the only mode of reproduction in *Blastocystis* with clear and established proofs (Tan, 2008; Yamada and Yoshikawa, 2012). The conventional method for detection of *Blastocystis* is by microscopic observation in clinical (mainly fecal specimens) and environmental samples. This method, however, is not adequate to

differentiate *Blastocystis* STs (Santos and Rivera, 2013; Stensvold, 2013; Tan, 2008).

1.4 Clinical relevance of human *Blastocystis* infections

Blastocystis is considered an important water-borne pathogen (World Health Organization, 2008). It has been implicated in waterborne disease outbreaks (Anuar et al., 2013; Baldursson and Karanis, 2011). Infection with *Blastocystis* is usually asymptomatic but when symptoms are observed, they are usually self-limiting. The symptoms usually associated with *Blastocystis* include abdominal pain, diarrhea and flatulence. There were also surveys that indicated urticaria as a symptom. There were controversies regarding the pathogenic status of *Blastocystis*. Several reports indicated that it is an opportunistic parasite and that the symptoms linked with it are a result of bystander effects (Alemu et al., 2011; Chandramathi et al., 2012; Teo et al., 2014). *Blastocystis* has been associated with a number disease states such as irritable bowel syndrome (IBS), chronic diarrhea especially in children and colitis in numerous studies (Coyle et al., 2012; Kiani et al., 2016; Maçin et al., 2016; Poirier et al., 2012; Roberts et al., 2014b; Tan, 2008). In line with this, cell culture experiments showed that *Blastocystis* can adhere to epithelial cells and that it is capable of compromising epithelial barrier integrity. Animal studies have also reported the ability of the parasite to colonize the intestines, upregulate inflammatory cytokines and increase the intestinal permeability (Ajjampur and Tan, 2016; Wu et al., 2014).

1.5 Distribution of *Blastocystis* spp.

Blastocystis is the most common eukaryote isolated in humans. More than 1 billion people in the world are estimated to harbor the parasite. Infection rates vary from 0.5 to 62% in surveys conducted at different locations all over the world (Clark et al., 2013; Scanlan et al., 2014). These surveys, however, were not uniform in terms of methods of detection, and sampling factors related to social, environmental and economic backgrounds. In some of these studies, particular STs were not identified. A recent survey in Senegal has stretched the range of infection rates further. In a study among children living beside a river basin, *Blastocystis* infection was at 100% prevalence. (El Safadi et al., 2014). In general, there is higher prevalence in developing countries compared to developed ones (Beyhan et al., 2015; Clark et al., 2013; Nithyamathi et al., 2016; Ramírez et al., 2016).

Blastocystis ST1-9 are human isolates and, with the exception of ST9, can be found in other animal hosts as well. Surveys indicated that *Blastocystis* ST1 and ST3 were the most common isolated subtypes worldwide (Clark et al., 2013). The geographical distribution of subtypes however varied from one continent to another. *Blastocystis* ST4, for example, was detected also frequently in Europe (Alfellani et al., 2013). *Blastocystis* ST4, 6, 7 and 9 were common among Japanese patients (Yoshikawa and Iwamasa, 2016). In South American countries, ST4 was almost non-existent and ST2 registered high prevalence rates (Casero et al., 2015; Ramírez et al., 2014, 2016).

1.6 Antimicrobial peptides

Antimicrobial peptides (AMPs) are small molecules which may comprise 6 to 100 amino acids in length (Peters et al., 2010). AMPs are considered primitive molecules which evolved 2.6 billion years ago (Gordon et al., 2005). AMPs are found in many types of organisms from prokaryotic to eukaryotic, from unicellular (e.g. bacteriocins in bacteria) to multicellular organisms, from plants to insects, animals and humans (Li et al., 2012; Peters et al., 2010). More than 2,000 AMPs have been identified from various sources, and still more are being discovered (Li et al., 2012; Wang et al., 2015). In animals, AMPs can be found in different types of tissues. There are AMPs secreted by circulating leukocytes as well as epithelial cells lining the skin and the gut. There are also others produced by specialized cells such as Paneth cells in the intestines (Andreu and Rivas, 1998; Lehrer and Ganz, 1999).

For plants and animals, AMPs are important elements in the innate immunity against pathogenic microorganisms (Lehrer and Lu, 2012). Almost every AMP is composed of a hydrophilic, hydrophobic and cationic amino acids arranged in a molecule that can assume an amphipathic structure (Zasloff, 2002). The net positive charge is due to the presence of a higher content in arginine and lysine amino acids than in aspartic acid and glutamic acid. This property is further reinforced by a C-terminal amidation (Chow et al., 2013). Having cationic groups, AMPs can strongly bind to the surfaces of bacteria (which has more negative charges) while having weak affinity towards cell membranes of

multicellular organisms (Zasloff, 2002). All AMPs originate from larger molecules with a corresponding signal sequence (Zasloff, 2002).

AMP-mediated cell killing includes the following steps: Attraction of AMP to membrane surface by electrostatic bonding; then, attachment to the cell membrane by traversing several structures. In the case of bacteria, these structures may include capsular polysaccharides, teichoic and lipoteichoic acids. Last step would be peptide insertion with subsequent membrane permeability (Brogden, 2005). There are several hypotheses on how AMPs actually kill microbes. The main theory is that the killing of microbes is due to the molecule's ability to cause pores to form on the membrane. Another supposition is that AMPs may cause depolarization of the bacterial membrane or they can cause unequal distribution of lipids which lead to abnormal membrane functions. AMPs can also bind to internal and critical targets or that it can induce hydrolases that degrade the cell wall (Gordon et al., 2005; Zasloff, 2002). Many AMPs are known to have a fast killing effect on some microbial cells (Yu et al., 2016). LL-37 has been shown to saturate the outer membrane of *Escherichia coli* cells within one minute and permeabilize the cytoplasmic membrane within 16 min (Sochacki et al., 2011). Another AMP, Cecropin A, disrupts the bacterium's membrane within 2 min (Rangarajan et al., 2013). Aside from direct killing effect of microbial cells by various mechanisms, several AMPs could also have other functions (Wang, 2014). AMPs can serve as mediators for recruitment of other immune cells. They can also function as modulators for immune response by binding to antigens. In general, acquired

resistance against AMPs seems to be a rare phenomenon (Fjell et al., 2012; Wang et al., 2015).

1.7 AMPs of the human gut

AMPs are present in all human tissue which is normally exposed to microorganisms such as the skin and the mucosae (Wiesner and Vilcinskis, 2010). Aside from the physical barrier, AMPs secreted into the intestines also provide protection from pathogens (Table 1.1). Paneth cells, which are found in the small intestines, are main sources of AMPs. These cells however are fewer in the large intestines where most AMPs are produced by epithelial cells (Bevins and Salzman, 2011; Elphick and Mahida, 2005). Defensins and cathelicidins are among the major groups of AMPs found in the lower portion of the gastrointestinal tract (Bevins and Salzman, 2011). AMPs are significant factors in maintaining homeostasis in the gut along with the commensal and mutualistic microbiota (Muniz and Yeretssian, 2012; Ostaff et al., 2013). And along with mucins which line the intestinal tract, these three elements constitute the front line of host defense against invasion of harmful microorganisms (Moal and Servin, 2006).

Defensins serve as endogenous antibiotics with microbicidal activity against Gram-negative and Gram-positive bacteria, fungi, viruses, and protozoa. Defensins' molecular masses are low, usually at 3-6 kDa. They are 30–40 amino acids in length. All human defensins share a triple-stranded β -sheet core structure stabilized by three intramolecular disulfide bonds. Depending on the

position of these cysteine residues, defensins can be grouped into two major subfamilies: the α -defensins and the β -defensins. The cyclic peptide called θ -defensin has not been isolated so far among humans. In human α -defensins, cysteine pairing pattern is 1:6, 2:4, 3:5. The total of six α -defensins includes human neutrophil peptides 1–4 (HNPI–4) produced by granulocytes and human defensin 5 and 6 (HD5 and HD6) produced by Paneth cells. The- α defensins (also referred to as cryptdins in mice) are most highly expressed in Paneth cells and neutrophils in humans, rats and other mammals, but not in mice. Human β -defensins have 1:5, 2:4, 3:5 cysteine pairing pattern, although their three-dimensional structures are similar to α -defensins. β -defensins (Fig. 1.1) are expressed by many types of epithelial cell, including colonocytes, and their expression in the intestinal epithelium is inducible, except for the expression of human β -defensin 1 (hBD-1). β -defensins have four subtypes, designated hBD-1 to hBD-4. hBD-1 is ubiquitously expressed at all surfaces of the human body including the skin, the respiratory, urogenital and the gastrointestinal tract. hBD-2 and hBD-3 are inducible antimicrobial peptides expressed by enterocytes throughout the intestinal tract (Jäger et al., 2010). The six human α -defensin peptides are encoded by only five defensin- α (DEFA) genes and the sequences of HNPs 1, 2, and 3 are almost identical (Bevins and Salzman, 2011; Ganz, 2003; Jäger et al., 2013; Lehrer and Lu, 2012, 2012; Li et al., 2012).

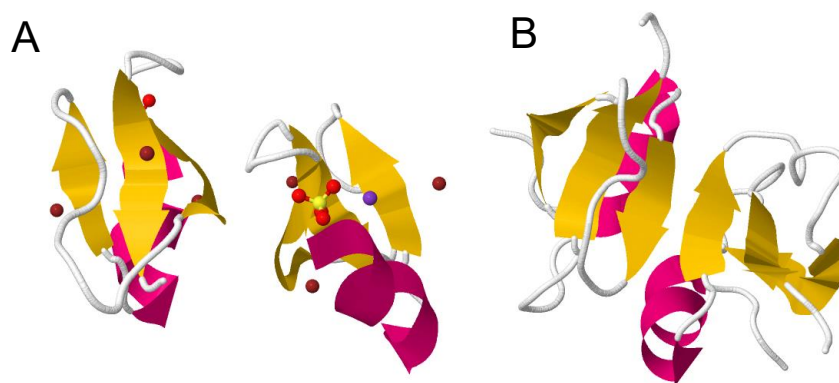


Fig. 1.1. Structures of human β -defensin 1 (A) and 2 (B) dimers. The β -sheets are in yellow while the flanking α -helix structures are in pink. Images obtained from Research Collaboratory for Structural Bioinformatics (RCSB) Protein Data Bank (PDB) with references (Hoover et al., 2000, 2001).

Defensins are effective against numerous bacterial pathogens (Oppenheim et al., 2003). Aside from this direct effect, defensins also have other roles in immunity. For example, hBD-1 and hBD-2 (also known as DEFB4A) have chemo-attractant activity for cells expressing CC-chemokine receptor 6 (CCR6), including dendritic cells. Some mouse intestinal α -defensins promote ion fluxes in epithelial cells. Human α -defensin 5 (HD5; also known as DEFA5) is a potent lectin and can neutralize bacterial exotoxins. Paneth cell defensins are stored as propeptides and require cleavage by trypsin, which is stored in Paneth cell granules as a zymogen as well. The exact mechanism by which defensins exert their bactericidal effect has still not been identified, but it has already become clear that they do not act with a uniform mechanism (Bevins and Salzman, 2011; Ganz, 2003; Jäger et al., 2013).

Cathelicidins are characterized by a conserved N-terminal domain that is proteolytically cleaved to generate the mature, active peptide contained within the C-terminus (Wiesner and Vilcinskis, 2010). The only cathelicidin identified in humans is termed LL-37 indicating the 37-amino acid sequence (Fig. 1.2). The Cathelicidin Antimicrobial Peptide (CAMP) is expressed in various immune cells, in salivary glands, and in epithelia of respiratory, digestive and reproductive tracts while keratinocytes and intestinal cells can be induced to enhance expression. Its main effect is pore formation in bacterial membranes. It is also found to be capable of modulating toxic effects due to bacterial infection (Bucki et al., 2010). LL-37's other activities include chemotactic effect on blood cells, activation of histamin release from mast cells, or induction of

angiogenesis. Absence of LL-37 has been associated with chronic periodontal disease (Wiesner and Vilcinskas, 2010).



Fig. 1.2. Structure of LL-37 from RCSB PDB showing the slightly bent α -helix construction (Wang, 2008).

Table 1.1. Antimicrobial peptides in the gastrointestinal tract¹

Antimicrobial peptide	Secretory stimuli	Distribution in gastrointestinal tract	Biological function
hBD-1	Constitutive in epithelial cells, IFN- γ and LPS in monocytes	Ubiquitous in epithelial cells of small and large intestine, monocytes, monocyte-derived dendritic cells	Antimicrobial, chemotactic
hBD-2, 3, 4	LPS, flagellin mediated by NF- κ B and AP-1	Epithelial cells, monocytes	- Antimicrobial, chemoattractant for macrophages and monocytes, - hBD-2: mast cells and neutrophils
HD-5 and HD-6	NOD2 activation (MDP, LPS) TLR	Granules of ileal Paneth cells (also metaplastic Paneth cells in other areas of intestinal tract)	Antimicrobial, induction of IL-8
Cathelicidin ("LL-37")	Butyrate, vitamin D, bile acids, MDP	Epithelial cells, leukocytes	Antimicrobial, chemotactic
Elafin	IL-1, TNF- α	Epithelial cells, leukocytes	Antiprotease with antimicrobial and chemotactic properties
Secretory phospholipase A2	LPS	Epithelial and inflammatory cells, Paneth cell granules	- Acute phase protein involved in Eicosanoide metabolism - Small intestinal mucosal defense
Lysozyme	?	Gastric, pyloric and duodenal glands, small intestine, macrophages and monocytes, not in colonic tissue	Antimicrobial against Gram-positive bacteria, chemotactic
BPI (bactericidal/Permeability increasing protein)	LPS	Epithelial cells, neutrophils	Antimicrobial, binds LPS-compounds

¹adapted from Jäger et al., 2013.

1.8 AMPs and Parasites

There are numerous studies on the effect of AMPs on several bacterial species. Fewer, however, are the investigations on its action on eukaryotic organisms particularly on unicellular parasites. Two α -helical AMPs were found to have antimalarial activity. A hybrid AMP also had a lytic effect on *Leishmania* (Vizioli and Salzet, 2002). Mammalian AMPs such as myeloid AMPs, defensins, histatin and plasmin inhibited the growth of *Leishmania* while angiotensin and NK-2 AMPs were effective against *Plasmodium*. AMPs purified from amphibians were also microbicidal against a number of protozoan parasites including intestinal parasites such as *Entamoeba histolytica*, *Cryptosporidium parvum* and *Blastocystis* (Rivas et al., 2009; Torrent et al., 2012). Regarding specific AMPs expressed in the human gut β -defensins 1 and 2 were found to kill *Cryptosporidium* (Zaalouk et al., 2004). Peptides belonging to cathelicidin were also found to be broadly cytotoxic to *Cryptosporidium* sporozoites (but not to oocysts) (Huang et al., 1990). Other cationic peptides such as indolicin, phospholipase and lactoferricin could also decrease their viability (Carryn et al., 2011). In another intestinal parasite, *Entamoeba*, LL-37 was not effective to kill it partly due to the organism's secretion of cysteine proteases (Cobo et al., 2012). However, other derivatives of LL-37 can kill the parasite (Rico-Mata et al., 2013).

For *Blastocystis*, no other studies could be found investigating the effect of AMPs on this ubiquitous eukaryote except a report on magainin. Magainin is an AMP secreted on the frog skin. Four analogs of this peptide were synthesized

and tested on several protistan parasites including *Blastocystis*. These peptides could kill the parasite to varying degrees depending on the α -helical content of the peptides (Huang et al., 1990).

1.9 Study Objectives

The barriers that may prevent or at least limit *Blastocystis* virulence include elements in both innate and adaptive immunity. Elements of innate immunity that are effective against most microorganisms may also be effective against *Blastocystis*. There are however limited studies exploring this aspect (i.e. immune responses) of host-pathogen interactions in the framework of human *Blastocystis* infections. The study's intent was to contribute to exploring the significance of host AMPs when *Blastocystis* infects humans. This goal falls within the broader context of elucidating host immune responses against *Blastocystis*.

This study in particular aimed to identify the effect of endogenous AMPs (e.g. defensins and cathelicidin) secreted by epithelial cells on various *Blastocystis* isolates (Fig. 1.3). The experiments also delved deeper into the lytic effects of one AMP which was found to affect all *Blastocystis* STs. Parallel to this, an alternative method for observing the effects of membrane-disrupting AMP on *Blastocystis* was sought. The result was the application of an imaging flow cytometry technique that focuses on *Blastocystis* shape as a determinant of viability of the parasite while also evaluating its various morphological forms. The resistance factors which cause variations in susceptibility among isolates

were also identified. Lastly, the ability of the parasite to modulate AMP expression and secretion in intestinal epithelial cells were also determined.

This study also contributed to exploring the potential applications of AMPs. AMPs could be used as novel therapies or provide templates for future drugs (Peters et al., 2010). This study therefore identified the therapeutic potential of a few AMPs which could also be extended to other parasitic diseases. The variation in susceptibilities to AMPs of various isolates of *Blastocystis* provided additional basis for speciation of *Blastocystis* STs. When definitive classification of the parasite down to species level is pursued, host immune responses in *Blastocystis* infections could be understood more clearly in the context of species-specific effects.

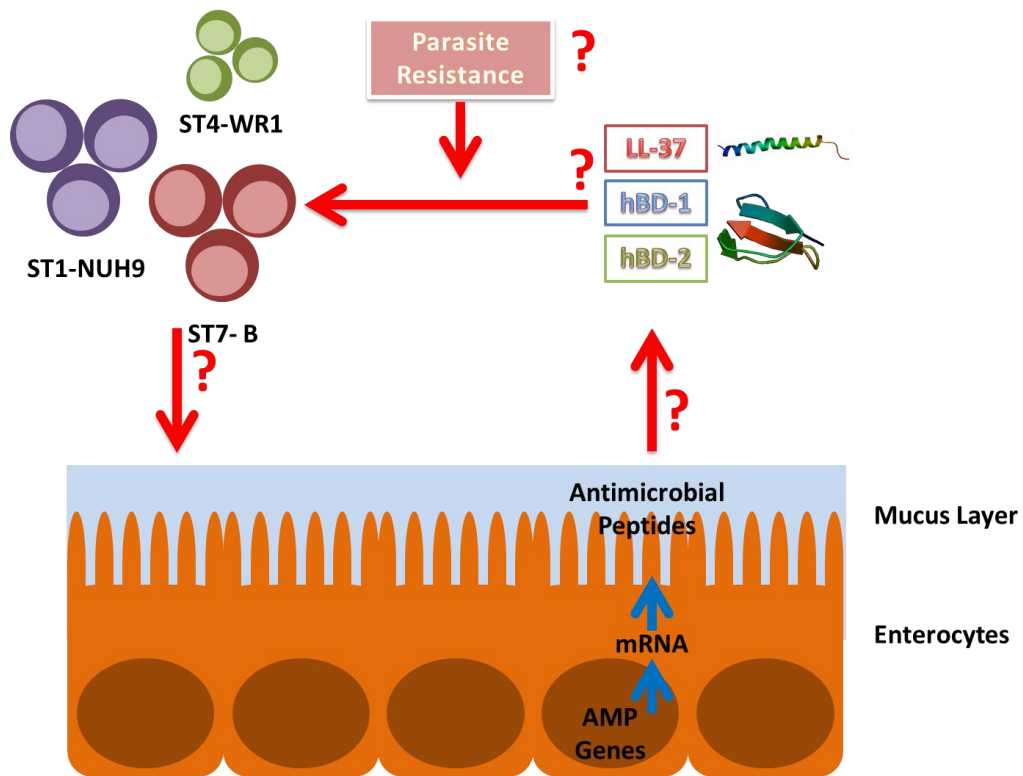


Fig. 1.3. Framework of the study exploring the roles of endogenous colonic AMPs in *Blastocystis* infections. The question marks indicate the particular aspects of this study: susceptibility of *Blastocystis* to AMPs, resistance factors against AMPs and modulation of AMP expression by the parasite.

Chapter 2

Susceptibility of *Blastocystis* to Antimicrobial Peptides

2.1 Introduction

Blastocystis is known to colonize the large intestines. When this happens, the host mounts a series of immune responses. Past in-vitro and in-vivo experiments indicated that the parasite can induce expression of GM-CSF and IL-8 in intestinal epithelial cells. *Blastocystis* secreted proteases can also stimulate other cytokines IL-1 β , IL-6 and TNF- α in macrophages (Ajjampur and Tan, 2016; Lim et al., 2014). Innate immune response against *Blastocystis* also includes production of nitric oxide (Mirza et al., 2011a).

Antimicrobial peptides (AMPs) are elements of innate immunity (Peters et al., 2010). This group of small molecules have wide-spectrum of activities and pathogens in general do not develop resistance against them. The mechanism of action by direct killing is by forming pores on the membrane of pathogens which may cause leakage of cytoplasmic contents. Some AMPs are also known to bind to intracellular targets and inhibit cellular processes (Li et al., 2012). AMPs can also serve as link between innate and adaptive immunity (Wiesner and Vilcinskas, 2010).

The objective of the experiments outlined below was to determine the susceptibility of *Blastocystis* against AMPs which are found in the colon and secreted by epithelial cells. LL-37, hBD-1 and hBD-2 were chosen because they are found in the colon and are secreted by epithelial cells (Table 1.1). These AMPs have direct killing effect on a number of bacterial species.

2.2 Material and Methods

2.2.1 Parasite cultivation and ethical approval

Nine (9) *Blastocystis* isolates (Chen et al., 1997; Ho et al., 1993; Wong et al., 2007) previously axenized representing 3 STs (ST1, ST4 and ST7) were used in the experiments. The isolates were cultivated in Iscove's modified Dulbecco's medium (IMDM) (ThermoScientific) supplemented with 10% horse serum (Gibco). Culture media were transferred in 12-ml culture tubes (ThermoScientific) at 8-9 ml volume. These were pre-reduced in anaerobic jars (Oxoid) for at least 18 h at 37°C using anaerobic gas packs (Oxoid) before inoculation with *Blastocystis*. Cultures were maintained in the same conditions.

Blastocystis isolates used in this study are maintained at the microbial collection of the Department of Microbiology and Immunology, Yong Loo Lin School of Medicine at the National University of Singapore (NUS). Isolate B, C, E, G and H were obtained from stool samples of patients admitted at the Singapore General Hospital in the 1990's before NUS established and Institutional Review Board (IRB). Isolates NUH2 and NUH9 were cultivated in 2007 from fecal samples submitted for routine health screening. Ethical approval was obtained from National Health Group IRB before project commencement and all samples were anonymized. Isolates WR1 and S1 were isolates and cultivated from Wistar and Sprague-Dawley rats, respectively.

2.2.2 Subtyping of *Blastocystis* isolates

The isolates were previously genotyped using primers in a polymerase chain reaction (PCR) assay based on the organism's small sub-unit ribosomal RNA (SSU rRNA) (Noël et al., 2005; Wong et al., 2007). To further confirm ST identity, another PCR assay using mitochondria-like organelle (MLO) (Poirier et al., 2014) gene fragments were used. Total DNA were extracted from 1×10^6 cells using Qiagen DNA stool kit (Qiagen) following the manufacturer's instructions. PCR was performed using Q5 High-Fidelity 2× Master Mix (New England BioLabs) with 500 ng of DNA sample. All PCR runs were completed using BioRad iQ5 thermocycler. PCR products were sequenced, and then compared to information found in National Center for Biotechnology Information (NCBI) (USA) nucleotide sequence database to confirm subtype identities. Specifically, these were isolates NandII (ST1), DMP/02-328 (ST4) and B (ST7). A phylogenetic tree was generated from gene sequences from representative isolates using DNADIST 3.5c. *Proteromonas lacertae* gene sequences were used as outgroup.

2.2.3 AMP susceptibility screening

To determine the susceptibility of the 9 *Blastocystis* isolates to various human intestinal AMPs, a high throughput viability assay developed by Mirza et al. (Mirza et al., 2011a) was applied. Briefly, flat-bottom 96-well plates (Greiner) were used with each well containing 0.5×10^6 *Blastocystis* cells. AMPs human beta-defensin 1 and 2 (hBD-1, hBD-2) and LL-37 were dissolved in complete

medium with concentrations ranging between 0 to 50 μM . After 24 h incubation in anaerobic conditions at 37°C, resazurin dye (Sigma-Aldrich) at 5% final dilution was added and incubated for another 3 h in anaerobic conditions at 37°C. Reading of fluorescence was taken at 550 nm excitation and 570 nm emission wavelengths using Tecan Infinite F200 microplate reader. Synthetic AMPs at 95% purity were obtained from Singapore Advanced Biologics. The experiments were done in triplicates.

2.2.4 Susceptibility of *Blastocystis* to AMPs and determination of IC_{50}

Half maximal inhibitory concentration (IC_{50}) values were calculated based on the relative fluorescence units of resazurin after incubation with AMP-treated-*Blastocystis* cultures. Using GraphPad Prism software, non-linear regression analyses were performed with the AMP concentration transformed into log-scale.

2.2.5 Statistical analyses

Statistical analyses in all the chapters in this study comparing variables and determination of significance were performed using ANOVA and Student's *t*-test in GraphPad Prism version 5. Experiments were done independently at least three times.

2.3 Results

2.3.1 *Blastocystis* isolates subtyping

Subtype identities of 9 *Blastocystis* isolates were confirmed (Fig. 2.1 A) using PCR assay based on the parasite's SSU rRNA and MLO gene fragments. MLO gene sequences from selected isolates from each ST were used to generate a cladogram using Neighbor-Joining/UPGMA method version 3.6a2.1 after aligning the sequences using ClustalW Multiple alignment (Thompson et al., 1994) (Fig. 2.1 B). DNA sequences from GenBank of known *Blastocystis* STs were used for identification.

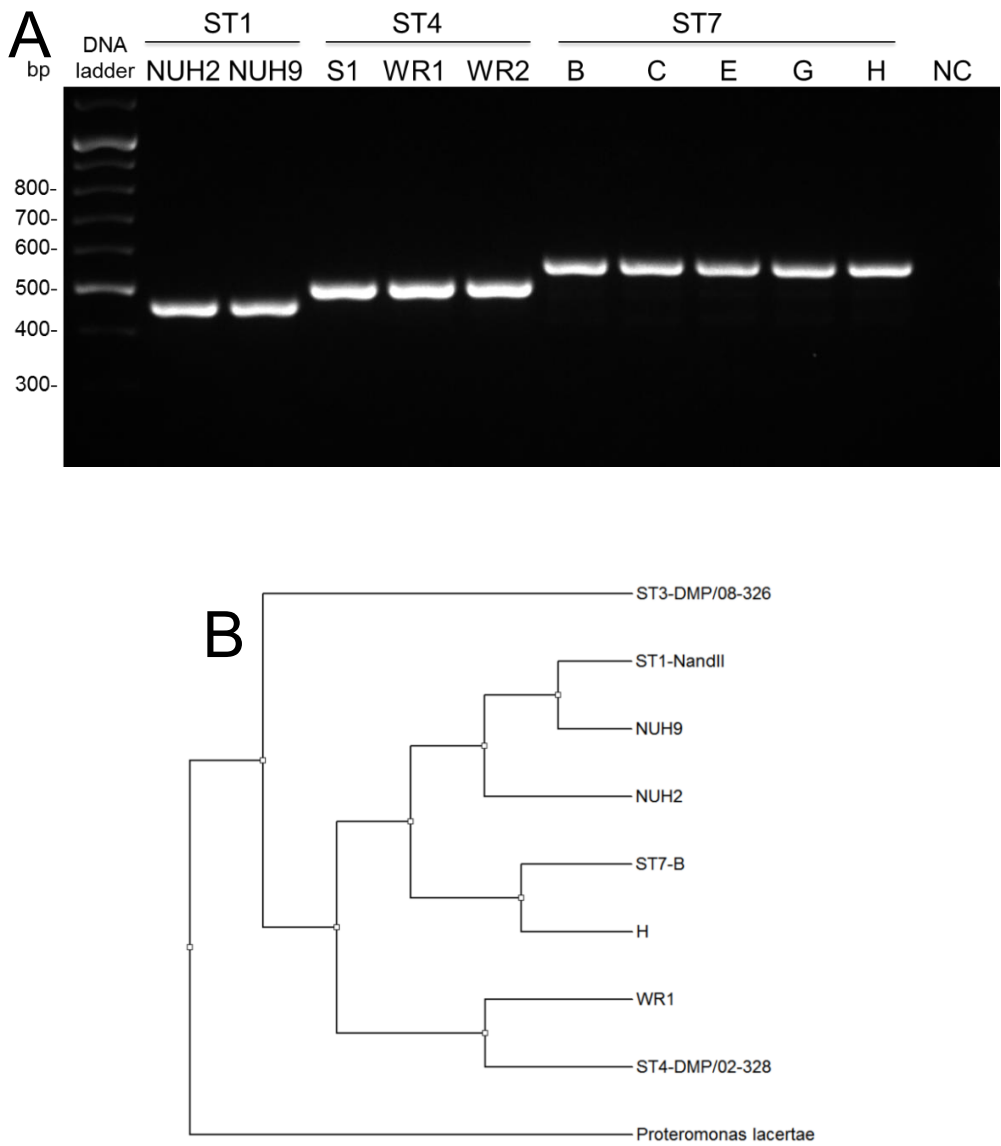


Fig 2.1. 2% Agarose gel showing amplified MLO gene fragments from various *Blastocystis* isolates. Each ST has a unique band size and they were of the expected sizes based on sequence data from NCBI nucleotide database. *Blastocystis* ST1, ST4 and ST7 isolates would show 477, 518 and 536 bp sizes, respectively (A). *Blastocystis* isolates representing different STs clustered with isolates with known STs in a cladogram generated using the parasite's MLO gene sequences (B).

2.3.2 Susceptibility of *Blastocystis* to AMPs and determination of IC₅₀ values

A resazurin-based assay was used to determine the susceptibility of *Blastocystis* against three AMPs secreted by intestinal epithelial cells. Resazurin is a compound that fluoresces when oxidized. It is useful for measuring the metabolic activity of cells in culture. This was used to develop drug-sensitivity assays on *Blastocystis* cultures (Mirza et al., 2011b). The same procedure was used to test the susceptibility of *Blastocystis* to different AMPs secreted by epithelial cells lining the intestines. After incubation of *Blastocystis* with synthetic AMPs, the fluorescent values which reflect the cultures metabolic activity were measured and plotted to generate graphs (Fig. 2.2). Linear regression analyses were performed to determine IC₅₀ values of each AMP (Table 2.1). hBD-1 did not inhibit *Blastocystis* while hBD-2 was only effective against ST4 isolates. Human beta-defensin 1, at 50 µM concentration, did not affect the activity of all *Blastocystis* isolates used in this study representing 3 STs. Human beta-defensin 2 was only effective on *Blastocystis* ST4 isolates (Table 1) at less than 50 µM concentration. In contrast, LL-37 displayed broad activity on all *Blastocystis* isolates representing 3 STs. LL-37 was found to inhibit the activity of 9 *Blastocystis* isolates at less than 50 µM concentration (Table 1). There was, however, variation in the IC₅₀ values for all the STs tested. At less than 10 µg/ml concentration, LL-37 was found to decrease the growth of *Blastocystis* ST1 and ST4 isolates by half. On the other hand, more than 20 µg/ml concentration is needed to decrease the growth of *Blastocystis* ST7 isolates by half (Table 1).

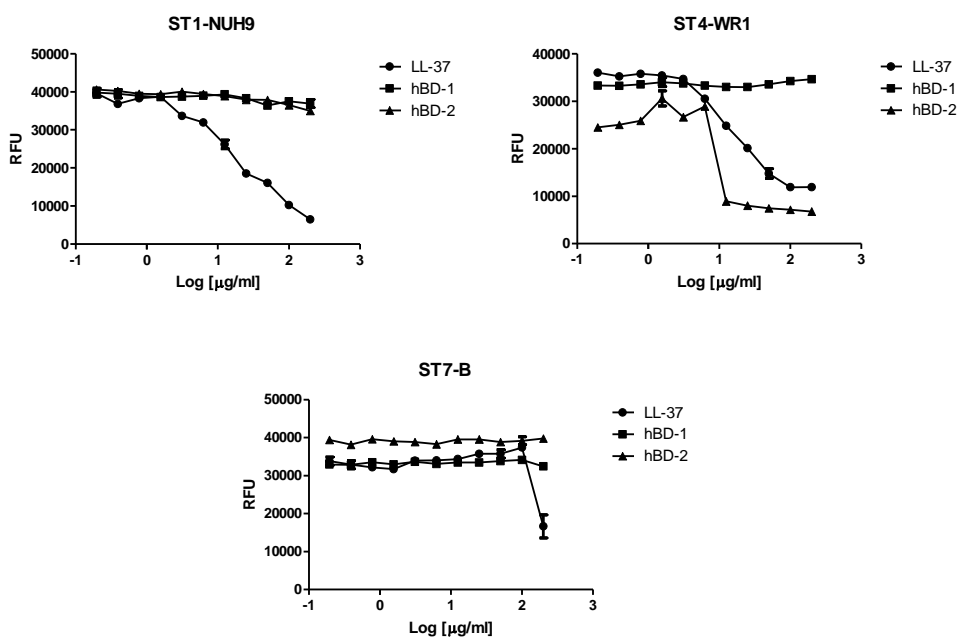


Fig. 2.2. Representative graphs showing relative fluorescence units (RFU) of *Blastocystis* isolates ST1-NUH9, ST4-WR1 and ST7-B treated with different concentrations of hBD-1, hBD-2 and LL-37.

Table 2.1 Half maximal inhibitory concentration (IC₅₀) of hBD-1, hBD-2 and LL-37 on *Blastocystis* STs.

Subtype	Isolate	HBD-1 (μM)	HBD-2 (μM)	LL-37 (μM)
ST1	NUH2	> 50	> 50	6.0
	NUH9	> 50	> 50	4.7
ST4	WR1	> 50	11.4	3.2
	S1	> 50	5.0	5.4
ST7	B	> 50	> 50	42.6
	C	> 50	> 50	23.4
	E	> 50	> 50	23.2
	G	> 50	> 50	27.7
	H	> 50	> 50	28.7

2.4 Discussion

There have been numerous studies showing the effectiveness of AMPs against bacterial, fungal and even viral pathogens. Few, however, are studies on AMPs' action on protozoan parasites. A review on the effect of AMPs against two neglected tropical diseases, leishmaniasis and malaria, outlined both the positive and negative aspects on using AMPs against these protozoans (Torrent et al., 2012). The pore-forming ability of AMPs may not be effective against all similar parasites down to all the stages of their respective life cycles. The developmental stages of these organisms may involve variations in cell membrane and cell wall structure so this may include changes in charges of the surfaces of the cells. As mentioned, hydrophobicity is an important factor in the binding of AMPs in membranes (Yin et al., 2012) and it is interesting to know if AMP can widely affect all life stages of the parasite. On the other hand, several forms of a particular parasite afford multiple targets of AMPs and other drugs. This is an advantage especially in terms of the broad-spectrum activities of AMPs (Torrent et al., 2012). On the use of AMPs for treating *Blastocystis* infections, one study found analogs of an anuran skin peptide called magainin effective against *Blastocystis hominis*, *Trypanosoma cruzi* and *Entamoeba histolytica* (Huang et al., 1990). This study was reported more than two decades ago and the mechanism of AMP-mediated killing was not identified. It showed however that this AMP could disrupt the cell membrane leading to leakage of cell contents and eventual death.

Blastocystis is widely considered a commensal thus the search for drugs that could eradicate the organism from human hosts did not progress rapidly. Infected but asymptomatic individuals may forego therapy but it is suggested that patients showing gastrointestinal and dermatologic symptoms undergo chemotherapy (Coyle et al., 2012). The usual drug of choice to treat *Blastocystis* infection is metronidazole, which is considered standard for many protozoan infections (Kurt et al., 2016). However, there were reports on the failure of this drug to remove *Blastocystis* from infected hosts and several subtypes have been identified as resistant to metronidazole treatment (Engsbro and Stensvold, 2012; Mirza et al., 2011a; Roberts et al., 2014a). There is a need therefore to find alternative strategies to treat *Blastocystis* infections. This study explored the potential of using AMPs to prevent further pathologies which are potentially caused by *Blastocystis* infection. AMPs' activities include membrane pore formation which may cause cell death directly, or allow other molecules to pass through the membrane and bind to intracellular targets (Peters et al., 2010). In the latter, AMPs could make classical drugs more effective. There were also studies on how to develop AMP-based antibiotics (Hancock and Sahl, 2006). AMPs found to be effective against *Blastocystis* could serve as templates for designing new and more effective drugs.

Out of the three endogenous AMPs tested, only a cathelicidin peptide had a broad activity against all the isolates while defensins only affected ST4 isolates. This, however, does not indicate that defensins fulfill no roles in *Blastocystis* infections. Synergistic effect of combination of AMPs may be common occurrence in immune responses against infection (Yu et al., 2016). It would be

interesting to study further if defensins and cathelicidins could act synergistically against *Blastocystis* by combining both AMPs in various ratios and performing killing assays.

Chapter 3

Cellular Effects of LL-37 on *Blastocystis* Subtypes Part A: Microscopy and Ultrastructure

3.1 Introduction

LL-37 is the C-terminal 37 amino-acid sequence fragment of cathelicidin antimicrobial peptide. Cathelicidin is a family of peptides and found in many mammalian species. At present, only one peptide has been identified so far in humans that belong to this family (Fabisiak et al., 2016). Cathelicidin is synthesized as a preproprotein ending up as a propeptide. It is processed by proteases and the fragment LL-37 is released. LL-37 assumes a helical structure in physiological pH, salt concentration and temperature (Kahlenberg and Kaplan, 2013; Vandamme et al., 2012).

In bacteriological studies, as well as fungal studies, LL-37 was found to cause membrane disruption. The exact mechanism of this process by LL-37 has not been elucidated. There are three models, however, which were proposed on the mechanism of AMPs to produce pores on membranes (Brogden, 2005; Huang et al., 2004; Oren and Shai, 1998). The barrel-stave model projects that the peptides can form barrel-shaped holes across the membrane. The peptides are oriented in such a way that their hydrophobic regions align with the lipid core region of the membrane. This has been determined in at least one AMP (alamethicin). In the toroidal-pore model, a “barrel-hole” is also formed but as a result of the peptides forcing the lipid bilayer to bend continuously towards the pore. In contrast to the barrel-stave model, the “barrel” is lined both by the peptides and the lipid heads of the membrane. The carpet model, on the other hand, proposes that peptides form a “carpet” on the membrane. The peptides are oriented parallel to the membrane. At high concentration, the peptide acts like

a detergent leading to the formation of micelles made up of lipid bilayer components. This disrupts the membrane which results into cytoplasmic leakage (Brogden, 2005). A study using Fourier-transform infrared spectroscopy indicates that the carpet model could be the mechanism for pore formation of LL-37. One reason is that LL-37 does not completely insert into the membrane as required in the two other previous models (Oren et al., 1999).

Using resazurin-based assay as discussed in Chapter 2, it was found that among all the AMP's tested, only LL-37 was effective in inhibiting all *Blastocystis* isolates representing 3 STs. However, the manner by which LL-37 acts on the parasite was not determined. In this series of experiments, the direct killing effect of LL-37 by lysis of the parasite was investigated using propidium iodide (PI) staining. PI is a viability dye which cannot penetrate intact membranes. Three *Blastocystis* isolates were used to represent 3 STs: ST1-NUH9, ST4-WR1 and ST7-B. LL-37 exerted a deleterious effect on all 3 STs but ST7 isolates showed relative resistance as evidenced by higher IC₅₀ values compared to both ST1 and ST4 isolates. It is therefore interesting to determine whether the lysis of *Blastocystis* membrane from three different STs would be dissimilar as well when treated with LL-37.

In this chapter, membrane disruption was investigated for three different isolates of *Blastocystis* using PI-staining and flow cytometry. Scanning electron microscopy was also used to look closely at certain morphological changes occurring when the parasite is treated with LL-37.

3.2 Materials and Methods

3.2.1 Parasite cultivation. (See Chapter 2)

3.2.2 Viability staining and flow cytometry

Propidium iodide (PI) (BioVision) was used to stain *Blastocystis* cells to assess viability after LL-37 treatment. *Blastocystis* ST1-NUH9, ST4-WR1 and ST7-B isolates (1×10^7 cells/ml) were treated with LL-37 at 0, 10 and 100 $\mu\text{g/ml}$ concentrations for 1 h. Necrotic control was added as a positive control. This was achieved by heating the cells at 80°C for 15 mins. PI was then added to the cell suspension according to the manufacturer's instruction. Cells were then analyzed using LSRFortessa (BD Biosciences). Data analysis was done using Summit software version 4.3 (Dako).

3.2.3 Time-lapse microscopic imaging

Blastocystis cells were treated with 100 $\mu\text{g/ml}$ LL-37. Aliquots were dropped onto glass slides and observed under Olympus BX60 light microscope. Images were taken every 5 min.

3.2.4 Scanning electron microscopy

The effect of LL-37 peptide on *Blastocystis* membrane and surface coat were visualized using scanning electron microscopy (SEM). *Blastocystis* cells at $1 \times$

10⁶ cells/ml density were treated with 100 µg/ml LL-37. These cells together with control were fixed overnight with 4% glutaraldehyde in PBS. The cells were then washed and attached to 0.1% poly-L-lysine-treated cover slips for 30 mins. The cells were dehydrated with increasing concentration of ethanol. The coverslips with attached cells were placed in critical point dryer (Balzers CPD 030) for carbon dioxide infiltration. After drying, the cover slips were coated with 5-10 nm of gold in a sputter coater. The cells were visualized in a JEOL JSM-6701F scanning electron microscope.

3.3 Results

3.3.1 LL-37 disrupts *Blastocystis* cell membrane

Three isolates (ST1-NUH9, ST4-WR1 and ST7-B) each representing a particular subtype were incubated with 0, 10 and 100 µg/ml LL-37 for 1 h and analyzed for membrane disruption by staining with PI. The proportion of cells with PI stain was determined by flow cytometry. All three isolates showed increase in proportion of permeabilized cells as the concentration of LL-37 increased. At 100 µg/ml LL-37, more than 50% of the *Blastocystis* ST1-NUH9 and ST4-WR1 cells had PI-staining while only 36% of that in ST7-B isolate (Fig. 3.1).

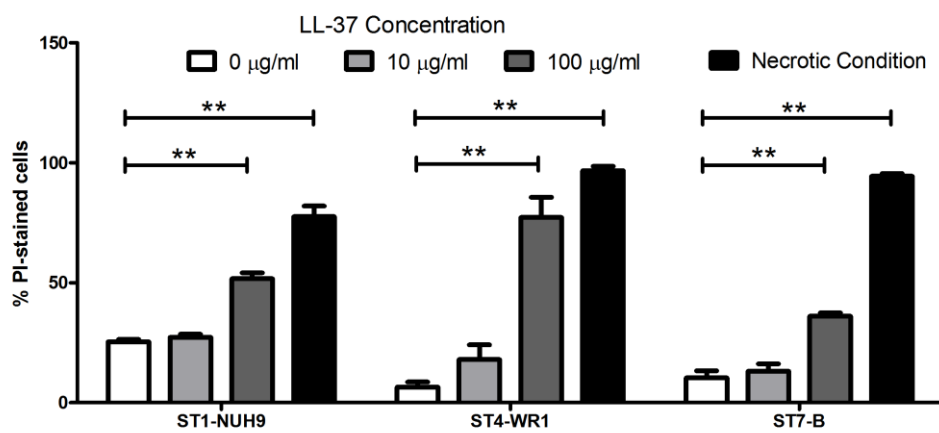


Fig. 3.1. LL-37 caused disruption of *Blastocystis* cell membrane. PI-staining and flow cytometry was used to detect cells with permeabilized membranes. Graphs show proportion of PI-stained cells in ST1-NUH9, ST4-WR1 and ST7-B populations after incubation with 0, 10 and 100 µg/ml LL-37 for 1 hour. Necrotic condition was used as positive control for PI-staining. This was attained by heating *Blastocystis* cells for 15 min at 80°C. There is an increase in proportion of permeabilized *Blastocystis* at higher concentration of LL-37. ST7-B isolate showed relative resistance to LL-37 compared to both ST1-NUH9 and ST4-WR1 isolates. **, p<0.001.

3.3.2 Time-lapse images of LL-37-induced lysis of *Blastocystis*

Time-lapse micrographs showed that as early as 5 minutes of incubation of *Blastocystis* ST7-B isolate with the peptide, smaller cells were already undergoing lysis. Bigger cells were observed being lysed after 20 minutes. Before complete lysis, vesicles were seen forming in a few sections of the cell membrane (Fig. 3.2). The cells appeared to flatten as well. In addition, the membrane-disruptive effect of LL-37 on a 'resistant' isolate (ST7-B) was slower compared to a 'sensitive' isolate (ST4-WR1). Flow cytometry analysis showed that more than 30% of ST4-WR1 had PI-staining at 15 min treatment of LL-37 while it took 30 min of treatment for ST7-B cells to reach this proportion (Fig. 3.2 B).

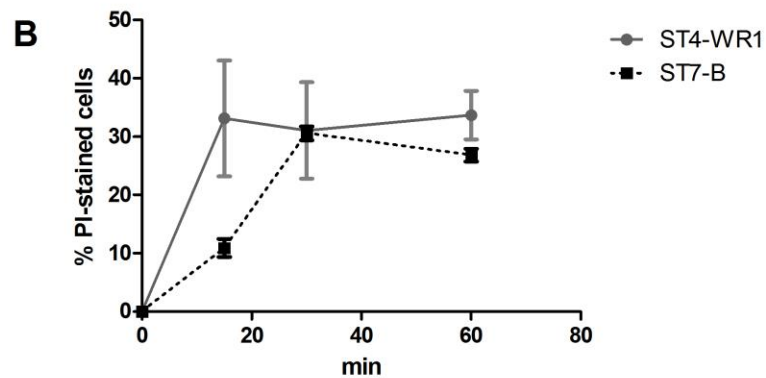
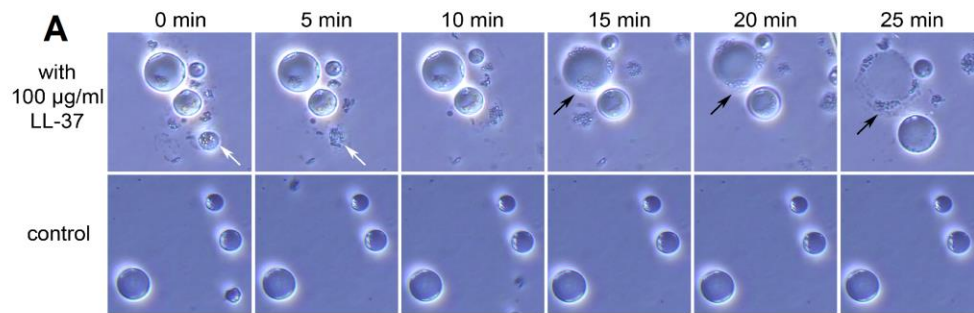


Fig. 3.2. Time-lapse images of *Blastocystis* ST7-B cells treated with 100 $\mu\text{g/ml}$ LL-37 (upper row) and control (lower row) (A). Images were taken every 5 minutes. Arrows point to cells undergoing lysis. Cells lysed as early as 5 minutes after addition of LL-37 (white arrow). Time course lysis experiments using PI-staining and flow cytometry were also done (B). Graph show that the membrane disrupting effect of LL-37 was faster among ST4-WR1 compared to ST7-B cells.

3.3.3 Scanning electron micrographs of LL-37 treated *Blastocystis*

Scanning electron micrographs of normal *Blastocystis* cells show the typical spherical shape particularly for *Blastocystis* ST1-NUH9 and ST7-B isolates (Fig. 3.3). *Blastocystis* ST4-WR1 cultures also showed slightly flattened cells. *Blastocystis* surface coat appear as rough, uneven covering of the cells. When treated with LL-37, *Blastocystis* ST1-NUH9 cells appear flattened and irregular. A few large pores were observed as well. ST4-WR1 cells appeared fragmented and loss of sphericity. ST7-B isolates also exhibited large holes when treated with the peptide. There also appeared smaller structures, which are probably cellular contents, in the cultures treated with LL-37.

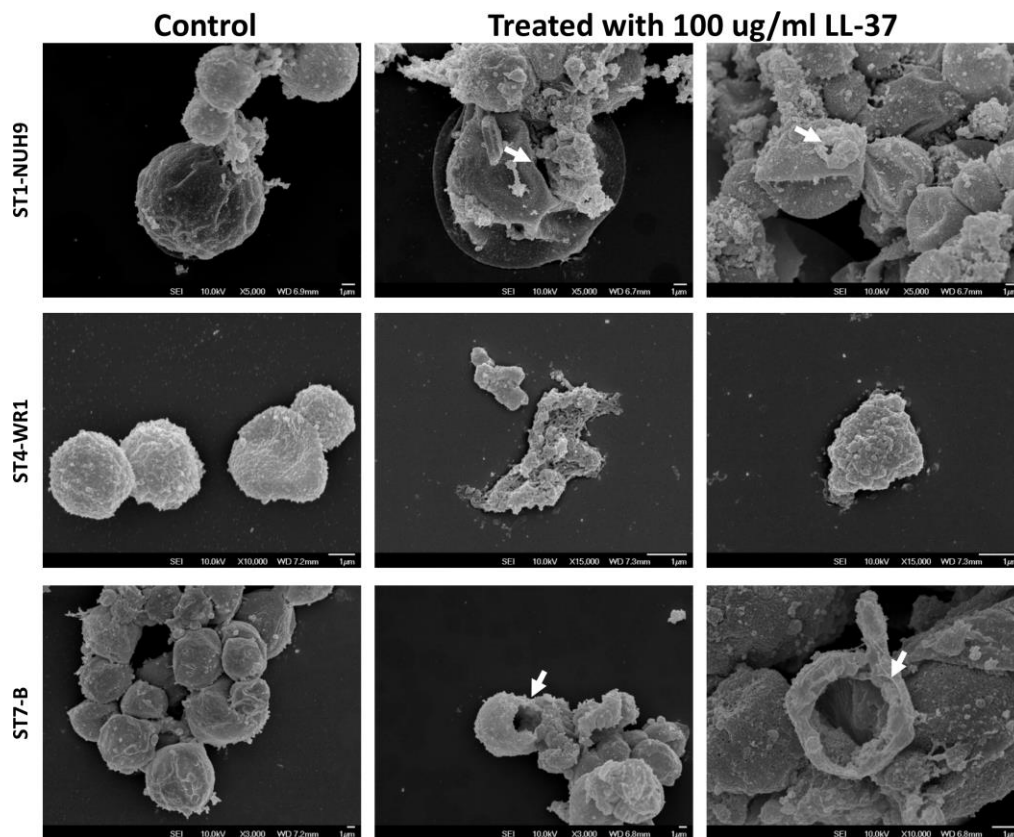


Fig. 3.3. *Blastocystis* membrane exhibited pores of various sizes when treated with LL-37 for 1 h. Scanning electron micrographs also showed cells assuming irregular shapes when treated with the peptide. The white arrows point to possible large membrane pores that could lead to cytoplasmic leakage. LL-37-treated *Blastocystis* ST4-WR1 cells show highly fragmented cells.

3.4 Discussion

This series of experiments showed that LL-37 causes membrane disruption in *Blastocystis*. The experiments also showed the fast killing action of LL-37 as seen in other treatment studies of bacteria and fungi (Bucki et al., 2010; Ordonez et al., 2014). In conjunction with the results in resazurin-based assay, LL-37 exerted lytic effects on all *Blastocystis* STs but ST7 isolates were less affected as shown by the lower proportion of PI-stained cells after treatment (Fig. 3.1). Moreover, the effect of membrane disruption was slower in a ST7 isolate compared to a sensitive ST isolate (i.e. WR1). *Blastocystis* STs exhibited various biological differences. For example, ST7-B isolate was significantly bigger in size compared to ST4-WR1 isolates. The former also has a slower growth rate compared to the latter. These and other factors may be responsible for the variation in AMP susceptibility and lysis rate among *Blastocystis* STs. Some of these factors will be considered later.

The fact that LL-37 caused permeabilization to *Blastocystis* indicates that the peptide has affinity to the parasite's membrane. It may also suggest that the surface coat does not completely protect the parasite from AMP attack by either preventing AMP binding to the membrane or shielding the negative charges in the membrane. In this context, the membrane of *Blastocystis*, a eukaryote, is similar to that of prokaryotes which makes the parasite susceptible to direct killing by AMP.

SEM images showed extensive morphological changes in *Blastocystis* treated with LL-37. The holes in the membrane were of different sizes. There were also other structures which could be cytoplasmic contents of the parasite. In bacteria, blebs were seen forming when treated with an AMP called SMAP29, a helical peptide similar to LL-37 (Brogden, 2005). In SEM images, these were difficult to find since the appearance of normal *Blastocystis* surface is rugged and features tiny bleb-like structures. It would require therefore a more specific approach to observe the process of membrane permeabilization in *Blastocystis* from beginning to end.

Going further, it would be interesting to study if inhibitors or proteases directed against LL-37 could abrogate ultrastructural changes in *Blastocystis* arising from LL-37 treatment. It is known that an analog of LL-37 with shorter sequence can still have an antimicrobial activity (Wang, 2008). LL-37 fragments cleaved by an *E. histolytica* protease was also found to maintain its antibacterial property (Cobo et al., 2012). Finding out if these observations could also apply to *Blastocystis* is compelling especially when considering microbiome-parasite interactions. Another technique that could be considered is the use of antibodies directed against LL-37. This could be an alternative in the use of inhibitors when these compounds affect the viability of *Blastocystis*.

Chapter 4

Cellular Effects of LL-37 on *Blastocystis* Subtypes Part B: Imaging Flow Cytometry

4.1 Introduction

The previous chapters discussed the effects of AMPs (particularly LL-37) on the growth and membrane integrity of *Blastocystis*. This chapter focused on the phenotypic changes caused by LL-37. The difficulty in this approach was that *Blastocystis* has a number of morphological forms, which are purported to have reproductive relevance (Govind et al., 2002, 2003; Tan and Stenzel, 2003; Windsor et al., 2003). These morphological forms observed both in culture and clinical samples still must be evaluated, however. For example, multivacuolar forms have been thought to be *Blastocystis* undergoing multiple fission or schizogony similar to what happens in other protozoan parasites (Govind et al., 2002). There were also suggestions that amoeboid forms may undergo plasmotomy (Yamada and Yoshikawa, 2012). Whether or not granular forms have specific biological functions is still yet to be discovered (Zhang et al., 2012). There was also a report on granular amoeboid forms expelling small granules in xenic cultures (Zhang et al., 2012). The authors however did not investigate further if these granules represent reproductive stages. Currently, only binary fission has been accepted as a mode of reproduction in *Blastocystis* since it can be readily observed under microscopy. Other investigators also suggested that other forms may be artefacts and do not represent reproductive stages (Clark et al., 2013; Tan, 2008; Vdovenko, 2000). There is, however, an interest on looking for alternative modes of reproduction. For some, binary fission alone could not explain the high number of cells in cultures and in fecal specimens (Govind et al., 2002). Just like the parable of the blind men and the elephant, various groups have reported on distinct forms without taking into

consideration the morphological complexity of the parasite. This often led to biases and confusion in the *Blastocystis* field. There is therefore a need to evaluate morphological forms exhibited by *Blastocystis* in terms of their biological importance.

In this chapter, an imaging flow cytometer was used to survey the morphological characteristics of 3 *Blastocystis* isolates representing 3 subtypes (ST1, ST4 and ST7). The Amnis ImageStream Mark II can acquire thousands of images in a sample. These images can then be analyzed based on specific characteristics such as size, aspect ratio, fluorescence staining intensity, etc. This technique was applied to characterize morphological features such as shape, size, granularity and location of nuclei that can identify unique population characteristics in each subtype. Fluorescence dyes were also used to visualize cellular structures such as vacuoles and nuclei. The proportions of cells showing these features were then calculated. This part of the study was the first to provide a comprehensive and unbiased overview of the various morphological forms of *Blastocystis* in culture and shed new light on the roles of certain forms of the parasite. After these baseline assessments, the technique was applied to LL-37-treated *Blastocystis* cultures. The flow imaging cytometry was used to visualize and quantify the localization of LL-37 molecules on the surface of *Blastocystis* and determine the proportion of permeabilized cells among those with bound LL-37. With this, it was possible to compare the affinity of LL-37 to membrane surface as well as the effect of surface-bound LL-37 among different *Blastocystis* STs.

4.2 Materials and Methods

4.2.1 Parasite cultivation. (See Chapter 2)

4.2.2 Fluorescence staining and imaging flow cytometry

In order to analyze cultures at the same stage of growth, 2-day old cultures of *Blastocystis* isolates WR1 and B and 7-day old culture of isolate NUH9 were harvested. The cells were washed twice by centrifugation at $1,000 \times g$ using warm PBS. 2×10^7 cells in 200 μL PBS were collected into 1.5 μL microtubes. The cell suspensions were then stained with 1 $\mu\text{g}/\text{mL}$ PI (BioVision), 5 μM carboxyfluorescein succinimidyl ester (CFSE) (Life Technologies) and 1 $\mu\text{g}/\text{mL}$ Hoechst 33342 (Life Technologies) for 15 mins. PI stain was used to select for viable and non-viable cells. Cells will only take up PI when there is membrane disruption. CFSE is used in proliferation studies and is found to stain vacuolar compartments of *Blastocystis* (Wu et al., 2014). Hoechst stains the DNA and is useful for cell-cycle analysis. Actively dividing cells will have higher emission while dying cells undergoing DNA fragmentation will have lower fluorescence readings. The cells were then washed to remove excess stains and fixed in 2% formaldehyde. Single stained cells were also prepared and used to create a compensation matrix. *Blastocystis* cell suspension heated to 80°C for 15 mins was used as positive control for PI-staining. Amnis ImageStream MarkII (Merck Millipore) with 4-laser attachment (375, 488, 561 and 642) was used to acquire *Blastocystis* cell images. 2,000 events were obtained with low flow speed at $60\times$ magnification. Images at extended depth

of field (EDF) setting were also acquired. EDF involves deconvolution to obtain highly focused images. Gating strategy involved selecting for focused cells using RMS gradient values, then for single cells using brightfield aspect ratio (Fig 4.1). Viable *Blastocystis* cells were identified as those without PI-staining. Cell shapes were characterized using aspect ratios from brightfield and CFSE staining. Acquisition was done using 3 different batches of cultures. Analysis of images was performed using IDEAS software version 6.1.

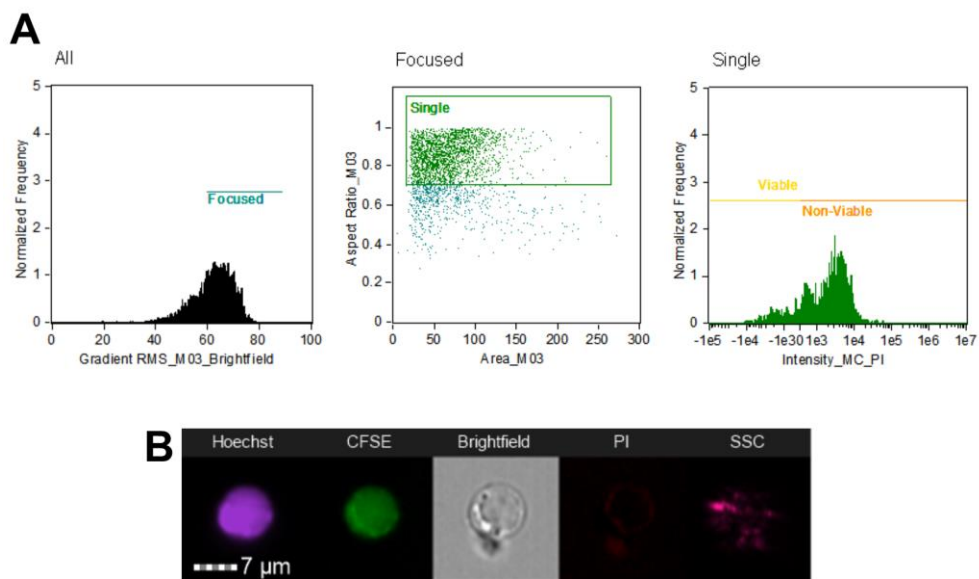


Fig 4.1. Initial gating strategy to analyze *Blastocystis* cells. Cells were gated for focused cells using brightfield channel, then selection of single cells using aspect ratio and area units, and finally to classify viable and non-viable cells using PI-staining characteristics. The above graphs show the analysis for *Blastocystis* ST1-NUH9 isolate (A). Subsequent analyses made use of features arising from Hoechst and CFSE staining characteristics as well as features from brightfield and side-scatter channels (B).

4.2.3 LL-37 treatment of *Blastocystis*

Blastocystis cultures of NUH9, WR1 and B isolates were harvested at the log phase of their corresponding growth curves. NUH9 has the slowest growth rate and cultures from this isolate were harvested after 7 days. Two-day old WR1 and B cultures were collected and used in the experiments. Cell suspensions with of 1×10^7 cells/ml were prepared and treated with LL-37 at 0, 10 and 100 $\mu\text{g/ml}$ concentrations for 1 h. The cells were then centrifuged and washed with PBS. These were the run in the imaging flow cytometer.

4.2.4 Localization of LL-37 bound on *Blastocystis* surface

LL-37 bound to the cell surface of *Blastocystis* were also visualized using imaging flow cytometry. Before running the samples, 1×10^7 cells were treated with 50 $\mu\text{g/ml}$ LL-37 at room temperature. PI was added and the cells were fixed using 4% formaldehyde for 30 mins. The cells were washed twice and suspended in PBS. LL-37 bound to *Blastocystis* cell surface was probed with 1:1000 rabbit polyclonal anti-LL37 human IgG antibody (Abcam) for 30 mins. Goat polyclonal secondary antibody to rabbit IgG FITC-conjugated antibody (Abcam) at 1:500 concentration was then added and incubated for 30 mins. All the reactions were done at 25°C.

4.3 Results

4.3.1 Round and irregularly-shaped cells found in *Blastocystis* STs

Using imaging flow cytometry, both round and irregular shapes were found in all *Blastocystis* isolates (Fig. 4.2, 4.3). The proportion of these shapes however differed from one subtype to another. Viable *Blastocystis* ST1-NUH9 was exclusively round, but only 76% round (the rest are irregular) in non-viable cells. Viable *Blastocystis* ST4-WR1 and ST7-B isolates were 83% and 92% round-shaped, respectively. These proportions were slightly lower (82% for ST4-WR1 and 88% for ST7-B) in non-viable cells (Fig 4.2 A).

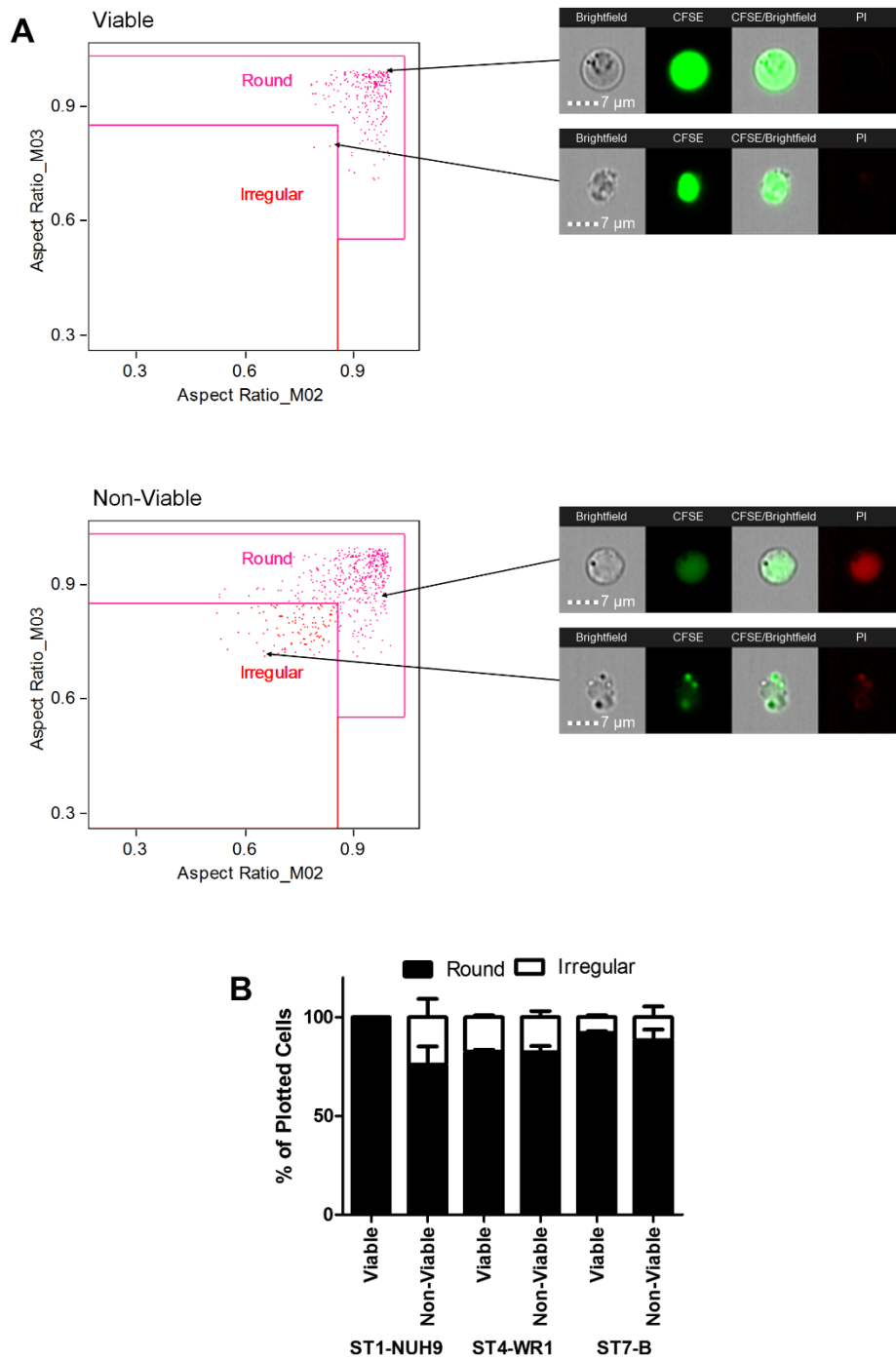


Fig. 4.2. Gating for round and irregular shapes of *Blastocystis*. The shapes of *Blastocystis* were selected based on aspect ratios from the brightfield channel (M03) and CFSE staining (M02). Viable and non-viable cells were plotted separately. The above graphs show the gating for *Blastocystis* ST1-NUH9 isolate (A). The average proportion of round and irregular shapes found in cultures of *Blastocystis* ST1-NUH9, ST4-WR1 and ST7-B were then plotted in a graph (B). These were based on three separate batches of cultures and independent runs in ImageStream. Error bars signify standard error values. p -values comparing the proportion of round cells between viable and non-viable populations are 0.06, 0.47 and 0.31 for ST1-NUH9, ST4-WR1 and ST7-B isolates, respectively.

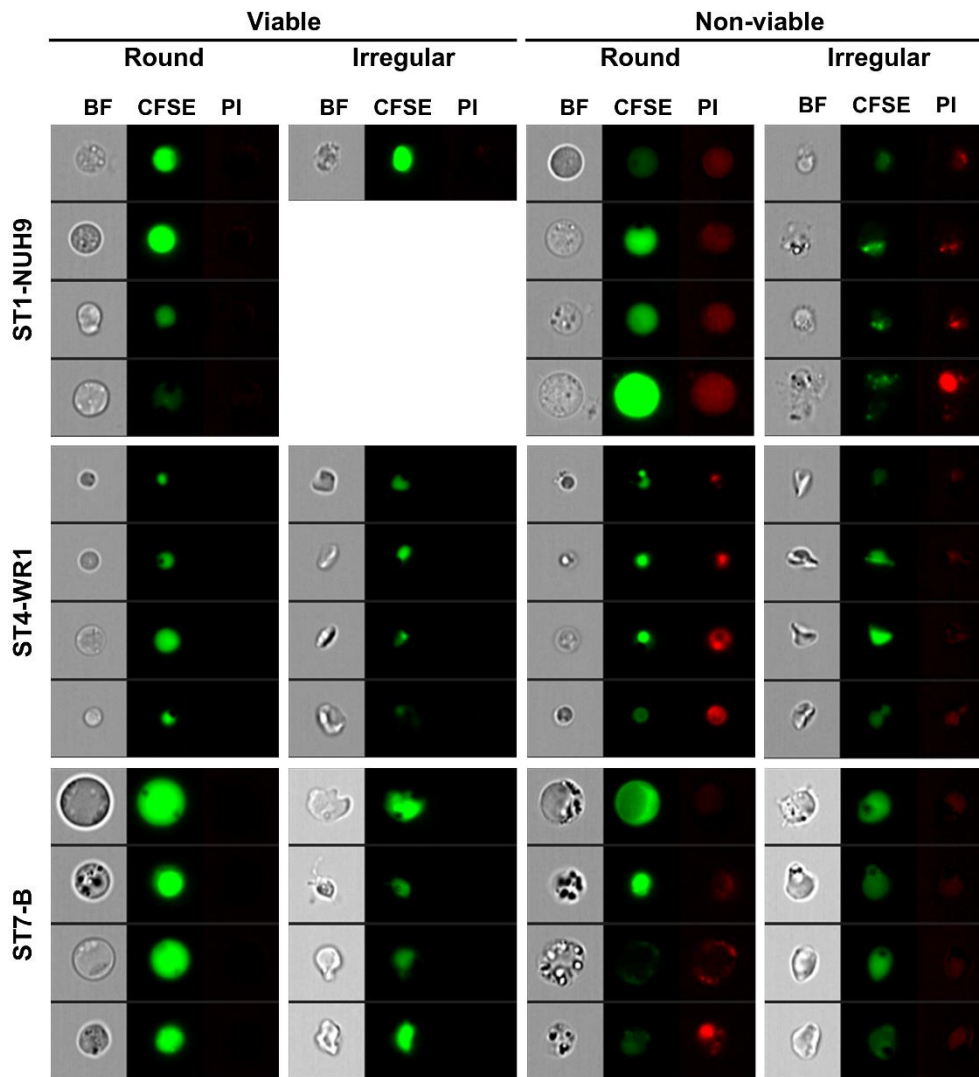


Fig. 4.3. *Blastocystis* STs display various shapes from both viable and non-viable populations. Image gallery of *Blastocystis* cells showing round and irregular shapes from viable and non-viable populations. Each cell shown in the brightfield view has corresponding images which display CFSE-staining, brightfield-CFSE composite and PI staining. The latter was used to determine viability. Irregular-shaped cells show elongated cells and amoeboid forms. Amoeboid forms with prominent pseudopodia and filamentous attachments were restricted to non-viable forms ST1-NUH9 and ST4-WR1. There were rare (0.1%) cells in viable ST7-B population that show an amoeboid-like morphology.

4.3.2 Profile of *Blastocystis* cells according to Hoechst staining and circularity

Analysis of single Hoechst-staining was also done to further correlate *Blastocystis* shape and reproductive status. Hoechst-staining is used for cell-cycle analysis. In general, actively dividing cells registered higher fluorescence compared to inert cells. The imaging flow cytometry can arrange the cells based on circularity which in turn is based on the images acquired using the brightfield channel. In all the isolates studied, round-shaped cells had higher average Hoechst-staining compared to irregularly-shaped cells (Fig. 4.4 B-C). This finding linked well with the observation using PI-staining that most irregularly-shaped may not have biological or reproductive roles at all.

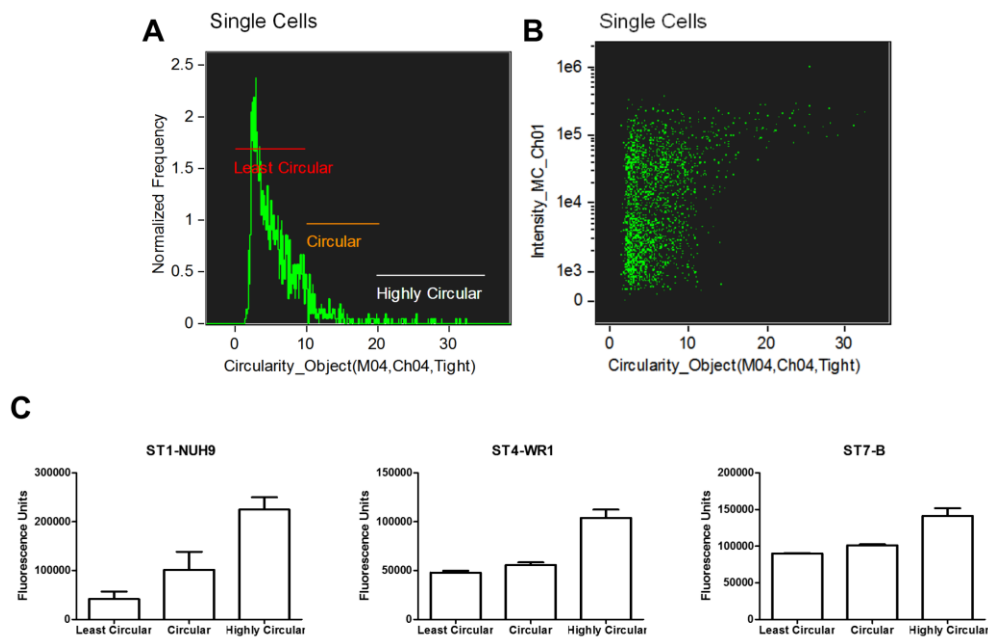


Fig. 4.4. Round *Blastocystis* have higher DNA content. *Blastocystis* cells were plotted according to circularity using the software's shape wizard.

4.3.3 Profile of *Blastocystis* cells according to granularity

The side-scatter channel was used to measure granularity of the cells. The average intensity coming from the channel in all STs in non-viable cells are higher compared to viable cells. Cells that are more granular can be found mostly among non-viable cells as seen among the population with PI staining (Fig 4.5 A-B). Non-viable cells have wider range in terms of granularity in contrast to viable cells where these tend to have lower side-scatter channel intensity. Samples of granular cells from the three *Blastocystis* isolates are shown (Fig. 4.5 C).

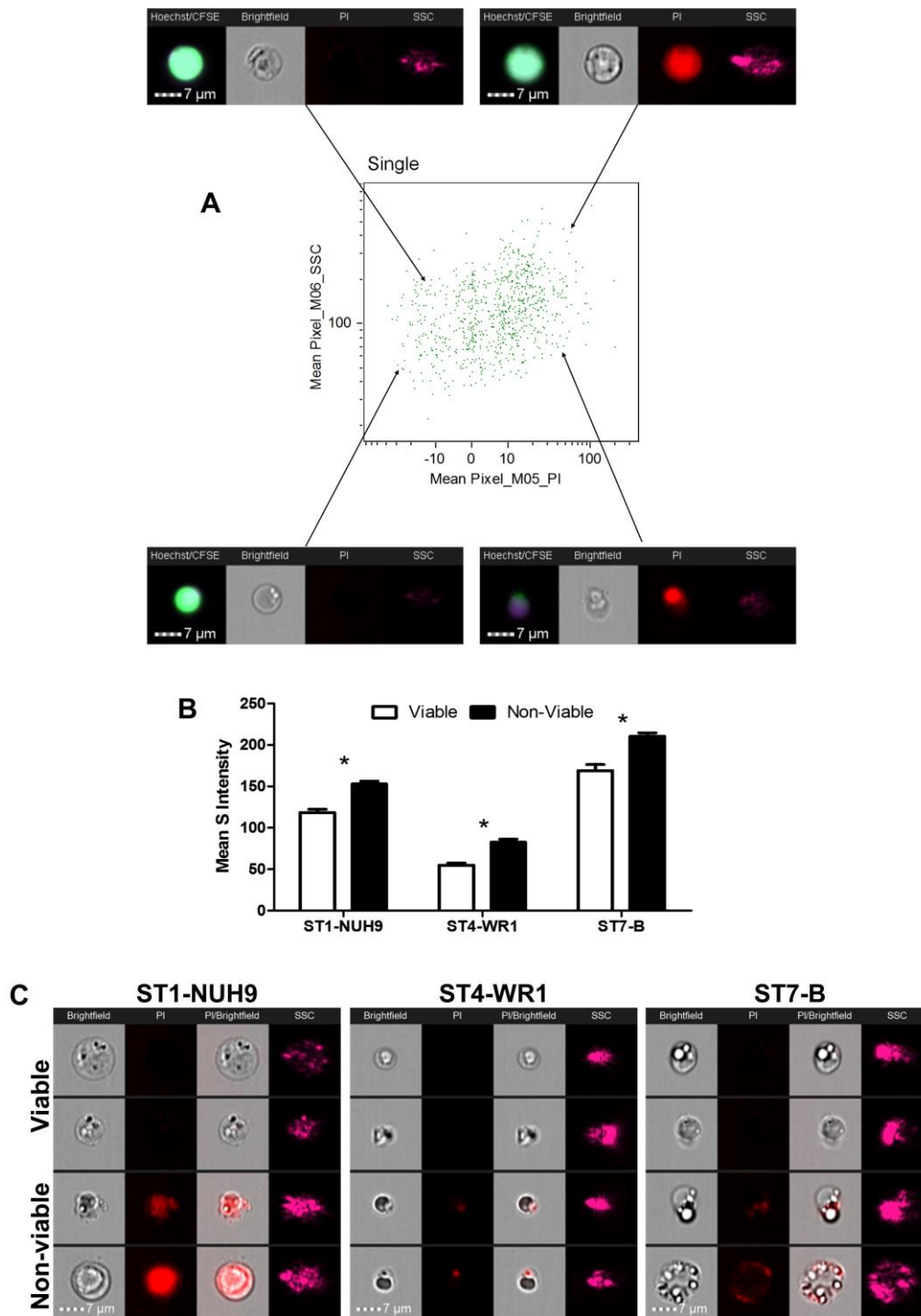


Fig. 4.5. Analysis of *Blastocystis* based on granularity. *Blastocystis* populations were plotted according to mean pixel intensities of both side scatter channel and PI staining to determine the cells' granularity and viability, respectively (A). Cells with higher PI staining have more granularity compared to cells with lower PI staining. This observation was common to all subtypes used in this study as shown in a graph (B). Sample images showing cells with high granularity among viable and non-viable populations (C). These cells may represent true granular cells and degenerating cells, respectively.

4.3.4 Profile of viable *Blastocystis* cells according to granularity and Hoechst staining

Both the side-scatter channel and Hoechst-staining characteristics were used simultaneously to analyze the DNA content of viable granular cells. Dot-plots showed that viable granular cells tend to have higher DNA content (Fig. 4.6). This observation was present in all the isolates representing three *Blastocystis* STs.

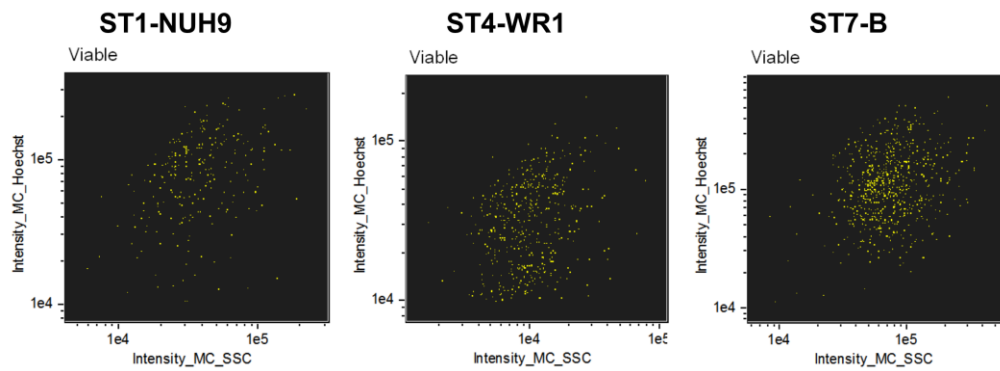


Fig. 4.6. Viable *Blastocystis* cells with high granularity have higher DNA content. Dot-plot shows the populations of *Blastocystis* cells plotted according to circularity and Hoechst staining.

4.3.5 Size range of *Blastocystis* isolates

Using the images obtained from brightfield channel, the size ranges of viable cells in each of the three subtypes were determined. ST1-NUH9 and ST7-B isolates were bigger compared to ST4-WR1 isolates (Table 4.1). Furthermore, more than half (51.7%) of ST1-NUH9 cells have diameter of greater than or equal to 5 μm while only 37.3% of ST7-B cells have this size. ST4-WR1 cells were generally small with diameter of less than 5 μm in 98.3% of the population.

Table 4.1. *Blastocystis* size profiles indicated by cell diameter range and average diameter.

Subtype- Isolate	Diameter Range (μm)	Average Diameter (μm)	Cells with diameter $\geq 5 \mu\text{m}$ (%)
ST1-NUH9	2.7-8.7	5.0	51.7
ST4-WR1	2.2-6.2	3.6	1.7
ST7-B	3.2-7.5	4.9	37.3

4.3.6 Imaging of *Blastocystis* showing classical morphological forms

The images of classical morphological forms of *Blastocystis* were acquired using EDF function of the imaging flow cytometer. Except for the size differences, the three isolates showed cells each with a large vacuole that pushes the nucleus to the edge (Fig. 4.7). The intensity of the staining for vacuoles varied even within the isolate's population.

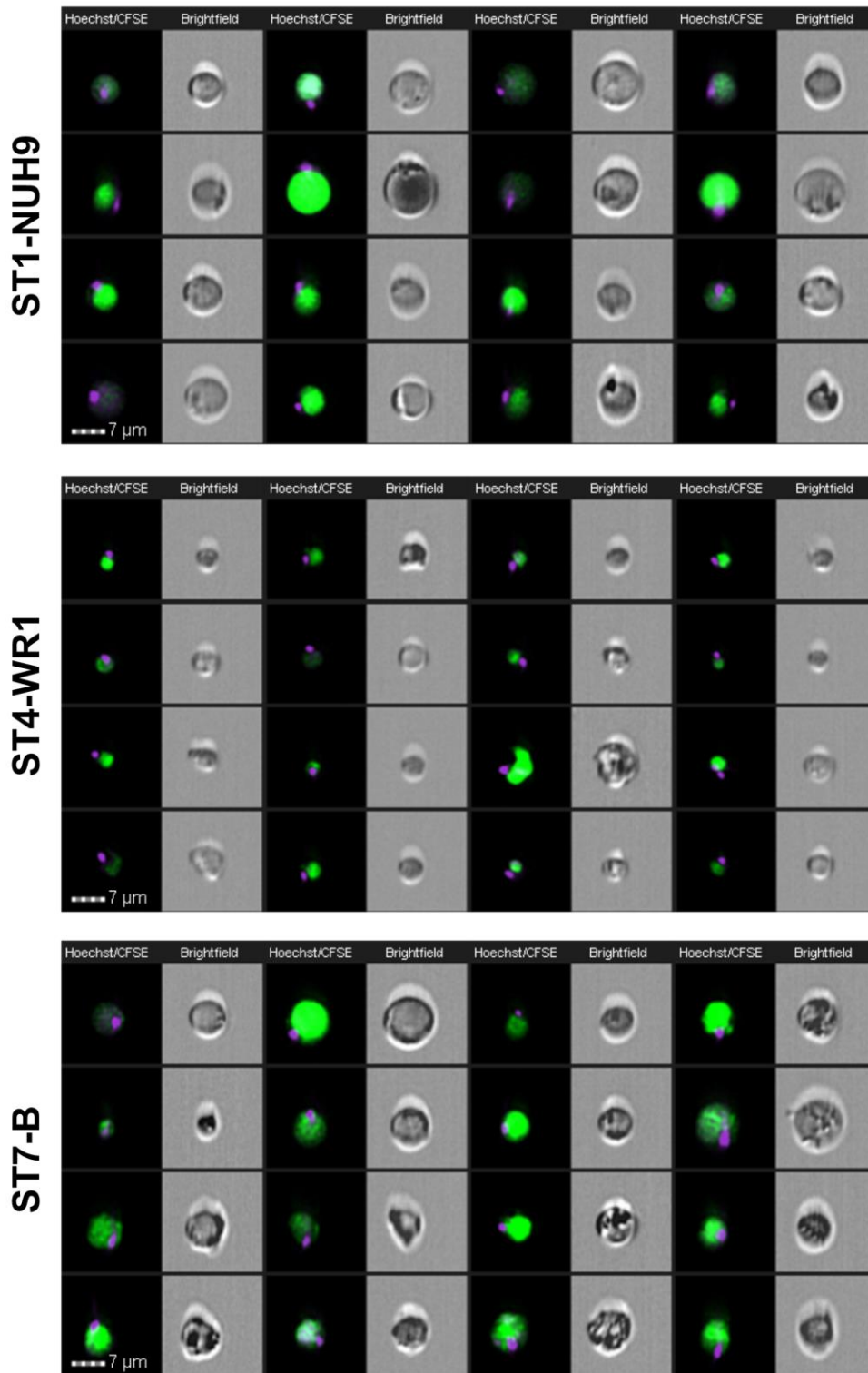


Fig. 4.7. Image gallery of *Blastocystis* showing classical morphological forms at varying sizes in the viable populations. Images were acquired using EDF setting of the imaging flow cytometer. Each cell is represented by two images: Hoechst-CFSE-staining composite and brightfield image. The nuclei were stained with Hoechst and the vacuole with CFSE. These round forms showed a single nucleus located at the edge of the cell. These forms comprised more than half of the population in all the subtypes studied.

4.3.7 Imaging of rare *Blastocystis* multinucleated cells

Blastocystis multinucleated cells were also observed using the imaging flow cytometer. However, only ST1-NUH9 and ST7-B populations had cells with 3 or more nuclei (Fig. 4.8 A). There were also small structures present in the cultures which indicated DNA content (Fig. 4.8 B). At present, they have unknown status and has not been reported in other studies.

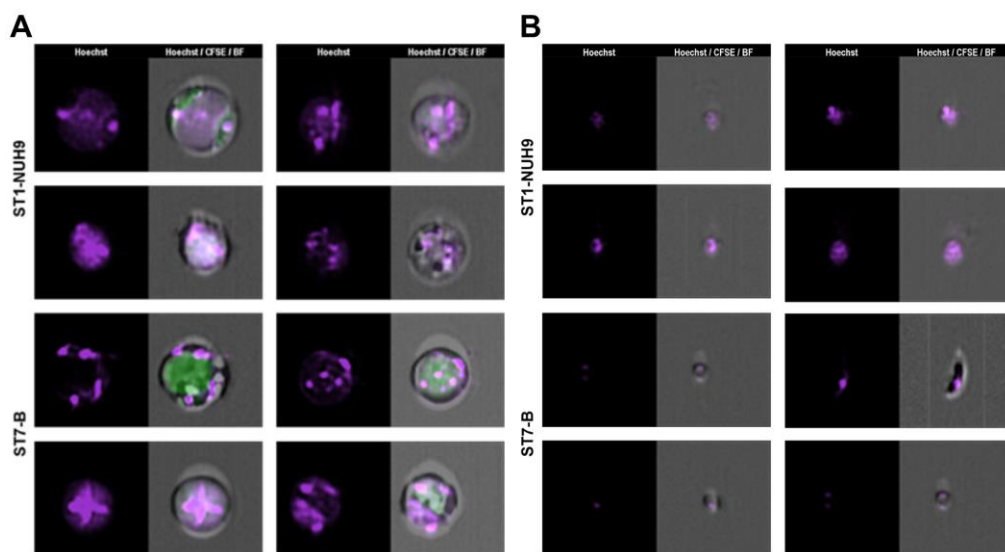


Fig. 4.8. Image gallery of rare *Blastocystis* multinucleated cells. The nuclei are visualized by Hoechst staining. The nuclei numbered more than three and some appeared to be concentrated in the center and not along the edges (A). Some of these cells also appeared to show nuclear condensation. (B) Image gallery showing small structures which contains DNA.

4.3.8 Application of imaging flow cytometry to *Blastocystis* treated with LL-37

With the establishment of comprehensive and baseline data on *Blastocystis* morphological forms, the same technique to achieve this was used to investigate LL-37-treated *Blastocystis* cultures. Brightfield images included round and irregularly-shaped cells (Fig. 4.9 A). Upon treatment with LL-37, the proportion of round cells decreased in the population (Fig. 4.9 B). The greatest change in the proportion of round cells was observed in the cell suspension with the highest concentration of LL-37. At 10 $\mu\text{g/ml}$ LL-37, the change in percentage of round cells was minimal. At 100 $\mu\text{g/ml}$ LL-37, there was a reduction of at least 50% of round cells in all the STs' populations compared to untreated cultures.

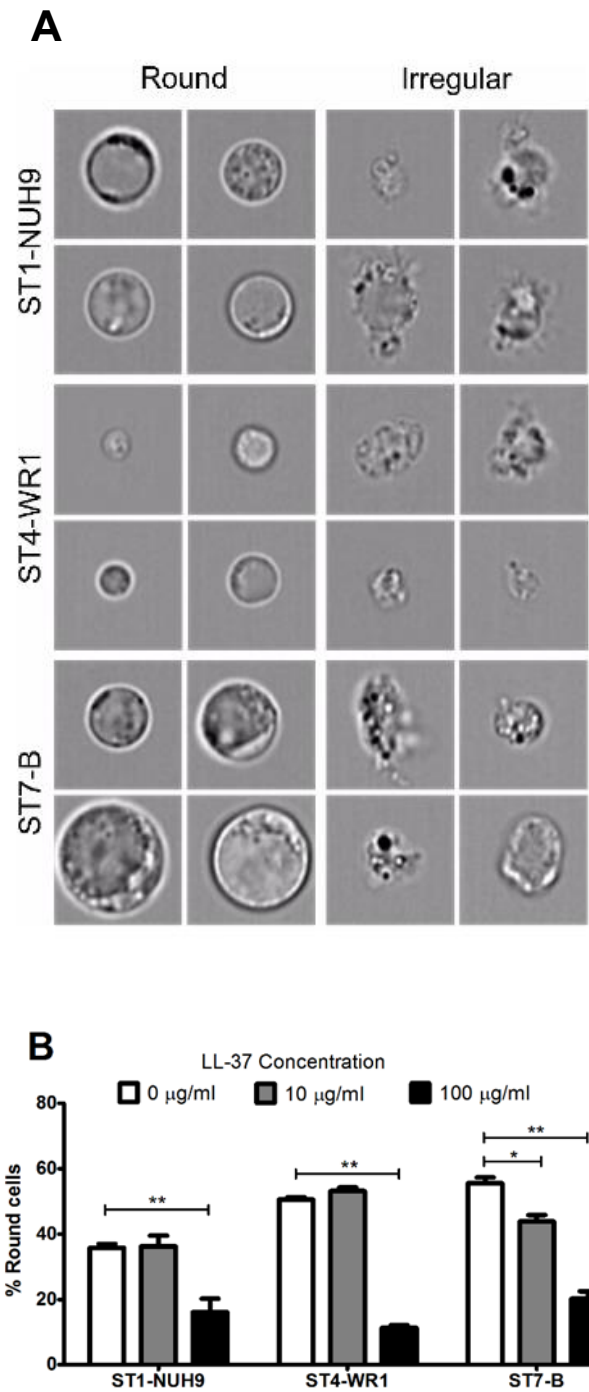


Fig. 4.9. LL-37 causes morphological changes in *Blastocystis* isolates. *Blastocystis* were incubated with LL-37 for 1 h and analyzed using an imaging flow cytometer. Images (A) show round and irregular cells as determined by circularity index generated by the software. Bar graphs (B) show that treatment of *Blastocystis* STs with LL-37 decreased the proportion of round-shaped cells. *, $p < 0.05$; **, $p < 0.001$.

4.3.9 Localization of LL-37 to *Blastocystis* surface

An imaging flow cytometry was used to visualize LL-37 bound to *Blastocystis* (Fig. 4.10 A). The proportion of cells with bound LL-37 is higher in ST4-WR1 isolates compared to ST7-B isolates (Fig 4.10 B). Gating for cells with bound LL-37, a higher percentage of ST7-B cells were found to be viable compared to ST4-WR1 cells (Fig. 4.10 C). Single antibody controls (primary and secondary) were prepared to check their respective specificities (Fig. 6.3).

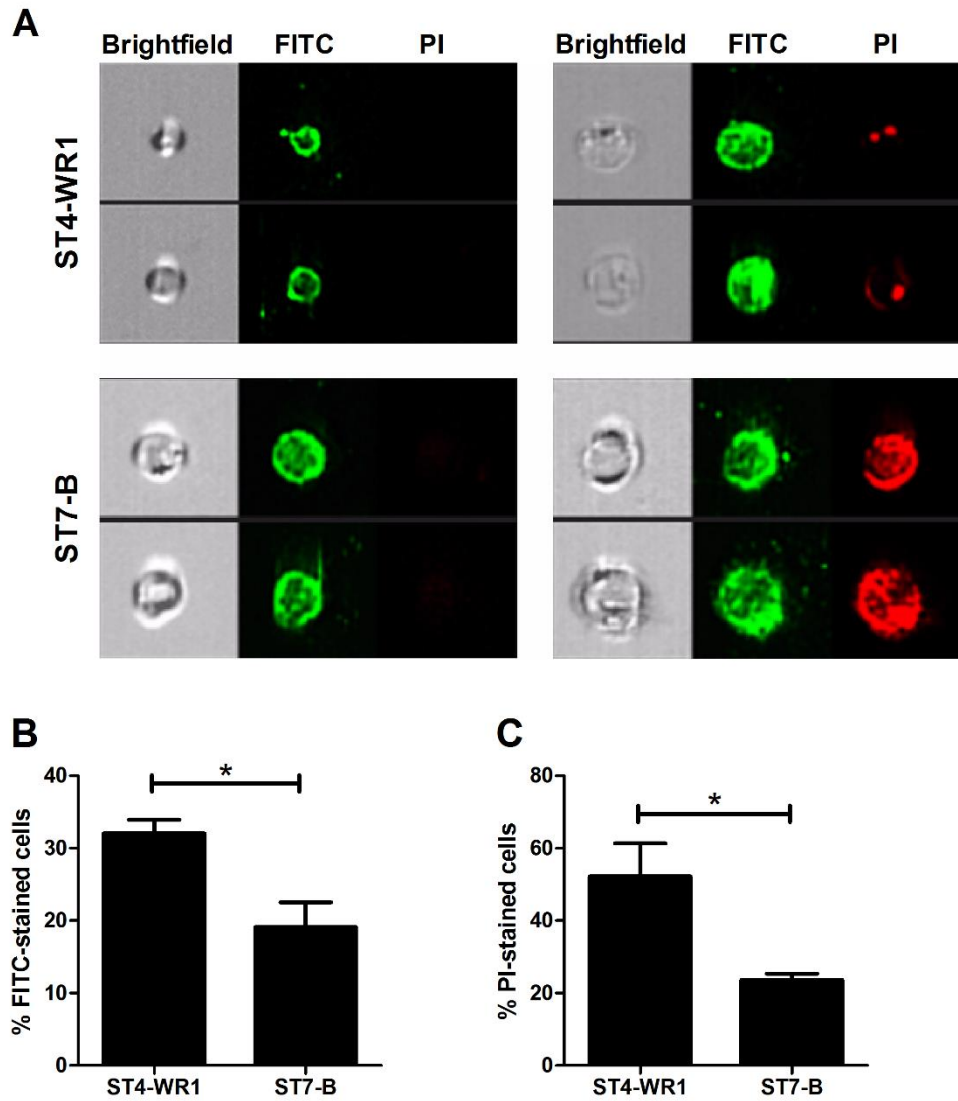


Fig. 4.10. LL-37 binds to the cell surface of *Blastocystis*. Images from the brightfield, FITC and PI channels are displayed showing both the viable and non-viable cells with bound LL-37 (A). LL-37 was detected using FITC-conjugated antibodies. Viability was determined using PI-staining. *Blastocystis* ST4-WR1 had a higher proportion of cells with bound LL-37 peptide (B). Among the cells with bound LL-37, *Blastocystis* ST4-WR1 had lower viability (C). *, $p < 0.05$.

4.4 Discussion

In these series of experiments, analyses of three STs of *Blastocystis* based on shape, size, granularity and nuclear arrangement were done using high content imaging flow cytometry. The features have been used to compare one *Blastocystis* ST to another. Rare forms which could possibly point to alternative modes of reproduction in the parasite have also been identified. Data from this study provided an important and useful reference on the morphological profile of *Blastocystis* STs. The methods outlined in this study have been used to detect changes in *Blastocystis* upon treatment of LL-37.

Several studies have attached significance to amoeboid forms in terms of reproduction and pathogenicity and these appear as irregularly-shaped cells (Govind et al., 2002; Rajamanikam and Govind, 2013; Windsor et al., 2003). These reports however did not identify the subtype of *Blastocystis* they have observed. Past studies also did not take into account the viability of these cells. In this study, morphological features of *Blastocystis* were analyzed while determining their viability using PI-staining. Irregularly-shaped cells in ST1 were found to be non-viable and therefore may not have any biological significance in this particular *Blastocystis* subtype. Isolates from ST4 and ST7, on the other hand, have viable irregularly-shaped cells. This irregularity could be due either to the cells' elongated shape or due to amoeboid features such as pseudopod-like structures. Analyses of the images showed that these amoeboid forms were rare among viable populations as most irregularly-shaped cells (especially in ST4) were elongated. In ST1 and ST4, these forms were more

numerous but all were non-viable. Analysis of cells from viable ST7 isolates showed only one cell (out of ~1000 cells) that could be characterized as amoeboid (Fig. 4.3).

Aside from the round vacuolar forms, round granular forms were also commonly observed in clinical samples and in cultures (Tan, 2008; Zhang et al., 2012). Vdovenko (2000) observed that these forms can naturally arise from vacuolar forms possibly by environmental exposure or fixation artefact. A more recent study has also mentioned this phenomenon (Zhang et al., 2012). These findings were consistent among the 3 STs studied (Fig. 4.4 B). Nevertheless, cells that were more granular can also be found among viable cells. Analysis of the images suggests that there exist two populations of granular cells: true granular cells and those that are degenerating (Fig. 4.4 C) as reported previously (Clark et al., 2013; Vdovenko, 2000). In addition, granularity of these dying cells may be due more to environmental exposure rather than caused by fixation since the same proportion of granular forms have been observed in both fixed and unfixed samples.

The diameter of *Blastocystis* vacuolar forms have been estimated to be between 2 and 200 μm (Tan, 2008). A study (MacPherson and MacQueen, 1994) indicated that the diameter of 80.8% of the *Blastocystis* they observed fell between 5 and 15 μm . That study, however, was published before the genotyping era and so the particular ST of the isolate is unknown. Mirza et al. have previously reported differences in sizes between ST4 and ST7 isolates using flow cytometry (Huang et al., 1990). In that study, the diameter of

majority of *Blastocystis* cells after 48 hours of culture were 6 to 10 μm and 3 to 6 μm for ST7 and ST4 isolates, respectively. The calculations made for ST4 in this study mirrors that of the previous report. However, the measurement in this study for ST7 is smaller (Table 4.1). The previous study has determined the sizes indirectly using known-sized beads and set them as standards for the forward scatter channel values in flow cytometry. This study however makes use of actual images of the cells and converting the pixel measurements to micrometers. Using the present technique, it was possible to exclude the doublets from the measurement by confirming the arrangement using the images themselves. There might be bigger-sized cells depending on the type and age of samples as well the amount of initial inoculum. The analyses highlight the importance of taking into account the subtype used in any morphological studies. The size range of *Blastocystis* is not as wide as between 2 and 200 μm , but narrower when ST identity is established. In addition, it was possible to measure just the viable cells alone as the non-viable cells may feature degenerating cells and assume irregular shapes (Fig. 4.3).

Hoechst staining and the EDF setting of the imaging flow cytometer was used to analyze nuclear arrangement of viable *Blastocystis* cells. More than 80% of the population from the three subtypes studied featured 1-2 nuclei (Fig. 4.7) located at the edge of the cells. ST4-WR1 isolates all feature one or two nuclei (and not more). This reflected the previous observation (MacPherson and MacQueen, 1994) whereby 98.4% of the cells have a similar arrangement. This study therefore supported the classical representation of *Blastocystis*. More infrequently, in the other STs (1-2% in ST1 and 2-8% in ST7), other nuclear

features were observed. These cells either showed more than 2 nuclei or that the nucleic acid stain covered a large area of the cell (Fig. 4.8). The latter showed an apparent nucleic acid condensation which could represent cells about to undergo binary fission. Surprisingly, multinucleation have been identified only in round cells in these two subtypes. No evidence was found to support alternative modes of reproduction such as plasmotomy and budding in *Blastocystis* as suggested by others (Govind et al., 2002; Yamada and Yoshikawa, 2012; Zhang et al., 2012) since multinucleation was not observed in irregularly-shaped viable cells. Some of the multinucleated cells showed the nuclei located in the center of the cell with the size of the central vacuole diminished (as indicated by lower intensity of CFSE staining). If this was a reproductive stage, it may be an evidence of a multiple fission event in *Blastocystis* as suggested (Suresh et al., 1994). Small structures containing nucleic acid have also been observed. These structures were rare (2-4% of viable cells). They also do not appear to have vacuoles as indicated by low CFSE staining but consist mainly of nucleic acid material in its compartment. Experiments in this chapter did not determine whether these structures originate from bigger and multinucleated cells. It may also be possible that these represented starving cells or a state where *Blastocystis* sheds off its vacuole.

Finally, after morphological forms have been assessed for relevance, the method and data obtained were applied to LL-37-treated *Blastocystis* cells. LL-37, as determined from the previous chapters, caused lysis of *Blastocystis* cells. SEM images also showed deformation and breakage of cells. The imaging flow cytometry analyses also showed this phenomenon occurring in the parasite. The

advantage of this method from SEM was that whole populations of the organism can be analyzed. It was possible to evaluate the extent of the effect of LL-37 on *Blastocystis* cells in cultures and calculate the proportion of the cells being affected. The ability to observe the cells in this way also made it possible to evaluate the viability of *Blastocystis* using morphological changes alone. In addition, the imaging flow cytometry was also able to identify *Blastocystis* cells with bound LL-37 and determine their corresponding proportion in the population (Fig. 4.10). This was made possible using fluorescence-tagged specific antibodies. As the results showed, *Blastocystis* ST4-WR1 have higher proportion of cells bound with LL-37 compared with ST7-B when these two isolates were treated with the same peptide concentration (Fig. 4.10 B). This difference in LL-37 affinity in different surfaces of *Blastocystis* isolates may be associated with the differences in susceptibilities of the isolates to AMPs. As the peptides are attracted to negatively-charged surfaces, structures outside the *Blastocystis* cell membrane may modify these charges or make the membrane less exposed to AMPs. It would therefore be interesting to have a closer look on the surface coat of *Blastocystis* and its function in the survival of the parasite. Specifically, its ultrastructure and its residues need to be identified and characterized. These may provide clues on whether the coat can trap AMPs or decrease the affinity of the peptides with the *Blastocystis* membrane.

Chapter 5

Resistance Mechanisms of *Blastocystis* isolate B against LL-37

5.1 Introduction

Previous chapters have shown the broad activity of LL-37 on *Blastocystis*. However, the STs showed variations in their sensitivity to the peptide. *Blastocystis* isolate B which belongs to ST7 showed relative resistance to LL-37 compared to ST1 and ST4 isolates as shown in the IC₅₀ values and flow cytometry with PI staining data. In this chapter, the factors which contributes to the resistance of ST7-B isolate will be explored.

While developing resistance against AMPs is a rare phenomenon, several bacterial species possess the ability to mitigate the effects of AMP. In a review paper (Cole and Nizet, 2016), several of these factors were highlighted. Briefly, these factors include: modification of the surface charges to decrease binding affinity of AMPs; use of surface molecules to trap AMPs; secretion of proteases that can degrade AMPs; efflux systems that pumps out AMPs and prevent them from binding to intracellular targets; induction of regulatory networks that synergistically protects the bacteria from AMP attack, and; suppression of AMP expression. Since AMPs effect of unicellular eukaryotic parasites are few, only several of these factors have been investigated.

In this chapter, resistance factors of ST7-B isolate have been identified. Experiments made use of sensitive strains to present comparisons. *Blastocystis*, as a eukaryotic unicellular organism, possesses complex surface structure. It's known to secrete proteases which affects the immune responses. It is also

significantly bigger in size compared to prokaryotic organisms. These factors then could lessen the effects of AMPs particularly LL-37.

5.2 Materials and Methods

5.2.1 Parasite cultivation (see Chapter 2)

5.2.2 LL-37 degradation and viability assay

Blastocystis ST7-B and ST4-WR1 excretory-secretory products (ESPs) were harvested from 24-h cultures. The cultures were washed twice in serum-free IMDM. The cells were then incubated for 2 h in pre-reduced serum-free IMDM at 37°C in anaerobic conditions at 1×10^8 cells per ml of IMDM. Culture supernatants were then collected by centrifugation at $1,000 \times g$ for 10 min and filtered twice using 0.2 μm -pore filters (Millipore). *Blastocystis* secreted products were stored at -80°C until use. The effect of *Blastocystis* ESPs on peptide integrity was quantitatively determined by ELISA. Briefly, 50 μl of LL-37 at 2 $\mu\text{g}/\text{ml}$ concentration were coated onto each well in flat-bottom 96-well Nunc Maxisorp plates for 18 h at 4°C. Coated LL-37 were exposed for 2 h to *Blastocystis* ESPs alone or ESPs previously incubated for 6 h with 1 \times Halt protease inhibitor cocktail (BioRad) at 37°C. The wells were then washed with PBS and concentration of intact LL-37 were determined using ELISA outlined above. LL-37 peptide solution previously incubated with *Blastocystis* ESPs were also used for treatment of *Blastocystis* cultures. Viability was determined

using flow cytometry and PI-staining after treatment. Denatured ESPs were also used in this assay which entailed heating the ESPs for 15 min at 95°C.

5.2.3 pH adjustment of *Blastocystis* culture medium

Three sets of *Blastocystis* culture medium were prepared with different pH: 6.5, 7.1 and 8.0. The pH of the media were adjusted using 6N HCl or 6N NaOH. pH measurements were made using Beckman Coulter PHI 350 pH meter.

5.2.4 Transmission electron microscopy

24-h cultures of *Blastocystis* cells (1×10^7) were harvested, washed and treated with 100 µg/ml cationized ferritin (Sigma-Aldrich) for 2h. Cationized ferritin binds to negatively-charged surfaces (26). This was useful to visualize the surface coat of *Blastocystis* by providing better contrast and maintaining its integrity during the preparation of cells for electron microscopy. The cells were then fixed overnight at 4°C with 8% glutaraldehyde. The cells were then washed 3 times with PBS. Post-fixation included incubating the cells with 1% osmium tetroxide and 1% potassium ferrocyanide in PBS for 2 h. The cells were then washed 3 times. The cells were dehydrated with absolute ethanol 5 times. Embedding was done for 48 h using London resin white. The solidified blocks were sectioned, mounted and viewed using transmission electron microscope (Jeol JEM-1010).

5.3 Results

5.3.1 *Blastocystis* ST7-B secretes proteases that can degrade LL-37

A modified ELISA was used to determine if *Blastocystis* ESPs can degrade LL-37. ESPs from ST7-B and ST4-WR1 cultures were used to represent LL-37-resistant and LL-37-susceptible isolates, respectively. Absorbance of wells after incubation with ST7-B isolate's ESP was lower compared to ST4-WR1's (Fig. 5.1 A). This suggests that ST7-B isolates produce proteases that can degrade LL-37. This degradation was inhibited when ESPs were incubated with a protease cocktail inhibitor prior to the degradation assay. In addition, PI staining was also used to determine viability of *Blastocystis* after treatment with LL-37 previously incubated with ST7-B ESP (Fig. 5.1 B). The secreted proteases in ST7-B ESP inactivated LL-37 activity on *Blastocystis*. This however was reversed when ESP were previously heat-denatured before incubation with LL-37.

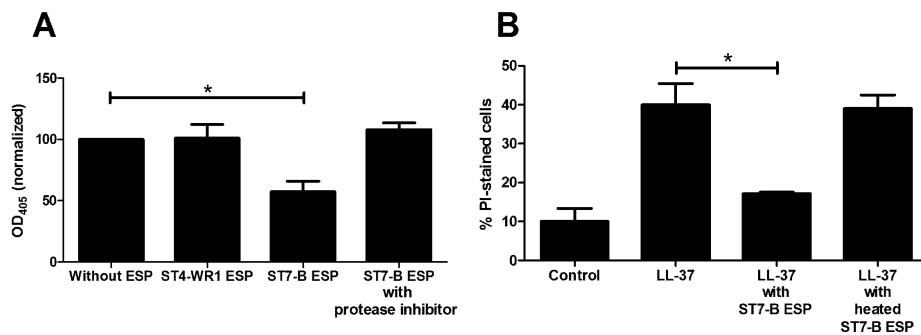


Fig. 5.1. *Blastocystis* ST7-B isolate (but not ST4-WR1) excreted-secreted products (ESP) degrade LL-37 as shown in ELISA results (A). LL-37 peptide was coated on ELISA plates and incubated with *Blastocystis* ESP for 2 h. Degradation was prevented when ST7-B ESP were incubated with a protease inhibitor cocktail prior to incubation with the peptide. Viability experiments were also done using LL-37 previously incubated with ST7-B ESP (B). Graph shows that ST7-B ESP attenuated LL-37 activity. This was reversed when ESP was first heated to denature proteins. *, $p < 0.05$.

5.3.2 *Blastocystis* ST7-B lowers the pH in culture and attenuates LL-37 activity

The pH of complete medium for *Blastocystis* were adjusted and used to determine if it has effect on the activity of LL-37 on *Blastocystis*. At pH 6.5, LL-37 had minimal effect on *Blastocystis* ST7-B and ST4-WR1 isolates with cell count at 90% and 88%, respectively, compared to untreated cultures. At pH 7.1, the relative resistance of ST7-B isolates was compared to ST4-WR1. Cell counts at this pH with LL-37 was 76% and 41% for ST7-B and ST4-WR1 isolates, respectively, normalized to untreated cultures. At pH 8.0, ST7-B and ST4-WR1 cell counts were 44% and 38%, respectively, of untreated cultures. At this pH, the highest level of activity of LL-37 was observed which negated the relative resistance of ST7-B isolate (Fig. 5.2 A). The pH of *Blastocystis* culture medium after 24 hours was also determined. *Blastocystis* ST7-B culture's average pH was 6.8 while ST-WR1 was 7.0 (Fig. 5.2 B).

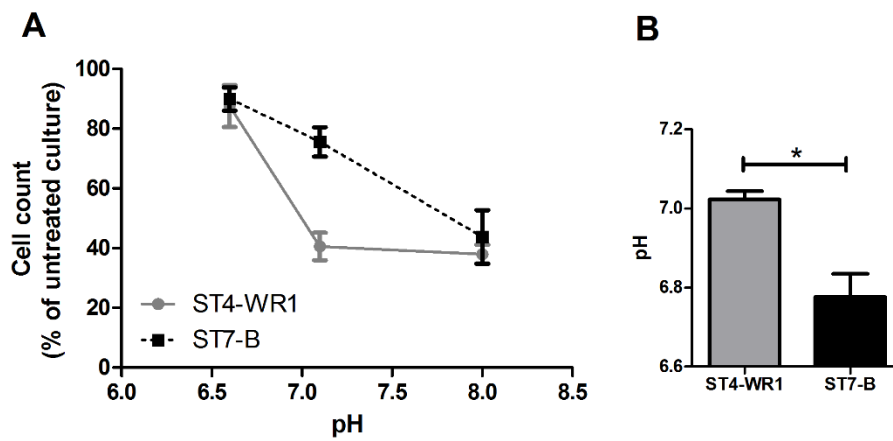


Fig. 5.2. pH affects the activity of LL-37 on *Blastocystis*. In acidic pH, LL-37 did not inhibit both *Blastocystis* STs (A) while at neutral and alkaline pH, both ST4-WR1 and ST7-B were inhibited by the AMP. *Blastocystis* ST7-B (but not ST4-WR1) cultures caused the medium to be acidic after 24 hrs (B). *, $p < 0.05$.

5.3.3 Surface coat of *Blastocystis*

India ink was used as negative stain to visualize the surface coat of *Blastocystis* cells. Most cells from ST7-B cultures showed thicker surface coats (Fig. 5.3 A-B). To observe the surface closely, transmission electron microscopy (TEM) was used. Cationized ferritin was used to label negatively-charged elements in the cell surface. Again, TEM showed a thicker surface coat for ST7-B cells compared to ST4-WR1 (Fig. 5.3 C-F). The coat's thickness in ST7-B isolates was almost three times than that of ST4-WR1 isolates (Fig. 5.3 G). Furthermore, ST7-B surface coats also appeared to be denser.

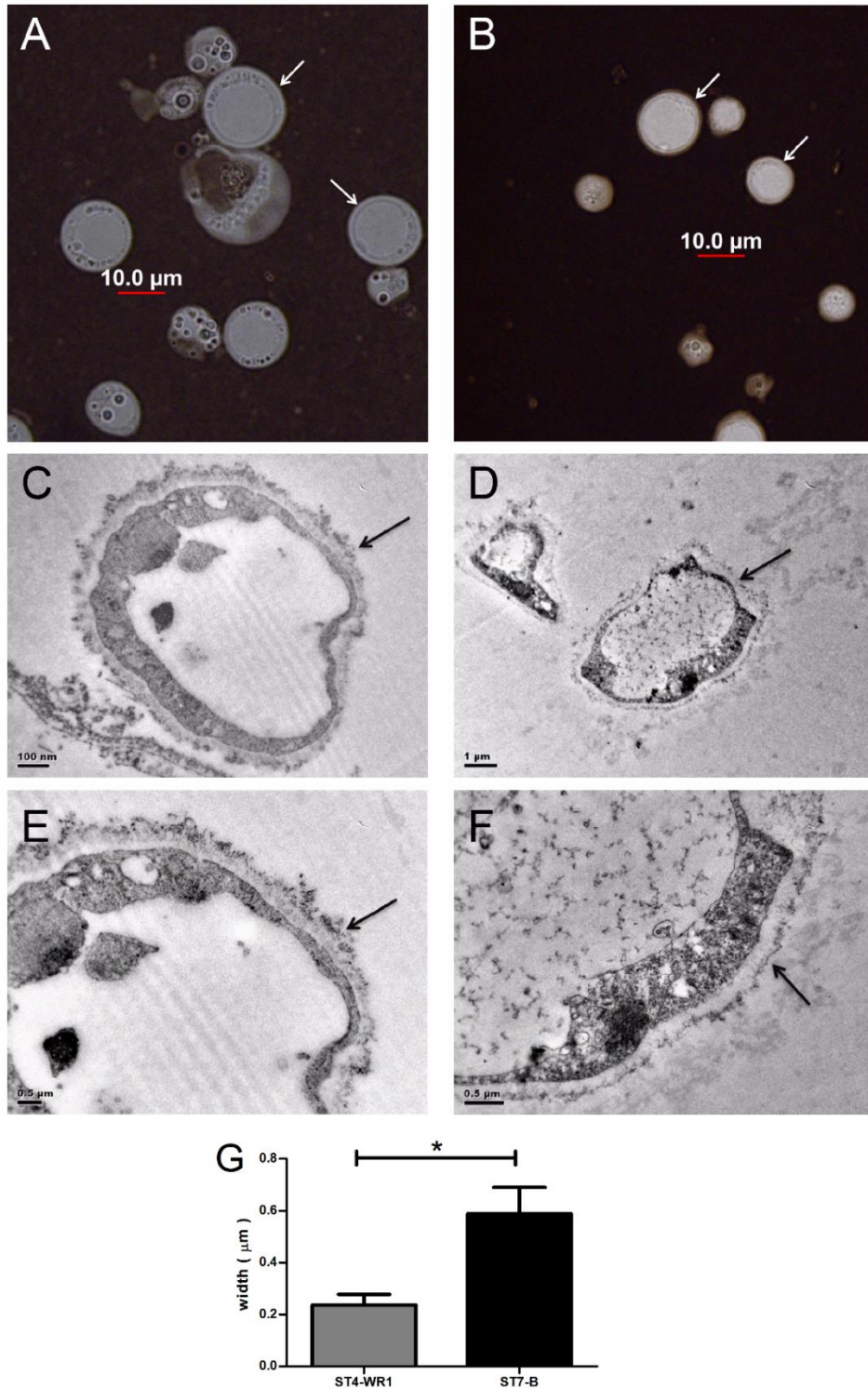


Fig. 5.3. *Blastocystis* ST7-B (A, C and E) isolates have thicker and denser surface coats (arrows) compared to ST4-WR1 (B, D and F) isolates as shown using India ink as a negative stain in bright microscope (A and B), and using transmission electron microscope (C, D, E and F). Images from TEM was used to measure the thickness of the surface coat. The surface coat of ST7-B isolate is more than double in thickness compared to ST4-WR1 isolate (G). *, $p < 0.05$.

5.4 Discussion

Blastocystis spp. constitute several isolates with significant biological differences. In the previous chapters, susceptibility assays showed that ST7 isolates B, C, E, G and H had higher IC₅₀ values for LL-37 compared to both ST1 and ST4 isolates. Expectedly, a representative isolate of ST7 (B), required higher concentration of LL-37 to reach the same proportion as with ST4-WR1 in PI-staining. These indicate some resistant factors are present in ST7 isolates. *Blastocystis* is known to secrete proteases. Particularly for ST7-B, its lysates were found to have high protease activities (Sio et al., 2006). In another study, proteases from ST7-B isolate were specifically able to degrade IgA (Puthia et al., 2005). Interestingly, ST4-WR1 isolate also contain proteases which have the same activity. Other studies on proteases of *Blastocystis* focused on their link in cell-death pathways and inflammatory responses (Lim et al., 2014; Puthia et al., 2008; Yin et al., 2010). The two identified proteases in *Blastocystis*, cathepsin B and legumain, were found to act on intestinal epithelial cells which links them to gut disorder (Wawrzyniak et al., 2012). In this study, secreted proteases from *Blastocystis* ST7-B isolate was found to degrade LL-37. Secreted proteases from ST4-WR1 isolate did not have this activity. It would be interesting to investigate on whether the two known *Blastocystis* proteases affect LL-37 activity. LL-37 can be degraded by proteases expressed by some pathogenic bacteria (Schmidtchen et al., 2002). *Staphylococcus aureus*, for example, secretes two different proteases that can cleave L-37 at different positions (Sieprawska-Lupa et al., 2004). Metalloproteases of *Bacillus anthracis* could also degrade the peptide, but these resistant factors are not

present in other *Bacillus* spp. (Thwaite et al., 2006). For another intestinal eukaryotic parasite, *E. histolytica*, a cysteine protease can also be produced that can degrade LL-37 (Cobo et al., 2012). In this study, the proteases present in *Blastocystis* secreted products could inactivate LL-37. This, however, was only present in a ST7 isolate and not in ST4 isolate. This partly explains why ST7 is relatively resistant to LL-37 compared to the other STs.

LL-37's antimicrobial activity is dependent on its conformation in solution (Johansson et al., 1998). This, in turn, is dependent on temperature, salt concentration and pH. Below pH 5, there is a decrease in helical structure. On the other hand, LL-37 helical structure is maintained at basic pH, even up to pH 13. This was further proven in a study in which at pH 6.8, the killing of *Staphylococcus aureus* and *Pseudomonas aeruginosa* was mitigated (Alaiwa et al., 2014). In this study, the effect of acidic pH on LL-37's activity on *Blastocystis* was investigated. After 24 hr, the pH of culture medium became acidic for ST7-B isolate, while it stayed neutral for ST4-WR1 (Fig. 5.2 B). The acidic medium in the former was enough to attenuate LL-37 activity. However, when the culture medium was adjusted to basic pH, even ST7-B cells became susceptible to LL-37 at an equal proportion as observed in ST4-WR1 populations. In physiological setting, the low cell number of *Blastocystis* may not be enough to affect the pH of the colon. However, this could still be a factor in AMP resistance when the microenvironment of *Blastocystis* colony is considered. The surface coat also may trap or at least slow down the binding of AMPs to the membrane. If this happens, the acidic pH in the microenvironment

could then attenuate AMP activity by, for examples, changing the peptide's structure.

Blastocystis has been known to possess a surface coat that covers the plasma membrane and is composed of polysaccharide residues (Lanuza et al., 1996; Zaman et al., 1999). As mentioned, the presence of structures outside the bacterial membrane could provide resistance to the organism from AMP killing. Bacterial capsules have been found to protect bacteria from LL-37 and other helical AMPs (Cole and Nizet, 2016). The sugar structures trap AMPs and prevent them from interacting with the bacterial membrane. Or they could decrease the affinity of the membrane to AMP binding by modifying the net charge (Peschel and Sahl, 2006). Some elements in these capsules also have more activity. For example, Group A *Streptococcus* has M1 protein that traps and inactivates LL-37. Furthermore, this protein prevents maturation of LL-37 by binding to cathelicidin (LaRock et al., 2015).

Blastocystis' surface coat could possibly be a resistant factor for the parasite to lessen LL-37 activity. Analyses of the parasite's coat by India ink staining and TEM indicate that ST7-B's has thicker and denser coat compared to ST4-WR1 isolate (Fig. 5.3). Imaging flow cytometry also revealed that LL-37 has higher affinity to the surface of ST4-WR1. In addition, for the *Blastocystis* cells with attached LL-37, ST4-WR1 cells had higher proportion of dead cells (Fig. 4.10 C). A possible explanation would be that the thicker surface coat of ST7-B cells could trap more LL-37 and prevent it from interacting with the surface.

Chapter 6

Blastocystis-Mediated Modulation of LL-37 Expression in Intestinal Epithelial Cells

6.1 Introduction

The previous chapters discussed the effects of LL-37 on *Blastocystis* isolates. This chapter focused on the modulation of the peptide's expression by *Blastocystis*. This chapter aimed to complete the picture of the role of AMP in *Blastocystis* infections in the context of host-pathogen interactions. Most AMPs including cathelicidin/LL-37 have upregulated expression during inflammation and infection of the colon (Ho et al., 2013). LL-37 and other AMPs are secreted by epithelial cells to maintain homeostasis in the gut physiology. LL-37, like other AMPs have other downstream immune functions aside from being solely and directly antimicrobial. They can recruit other cells, provide stronger antigen presentation, activate regulatory networks and stimulate cytokine production (Jäger et al., 2013; Ostaff et al., 2013). The modulation of AMP expression by an invading pathogen is therefore relevant as this may provide additional information to explain the outcome of the infection.

LL-37 production is modulated in many ways. As a response to endoplasmic reticulum stress, sphingosine-1-phosphate is produced leading towards cathelicidin expression through NF- κ B pathway (Park et al., 2011, 2013). The vitamin D pathway in the induction of cathelicidin expression is also extensively studied as the peptide is important in skin diseases (Liu et al., 2007; Schaubert and Gallo, 2008). However, ligands that signal cathelicidin expression in keratinocytes may not have the same effect in colonocytes (Peric et al., 2009). In the intestines, normal microbiota is among the factors responsible for basal AMP presence (Verdu et al., 2015). Cathelicidin gene expression was also

stimulated by LPS (Wu et al., 2000). Cell differentiation stimulated by short chain fatty acids also lead to increased cathelicidin production (Hase et al., 2002; Schaubert et al., 2003). Several bacterial species can induce cathelicidin production in the intestines such as *Salmonella enterica*, invasive *E. coli* and *Mycobacterium tuberculosis* (Hase et al., 2002; Rivas-Santiago et al., 2008; Wu et al., 2000). On the other hand, several bacterial products could downregulate cathelicidin expression. For example, cholera toxins from *Vibrio* have this effect on intestinal epithelial cells.

The fact that LL-37 and other AMPs' expression could be stimulated has led to further studies exploring on whether induction of their expression can resolve or alleviate known diseases (Agerberth et al., 2013). In *Blastocystis* infections, this could be relevant as the experiments discussed in previous chapters show the efficacy of LL-37 in killing the parasite. In this chapter, the gene expression modulated by *Blastocystis* in mouse intestinal explants and human intestinal epithelial cells were determined. LL-37 production and secretion inside the cell and in culture supernatant were also investigated.

6.2 Materials and Methods

6.2.1 Mouse intestinal explants exposure to *Blastocystis*

Mouse experiments were done by Dr. Sitara Rao Ajjampur. C57BL/6 mice were obtained from NUS and housed in an animal biosafety level 2 facility. Mice (7-9 wk old) were euthanized by CO₂ inhalation. The intestinal tract was dissected

out and placed in 50 ml tubes with complete media comprising of Dulbecco's modified Eagle's medium (HyClone) supplemented with 10% heat-inactivated fetal bovine serum and 1% each of sodium pyruvate and MEM and penicillin-streptomycin (Gibco) at final concentrations of 2,000 units/mL each of the antibiotics. The tissue was then dissected into segments of distal colon, proximal colon, caecum and terminal ileum, opened along the mesenteric edge and intestinal contents removed. The segments were washed gently in cold penicillin-streptomycin and cut into bits measuring 1.5 cm × 1 cm. The explants were affixed onto 2% agarose layers in 6 well plates with the serosal surface facing down in pre-warmed complete media with penicillin-streptomycin (Gibco). Explants were incubated with 5×10^7 live *Blastocystis* ST7-B parasites for 1 h at 37°C. For all assays, more than one litter was used in order to avoid any litter-specific effects. After incubation, the explants were frozen in Trizol (Invitrogen) at -80°C till further processing. The animal experiments were performed in accordance with the Singapore National Advisory Committee for Laboratory Animal Research guidelines. The protocol (R13-5890) was reviewed and approved by the NUS Institutional Animal Care and Use Committee.

6.2.2 Co-culture of *Blastocystis* with HT-29 intestinal epithelial cells

HT-29 epithelial cells were used to study whether *Blastocystis* parasites affect the expression of LL-37 in host cells. Cells were maintained in T-75 flasks (Corning) in humidified incubator with 5% CO₂ at 37°C. Complete culture medium consisted of 10% heat-inactivated fetal bovine serum (Gibco), 1% each

sodium pyruvate (Gibco), non-essential amino acids (Gibco) and penicillin-streptomycin in Dulbecco's modified Eagle's medium (DMEM) (ThermoScientific). Cells were seeded onto 6-well plates (Greiner) using complete medium. After reaching confluency, HT-29 cells were incubated for 48 h with serum-free media supplemented with 3mM sodium butyrate (Sigma-Aldrich). HT-29 cells were then co-cultured with *Blastocystis* cells at 10 MOI (multiplicity of infection) for 1 h. Culture supernatant were collected and set aside for determination of LL-37 secretion. The viability of HT-29 cells after co-culture were determined using trypan-blue exclusion assay.

6.2.3 Quantitative real-time PCR (qRT-PCR)

Induction of cathelicidin-related antimicrobial peptide (CRAMP) gene expression on mouse intestinal explants and CAMP gene on HT-29 cells were determined after exposure to *Blastocystis*. Mouse explants in Trizol were homogenized with ZrO beads in a tissue homogenizer (WisBioMed) and RNA extracted from homogenates using the Trizol method followed by further purification with the nucleospin RNA kit (Machery Nagel). HT-29 cells were homogenized and lyzed with RNazol (Molecular Research Center). Total RNA was extracted following the manufacturer's protocol. Synthesis of cDNA was done using iScript cDNA synthesis kit (Bio-Rad) with 1µg of RNA sample in iCycler (Bio-Rad) thermocycler using the suggested protocol. qRT-PCR was then performed using iTaq Universal SYBR Green Supermix kit (Bio-Rad), 1µl of cDNA and 500nM each of primers (Sigma-Aldrich): CRAMP-F: 5'-TTT TGA CAT CAG CTG TAA CG-3' and CRAMP-R: 5'-GCT TTT CAC CAA

TCT TCT CC-3' for mouse samples; CAMP-F: 5'-AGT GAA GGA GAC TGT ATG TG-3' and CAMP-R: 5'-ATT TTC TTG AAC CGA AAG GG-3' for HT-29 samples. Mouse beta-actin (mBA-F: 5'-GAT GTA TGA AGG CTT TGG TC-3' and mBA-R: 5'-TGT GCA CTT TTA TTG GTC TC-3') and human glyceraldehyde 3-phosphate dehydrogenase (GAPdH) (hGAPdH-F: 5'-CTT TTG CGT CGC CAG-3' and hGAPdH-R: 5'-TTG ATG GCA ACA ATA TCC AC-3') genes were used as endogenous controls. Gene expression analysis was done using iQ5 v2.1 software (Bio-Rad) which uses the $2^{-\Delta\Delta C_t}$ method.

6.2.4 LL-37 secretion assay

To quantitatively determine LL-37 secretion in HT-29 cells, supernatant (100 μ l) from co-culture with *Blastocystis* were used to coat flat-bottom 96-well Maxisorp plates (Nunc) for 18 h at 4°C. Excess supernatant was disposed and LL-37 peptide concentration was determined using an enzyme-linked immunosorbent assay (ELISA). The plates were washed 3 times using PBS with 0.05% Tween-20 (PBS-T) wash buffer and blocked with 1% bovine serum albumin (BSA) (Santa Cruz Biotechnology) for 2 h at 25°C. LL-37 were probed with 1:5000 rabbit polyclonal anti-LL37 human IgG antibody (Abcam) in blocking solution. After 1 h, the wells were washed 4 times with PBS-T. 1:1000 goat polyclonal secondary antibody to rabbit IgG HRP-conjugated antibody (Abcam) in blocking solution was added and incubated for 25°C. After 1 h, the wells were washed 4 times with PBS-T. The wells were then incubated with substrate 2,2'-Azinobis [3-ethylbenzothiazoline-6-sulfonic acid] (ABTS)

(Sigma-Aldrich) for 5-10 min. Absorbance was read at 492 nm using Tecan Infinite F200 microplate reader.

6.2.5 Fluorescence microscopy

To visualize expression of LL-37 in HT-29 cells, a fluorescence microscopy assay was used. HT-29 cells were grown to confluency in 24-well cell culture plates (Greiner) with poly-L-lysine treated glass coverslips. The complete medium was then replaced with 3mM sodium butyrate in serum-free medium. After 48 h, co-cultivation with *Blastocystis* ST1-NUH9, ST4-WR1 and ST7-B at 10 MOI for 1 h was done. HT-29 cells were then washed with PBS and fixed with absolute methanol for 15 min at -20°C. The cells were then washed with PBS and blocked with 5% normal goat serum in PBS for 2 h. LL-37 was probed using 1:500 rabbit polyclonal anti-LL37 human IgG antibody (Abcam) in blocking solution overnight at 4°C. After washing 3 times for 5 min each with PBS-T, incubation was done with 1:1000 goat polyclonal secondary antibody to rabbit IgG FITC-conjugated antibody (Abcam) in blocking solution for 1 h at 25°C. The cells were then washed 3 times. The glass coverslips were then mounted using Vectashield mounting medium and examined using Olympus BX60 fluorescence microscope. Total cell fluorescence was quantified using ImageJ software version 1.48 (NIH).

6.3 Results

6.3.1 *Blastocystis* induces cathelicidin expression and secretion

Increase in cathelicidin mRNA was detected in mouse intestinal explants and HT-29 human intestinal epithelial cells. Mouse intestinal samples were sectioned into terminal ileum, caecum, proximal colon and distal colon sections and subsequently inoculated with *Blastocystis* ST7-B cells. qRT-PCR analysis showed that mouse distal colon explants showed a net upregulation of CRAMP gene when exposed to the parasite (Fig. 6.1 A). HT-29 cells also showed upregulation of cathelicidin gene expression when co-incubated with *Blastocystis* ST1-NUH9, ST4-WR1 and ST7-B isolates (Fig. 6.1 B). ELISA results showed an increase in cathelicidin in HT-29 culture supernatant when incubated with *Blastocystis* (Fig. 6.1 C). At equal multiplicity of infection (MOI), ST1-NUH9 showed the highest induction, followed by ST7-B and ST4-WR1 isolates. HT-29 cells 95% viability in all the wells and no significant difference in viability was found between cells with parasite and those without (Fig. 6.2). Viability of HT-29 cells was checked using Trypan-blue exclusion assay to confirm that the peptide present in the supernatant is not due to dying cells (Fig. 6.2). Fluorescence microscopy also showed increase in FITC-staining of HT-29 cells when incubated with *Blastocystis* (Fig. 6.3). The specificity of the antibody used to detect LL-37 peptide was confirmed by flow cytometry (Fig. 6.4).

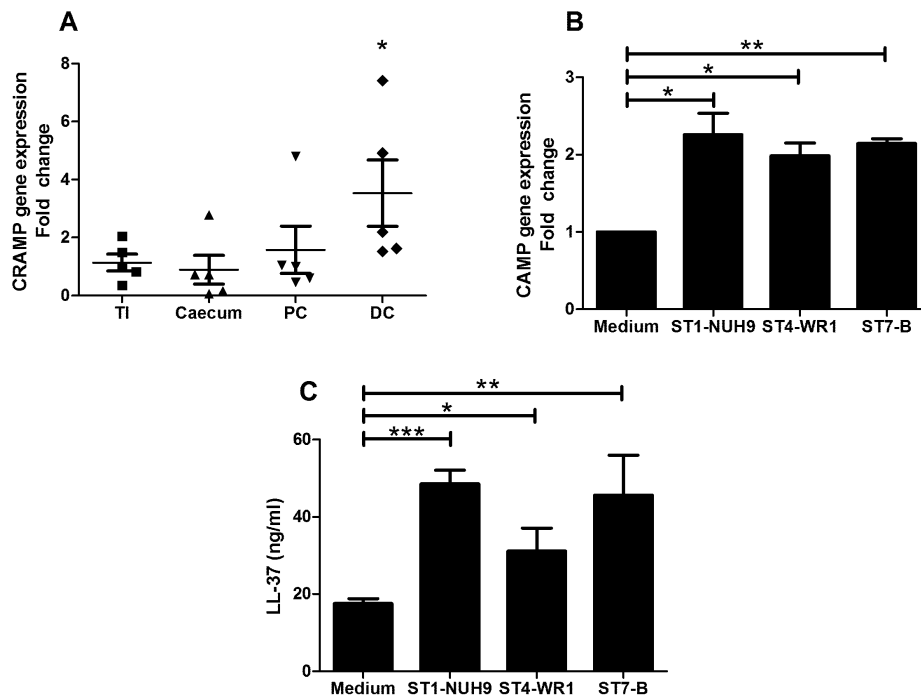


Fig. 6.1. *Blastocystis* induces LL-37 expression in mouse distal colon explants and HT-29 colonic epithelial cells. Intestines from five mice were externalized and partitioned into terminal ileum (TI), caecum, proximal colon (PC) and distal colon (DC) (A). These segments were exposed to *Blastocystis* ST7-B isolates for 1 h. CRAMP gene expression was determined using qRT-PCR. Distal colon explants showed significant upregulation of CRAMP gene. Three *Blastocystis* isolates (NUH9, WR1 and B) representing three STs (1, 4 and 7, respectively) also induced CAMP gene expression in confluent HT-29 cells after 30 min of co-incubation at 10 MOI (B). Supernatant from the co-culture showed significant increase in LL-37 content after 1 h of co-incubation as determined by ELISA (C). *, $p < 0.05$; **, $p < 0.001$; ***, $p < 0.0001$.

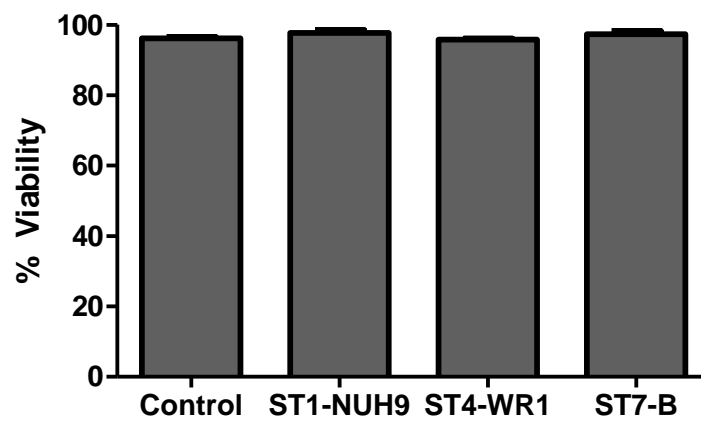


Fig. 6.2. Trypan-blue exclusion assay was used to determine viability of HT-29 cells after co-incubation with *Blastocystis*. No significant differences were found between the viability of the cells with or without the presence of the parasite.

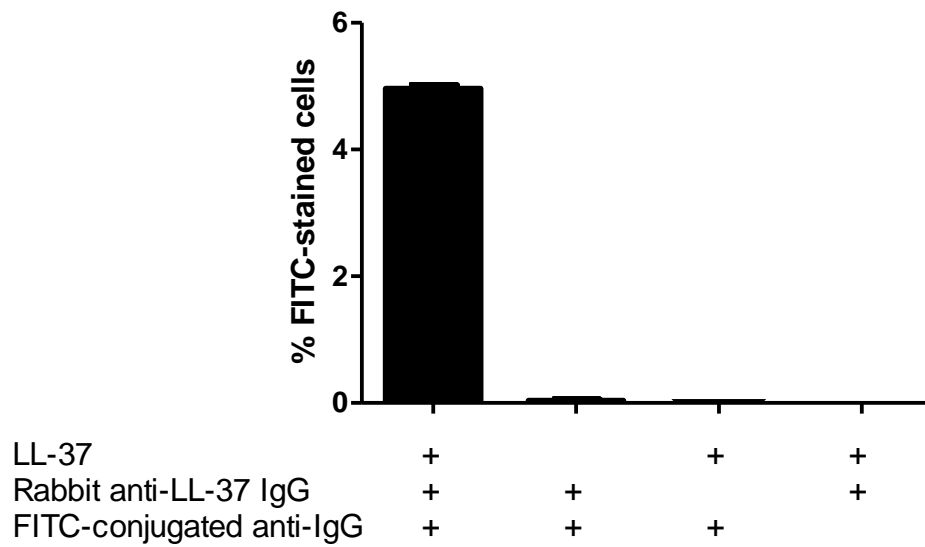


Fig. 6.3. Flow cytometry was used to demonstrate the specificity of anti-LL-37 antibody used in ELISA, fluorescence microscopy and imaging flow cytometry experiments. The graph shows FITC-staining of *Blastocystis* treated or untreated with 10 $\mu\text{g/ml}$ LL-37, with or without the presence of either one of the antibodies. Only cells treated with LL-37 and with the two antibodies present showed fluorescence.

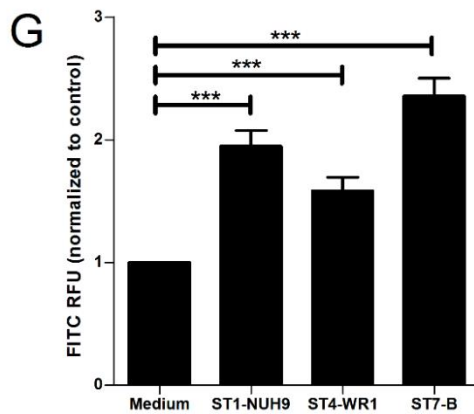
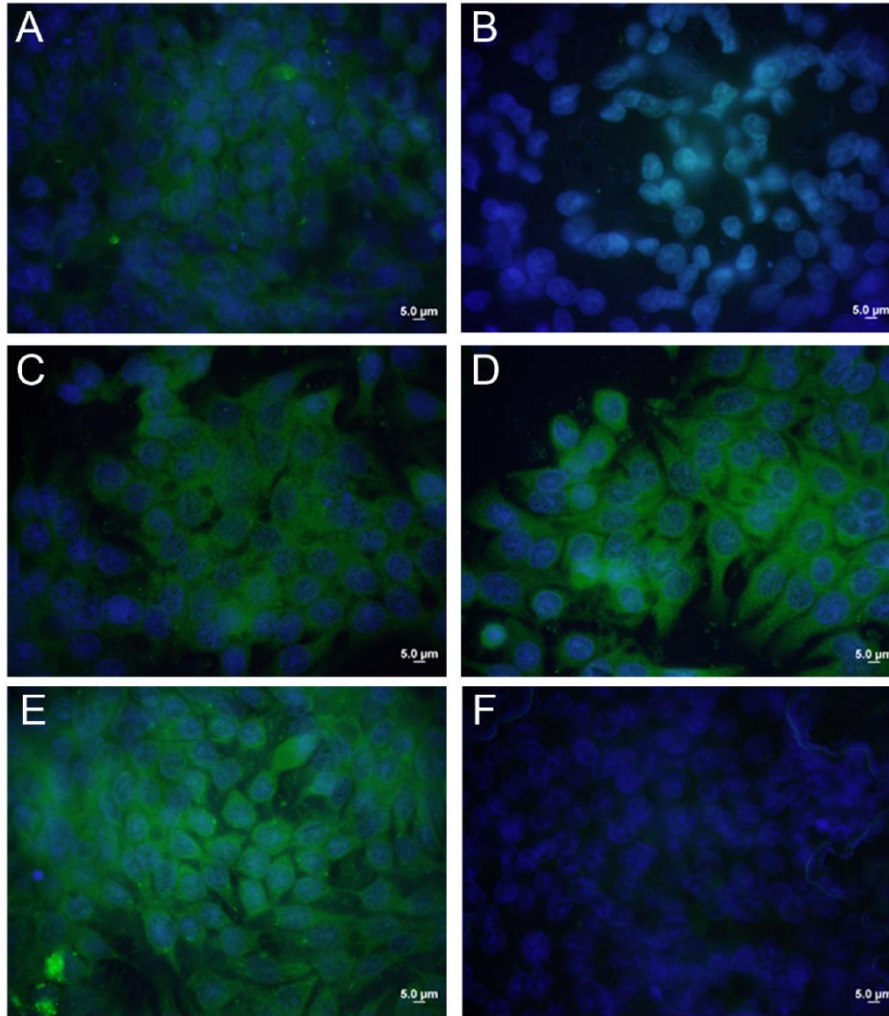


Fig. 6.4. Confluent HT-29 cells in monolayer increase production of cathelicidin after incubation with *Blastocystis*. Immunofluorescence assay images showed a basal level of cathelicidin production in differentiated HT-29 cells (A) but absent in undifferentiated cells (B). Differentiated HT-29 cells incubated with *Blastocystis* ST1-NUH9 (C), ST4-WR1 (D) and ST7-B (E) showed brighter fluorescence after 1 h co-incubation at 10 MOI. Negative control (F). Total fluorescence units were quantified using ImageJ software (G). ***, $p < 0.0001$.

6.4 Discussion

The experiments conducted in this chapter showed that *Blastocystis* upregulated LL-37 expression and secretion in intestinal epithelial cells. This was seen in other gastro-intestinal infections of protozoan parasites such as *Entamoeba* (Cobo et al., 2012) and *Cryptosporidium* (Huang et al., 1990). In the mouse model, the *Blastocystis* ST7-B isolates could induce mouse intestinal cells to express CRAMP genes, the homologue of human cathelicidin in mice. However, this upregulation was only seen in the distal colon of mice. This is relevant since *Blastocystis* is known to specifically colonize the large intestine in humans (Ajjampur and Tan, 2016). In the *in vitro* model using HT-29 cells, all *Blastocystis* isolates representing 3 STs could upregulate LL-37 gene expression, peptide production and secretion inside and outside the cell, respectively. The level of expression varied, however, from one isolate to another. This possibly contributed to the differences in symptomatology and pathogenesis in *Blastocystis* infections as reported in other studies (Casero et al., 2015; Das et al., 2016; Safadi et al., 2013).

That *Blastocystis* could upregulate LL-37 in intestinal cells was also relevant for another reason. The induction of AMPs can be used as indicator of a disease state. In a study comparing the concentration of human beta-defensin 2 levels in fecal samples from ulcerative colitis and irritable bowel syndrome patients and healthy controls, the latter had significantly lower level compared to the first two (Langhorst et al., 2007). While this study sought to detect only LL-37, it is probable that other AMPs could be upregulated as well. The modulation of

AMPs by *Blastocystis* could therefore contribute to the elucidation of pathogenesis of the parasite. LL-37 and other AMPs are elements of the innate immunity. *Blastocystis* induces a slight nitric oxide (NO) production in epithelial cells as reported (Mirza et al., 2011a). But this phenomenon is only observed in ST4-WR1 isolate. In contrast, ST7-B isolate downregulates NO production by inhibiting expression of nitric oxide synthase. In this light, it appears that host immune responses during *Blastocystis* infections are a complex array of events which depends on the ST of the parasite.

The concentration of induced LL-37 in the culture supernatant is at nanogram level (<100 ng/ml). This is consistent with the estimated concentration of LL-37 (or β -defensins) at mucosal sites which is less than 2 μ g/ml (Lai and Gallo, 2009). At this concentration, complete lysis of the parasite's population may not occur. However, AMPs are known to act synergistically (Alaiwa et al., 2014; Guo et al., 2013; Yu et al., 2016). It is probable that a lower LL-37 concentration is needed to control the parasite when the peptide is combined with other AMPs. There is also the presence of the mucus layer to consider. This structure covering the epithelial cells may act to concentrate AMPs in certain areas in the intestines.

Chapter 7

General Discussion and Conclusions

7.1 General Discussion

This research study sought to explore the role of AMPs and its effects on *Blastocystis* in the context of host-pathogen interactions. AMPs are diverse molecules found across different types of organisms. Some are endogenous to the host and fulfill several functions including direct killing of the pathogens. AMPs' binding to targets is not dependent of conformation but by electrostatic attraction. The pathogen's ability to develop resistance factors against them are generally non-existent (Ho et al., 2013; Li et al., 2012; Wang, 2014). These points make it attractive to use AMPs as antibiotics or at least utilize the AMP's structure as a template to design new drugs (Fjell et al., 2012; Peters et al., 2010). The importance of AMPs in innate immunity of multicellular organisms is now well established. Since the 1980's many AMPs from different organisms have been characterized and tested for a variety of functions especially on their antibacterial properties (Zasloff, 2016). Despite these advances, knowledge on the roles of AMPs in parasitic infections remains scant. In a list of thirty seven well-studied AMPs arranged by date of discovery, only 7 have been found to have anti-parasitic activities (Wang, 2014). One reason for this could be that very few studies are done to investigate the effect of AMPs on parasites. The results in this present study therefore contributes significantly to establishing the critical role of specific AMPs in a parasitic infection. In this study, LL-37, and endogenous AMP in human colon, was found to be effective in growth inhibition of *Blastocystis* across different STs. LL-37 has been found to kill other protozoan parasites (Scott et al., 2002). It had a deleterious effect on *E. histolytica* trophozoites at 10-50 μM concentration (Rico-Mata et al., 2013)

although the parasite could produce cysteine proteases that degrade the peptide (Cobo et al., 2012). But these kinds of studies are infrequent compared to other investigations involving bacteria considering that parasitic infections are still a burden in many countries. This study therefore contributes to this dearth of information with the inclusion of *Blastocystis* as a LL-37-susceptible eukaryotic parasite. The other set of AMPs tested on *Blastocystis* are the β -defensins. These peptides, in contrast to LL37, showed little or no direct effects on *Blastocystis*. Results in this study however could not completely dismiss the significance of these peptides in *Blastocystis* infections. In physiological setting, these peptides may still be significant as additive and synergistic activities of endogenous AMPs have been reported (Yu et al., 2016).

LL-37 inhibited the growth of *Blastocystis* but this effect varied between STs as indicated by different IC₅₀ values of the peptide on different *Blastocystis* isolates (Table 2.1). This variation in sensitivity of *Blastocystis* STs to LL-37 had been further investigated looking at membrane permeabilization with brightfield microscopy, scanning electron microscopy and flow cytometry. Again, a ST7 isolate showed that it is less affected by LL-37 compared to isolates from ST1 and ST4 as shown by flow cytometry with PI-staining. It also took a longer time to disrupt the membrane of ST7-B isolate compared to other isolates from different STs. LL-37-induced surface disruption correlated with the shape change happening in *Blastocystis* as more cells from ST1 and ST4 populations became more irregular in shape compared to ST7 (Fig. 4.9). During these investigations, there was an opportunity to resolve unknown status of several *Blastocystis* morphological forms. The imaging flow cytometry results in this

study indicated that some of these forms may not have biological or reproductive significance at all. For example, amoeboid forms were thought to be budding cells undergoing an alternative mode of reproduction (Yamada and Yoshikawa, 2012). The findings in this study could not verify this. However, the cytometry data indicated that most of these amoeboid cells are dying cells. The application of high-content imaging cytometry contributed to a better understanding of *Blastocystis* biology.

Aside from drug or host defense factors sensitivity, the pathogenicity of *Blastocystis* and corresponding host immune responses also need to be elucidated. It is known that *Blastocystis* colonizes the large intestines (Ajjampur et al., 2016) but specific events leading to the survival and colonization of the parasite still needs to be identified. With regard to innate immune response against *Blastocystis*, only one related study has been published which discussed the role of nitric oxide, an element of innate immunity, in *Blastocystis* infections (Mirza et al., 2011a). Results in this present study further added to the cellular events that occur when the parasite interacts with intestinal epithelial cells. Co-culture experiments showed that *Blastocystis* stimulates additional LL-37 secretion. However, LL-37 potency varied and can only be applied to ST1 and ST4 isolates. This meant that *Blastocystis* ST7 isolates could be more pathogenic by virtue of its ability to evade the first line of host defense including AMPs. Several other studies have already pointed the greater pathogenic potential of *Blastocystis* ST7 isolates. A clinical case could also be linked to this phenomenon as *Blastocystis* ST7-B isolate has been isolated from a symptomatic patient (Ho et al., 1993). These isolates are more adhesive, capable

of compromising the intestinal barrier and impedes nitric oxide production, which is not the case compared to isolates from different STs (Mirza et al., 2011a; Wu et al., 2014). The relative resistance of ST7 isolates against LL-37 is therefore an additional factor to the pathogenic potential of these isolates. The fact that *Blastocystis* ST7 isolates can withstand the presence of LL-37 (and probably other endogenous AMPs) while others could not, further differentiate it from other *Blastocystis* STs. The added value of the findings in this study was that several isolates of different STs have been used. This is significant since *Blastocystis* is a species complex and many studies indicate that one observation in one isolate may not necessarily be the case in another isolate of another ST (Tan, 2008; Teo et al., 2014).

The factors that are responsible for *Blastocystis* ST7 isolates' relative resistance to LL-37 were investigated. The starting point in this particular study was how some species of bacteria evade or negate the effect of AMPs particularly LL-37. Experiments in the present showed that some of these factors are also observed in a *Blastocystis* ST7 isolate. For example, ST7-B cells produced excretory-secretory products that contain proteases. These proteases were then able to degrade LL-37. The specificity of these proteases was not investigated but it is possible that these could have broad effects on different AMPs secreted by the host. Further studies could also focus on whether these proteases are induced or these are constitutively secreted by the parasite. Another interesting observation was the ability of *Blastocystis* to produce an acidic environment that attenuated LL-37 activity. This occurrence was only observed in a ST7 isolate. This suggests therefore an innate ability of this particular ST to

counteract LL-37 attack. As many AMPs are also sensitive to pH changes, this could mean that *Blastocystis* ST7 elimination could require more potent host factors. The presence of a surface coat in *Blastocystis* has also been studied specifically on its role in protecting the parasite from AMPs. The exact construction of this outer coat is still unknown. There have been sugar residues identified (Lanuza et al., 1996) but their role in the parasite's survival and infectivity had not been determined. In this study, the surface coat has been visualized and measured. Fluorescence-antibody tagging of the surface coat showed that it did not totally eliminate the affinity of LL-37 to the parasite's membrane. However, it may be possible that it could at least diminish the attraction of the peptide since the thickness of the surface coat correlates with the degree of saturation of LL-37 binding (Fig. 4.10 and 5.3). Aside from these factors, others may be involved as well in protecting the parasite from AMPs and other elements of innate immunity. For example, efflux systems present in some bacteria (Cole and Nizet, 2016), may also be present in some *Blastocystis* isolates. Sequestration of LL-37 by M1 proteins expressed on the surface of bacteria has been observed (LaRock et al., 2015). It would be interesting know if these proteins are also expressed in the surface coat of *Blastocystis*.

All *Blastocystis* STs used in co-culture with intestinal epithelial cells have been able to upregulate LL-37 expression and secretion in the host cells (Fig. 6.1, 6.4 and 6.5). The stimulation for LL-37 expression was also rapid, occurring within 30 minutes in terms of gene expression and within an hour in terms of secretion outside the cell. This suggests that AMPs in general are one of the immediate host responses triggered in the presence of a *Blastocystis* infection. The amount

of LL-37 however was not enough to significantly inhibit *Blastocystis* (Fig. 6.1 C). Nevertheless, the physiological concentration of the peptide may be more concentrated within the mucus layer. The synergistic effect of AMPs could also be considered and perhaps these and other factors may be sufficient to eliminate the parasite despite the low levels of induced LL-37 seen in cell culture studies. Furthermore, the concentration of the peptide in physiological setting is still unknown and would be difficult to estimate. This would probably require more sensitive measurements in clinical samples.

The ability of *Blastocystis* to stimulate LL-37 secretion in the host is a significant event not only because it could affect the parasite directly but also because it could result into an array of downstream host immune responses. While AMPs are elements of innate immunity, their functions go beyond it by serving as bridges to adaptive immunity (Scott et al., 2002). LL-37, for example, upregulates cytokines which includes interleukin (IL)-17A, IL-8 and interferon gamma (IFN γ) (Vandamme et al., 2012). On the other hand, *Blastocystis* were also observed to stimulate production of cytokines such as IL-8 and granulocyte-macrophage colony stimulating factor. It would be interesting to know whether these cytokines production is a direct result of the parasite's stimulation or mediated by LL-37. If it is the latter, then AMPs, and LL-37 in particular, do have an important role in combatting invasion by being a necessary mediator so that the adaptive immune response could proceed in case of infection.

Intestinal unicellular parasites have been reported to cause agitation in normal gut microbiota. And perturbation of microbiome results in pathologies (Collins, 2014; Flint et al., 2012). *Cryptosporidium*, for example, damages the intestinal epithelium which then affects the microbiome populations (Ras et al., 2015). Another intestinal protistan parasite, *Giardia*, has been shown to disrupt microbiota biofilms in mice leading to pathophysiology (Beatty et al., 2013). *Blastocystis* has also been found to cause changes in the members in microbiota. In a study of patients with IBS, the presence of *Blastocystis* had a negative correlation with the presence of *Bifidobacterium* sp., which is considered a probiotic. Another study reported on the association of the parasite with increased diversity of bacterial microbiota in the human gut (Audebert et al., 2016). This means that *Blastocystis* could be considered as a factor that promotes healthy gut and prevents dysbiosis. Although subtyping was done in the previous study, the sample size was small and *Blastocystis* ST distribution did not significantly differ between IBS and control. But whatever the scenario, it could be said that *Blastocystis* impacts the populations of microbiota in the human gut and the ramifications of this event could be investigated further along with other underlying factors.

In the light of present study, the ability of *Blastocystis* to modulate AMP could also affect microbiota populations in the human gut. AMPs are now known to shape the composition of gut normal microbiota (Muniz and Yeretssian, 2012). In the two studies mentioned concerning *Blastocystis* and microbiota, it would be interesting to investigate on whether the changes in the bacterial population is mediated by LL-37 and other AMPs. AMP expression is tightly regulated and

ability of *Blastocystis* to disrupt this could lead to loss of gut homeostasis. *Blastocystis* then would be indirectly responsible for the changes in the microbiome populations mediated by high AMP release in the intestinal lumen. The changes in microbiome then could lead to colonization of invading pathogens. In this study, LL-37 has been the only AMP identified to be upregulated by *Blastocystis*. In the future, modulation of other AMPs could be investigated as well. LL-37 has a potent antibacterial activity (Vandamme et al., 2012) which does not distinguish beneficial microbes from harmful ones. The sudden increase of LL-37 in the colon could lead to elimination of certain members of microbiota which then could cause intestinal disorders. Some AMPs toxic to harmful bacteria are not upregulated by invading pathogens but constitutively expressed due to the presence of microbiota. For example, the secretion of RegIII γ , which has antimicrobial activity against Gram positive bacteria, is triggered by commensal bacteria (Srikanth et al., 2008). In this scenario, *Blastocystis* would then be indirectly the cause of the disease state even if the parasite does not survive for long in the colon by preventing other immune factors from being secreted. These possible scenarios could then be investigated and contribute in solving questions in the host-pathogen interactions occurring in *Blastocystis* infections. In short the cross-talk between microbiota, host epithelial cells and immune effectors including AMPs which are the foundations for gut homeostasis (Öhman et al., 2015) could be disrupted by *Blastocystis*. And this study, which determined that *Blastocystis* can upregulate LL-37 expression, could provide a starting point for future investigations.

7.2 Future directions

This study explored the effects of AMPs on *Blastocystis*. The differences in susceptibilities of *Blastocystis* isolates have been studied further as well as some parasitic factors that could be linked to these variations. Further investigations could focus on specific secretory products of *Blastocystis* that could contribute to *Blastocystis* isolates' resistance against AMPs. For example, secretory products of ST7-B have been found to contain proteases that can degrade LL-37. These proteases can be isolated and characterized in future studies to give a clearer picture on the pathogenesis of the parasite. The potential of inhibiting these proteases could be relevant in developing drugs against *Blastocystis*. The surface coat of the parasite may also be worth studying. Aside from identifying its basic ultrastructure and residue content, functional studies could be done to ascertain its role in *Blastocystis* physiology. This could also be relevant in elucidating the parasite's virulence.

Additional experiments could also be done to provide more value to the findings in this study. The effect of low pH in attenuating LL-37 activity is a known phenomenon. In addition, the acidic pH caused by *Blastocystis* ST7-B isolates may also lead to the decrease in affinity of cationic AMPs to the parasite's membrane. This can be studied by chemically modifying surface charges in *Blastocystis*. As mentioned before, the use of LL-37 antibodies and inhibitors in *Blastocystis* AMP challenge could also give an idea on the potency of the peptide if there are minor changes in its structure or net charge.

Blastocystis could upregulate AMP expression in host epithelial cells. However, this study did not elaborate on how this could occur. Specifically, it could be interesting if physical contact between parasite and host cell is necessary to trigger expression of AMPs. If secretory products are enough to produce this effect, further studies could focus on identifying specific molecules from the parasite. This could be significant when therapeutic studies are conducted which are centered on increasing the expression of AMPs.

In this study, only three AMPs have been selected since these are secreted by epithelial cells. In the future, other AMPs could be investigated. For example, α -defensins in the small intestine could play a role in preventing the survival of *Blastocystis* as it passes through the gastrointestinal tract. These are produced by specialized cells and therefore, other techniques in co-culture experiments are needed. It would also be interesting to study the synergism of AMPs as well as the additive effects of the other elements of innate immunity in controlling *Blastocystis* colonization.

The experiments in this study involved *Blastocystis* and host epithelial cells. However, it should be acknowledged that in actual infections, there is also the presence of the microbiome in the gut. This element increases the complexity of the host-parasite interactions mediated by AMPs. Future studies therefore

could involve members of normal microbiota along with the parasite and host cells.

In general, findings in this study would be more significant when verified with *in vivo* studies. It may be necessary to use a mouse model which is incapable of expressing certain AMPs. Infection studies would then seek to investigate if a certain AMP is necessary in controlling and eliminating *Blastocystis* infection. The modulation of AMPs by *Blastocystis* could also be established in animal experiments. The microbiome study mentioned earlier could proceed with the availability of appropriate animal models.

7.3 Conclusions

Figure 8.1 provides a summary model encapsulating the major new findings of this study in relation to *Blastocystis*-AMP interactions.

1. *Blastocystis* is susceptible to growth inhibition by endogenous AMPs. LL-37 has a broad activity on all isolates representing *Blastocystis* ST1, 4 and 7. hBD-2 only affects ST4 isolates while hBD-1 does not show effects on all *Blastocystis* isolates tested.

2. LL-37 causes membrane permeabilization in *Blastocystis* as shown by flow cytometry. Scanning electron microscopy also shows breakage of the parasite's surface when treated with the peptide. Imaging flow cytometry indicates morphological changes from round cells to irregularly-shaped cells upon treatment of LL-37 to *Blastocystis* cells in solution.

3. There is a variation in the sensitivity of *Blastocystis* isolates to LL-37. ST7 are relative resistant to the AMP as indicated by higher IC₅₀ values. Moreover, a representative isolate (B) from ST7, when treated with LL-37, has lesser proportion of cells being permeabilized, takes longer time to lyse and has lesser morphological changes compared to isolates of ST1 and ST4.

4. The mechanisms of resistance of ST7-B isolate to LL-37 has been investigated. These include the parasites ability to secrete proteases that degrade the peptide. The acidic environment caused by the isolate also attenuates LL-37 activity. Lastly, the surface coat of the isolate is thicker compared to other STs and may play a role in protecting the cell from LL-37 attack. The surface coat of *Blastocystis* does not entirely prevent LL-37 from binding to the cell surface but it may obstruct the peptide from reaching the cell membrane.

5. This study also involved the development, optimization and application of a new method for studying *Blastocystis* which shed light on the significance of the different morphological forms of the parasite. Several observations using this method indicate that majority of the irregularly-shaped cells (some would label as amoeboid) are dying cells. The granular forms also have viable and non-viable population with the latter showing a higher mean granularity. The multinucleated cells in *Blastocystis* are rare and cells with more than three nuclei are virtually non-existent in ST4 isolates.

6. Lastly, expression studies indicate that *Blastocystis* upregulates LL-37 expression and secretion in intestinal epithelial cells. In mouse studies, upregulation of CRAMP was seen in the distal colon of mice when inoculated with the parasite. Co-culture studies coupled with qPCR, confocal microscopy and ELISA also showed higher LL-37 expression in an epithelial cell line when incubated with *Blastocystis* ST1, 4 and 7 isolates.

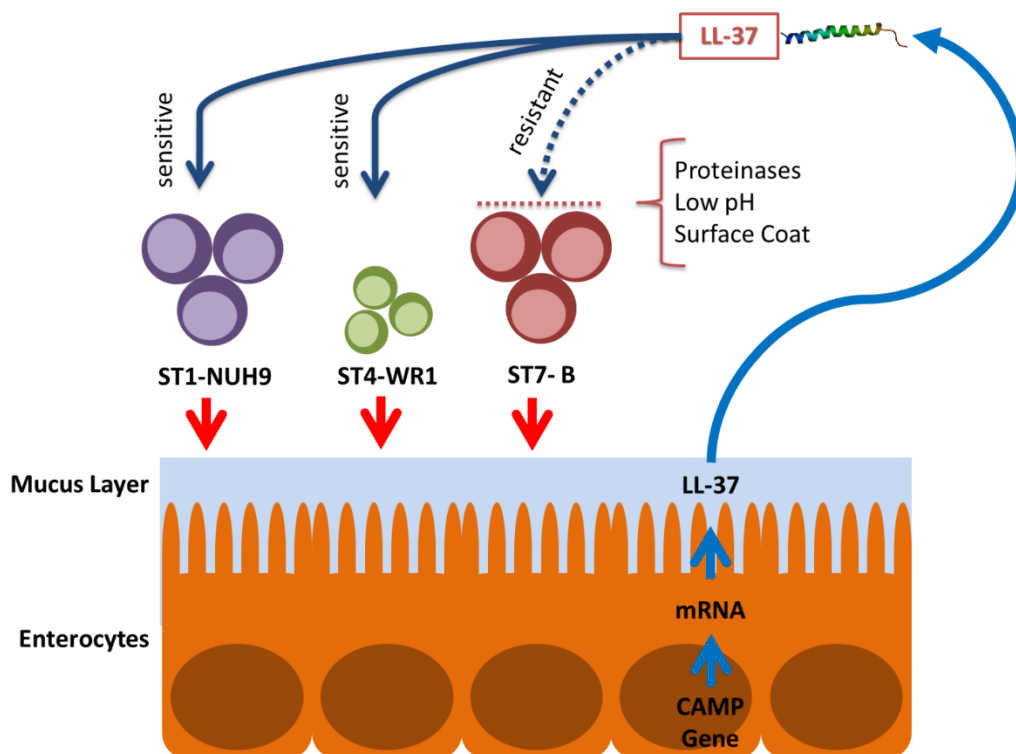


Fig. 7.1. The interactions between *Blastocystis* subtypes and LL-37. *Blastocystis* STs induce epithelial cells to secrete LL-37. ST1 and ST4 are susceptible to LL-37 attack while ST7 is relatively resistant. An isolate of ST7 (B isolate) was found to secrete proteinases that degrade LL-37. It could also lower the pH that attenuated LL-37 activity. It has a thicker surface coat that could possibly protect the parasite against LL-37 binding.

REFERENCES

- Adl, S.M., Simpson, A.G.B., Lane, C.E., Lukeš, J., Bass, D., Bowser, S.S., Brown, M.W., Burki, F., Dunthorn, M., Hampl, V., et al. (2012). The Revised Classification of Eukaryotes. *J. Eukaryot. Microbiol.* *59*, 429–514.
- Agerberth, B., Bergman, P., and Gudmundsson, G.H. (2013). Helping the Host: Induction of Antimicrobial Peptides as a Novel Therapeutic Strategy Against Infections. In *Antimicrobial Peptides and Innate Immunity*, P.S. Hiemstra, and S.A.J. Zaat, eds. (Springer Basel), pp. 359–375.
- Ajjampur, S.S.R., and Tan, K.S.W. (2016). Pathogenic mechanisms in *Blastocystis* spp. — Interpreting results from in vitro and in vivo studies. *Parasitol. Int.*
- Ajjampur, S.S.R., Png, C.W., Chia, W.N., Zhang, Y., and Tan, K.S.W. (2016). Ex Vivo and In Vivo Mice Models to Study *Blastocystis* spp. Adhesion, Colonization and Pathology: Closer to Proving Koch’s Postulates. *PLOS ONE* *11*, e0160458.
- Alaiwa, M.H.A., Reznikov, L.R., Gansemer, N.D., Sheets, K.A., Horswill, A.R., Stoltz, D.A., Zabner, J., and Welsh, M.J. (2014). pH modulates the activity and synergism of the airway surface liquid antimicrobials β -defensin-3 and LL-37. *Proc. Natl. Acad. Sci.* *111*, 18703–18708.
- Alemu, A., Shiferaw, Y., Getnet, G., Yalew, A., and Addis, Z. (2011). Opportunistic and other intestinal parasites among HIV/AIDS patients attending Gambi higher clinic in Bahir Dar city, North West Ethiopia. *Asian Pac. J. Trop. Med.* *4*, 661–665.
- Alfellani, M.A., Stensvold, C.R., Vidal-Lapiedra, A., Onuoha, E.S.U., Fagbenro-Beyioku, A.F., and Clark, C.G. (2013). Variable geographic distribution of *Blastocystis* subtypes and its potential implications. *Acta Trop.* *126*, 11–18.
- Andreu, D., and Rivas, L. (1998). Animal antimicrobial peptides: An overview. *Pept. Sci.* *47*, 415–433.
- Anuar, T.S., Ghani, M.K.A., Azreen, S.N., Salleh, F.M., and Moktar, N. (2013). *Blastocystis* infection in Malaysia: Evidence of waterborne and human-to-human transmissions among the Proto-Malay, Negrito and Senoi tribes of Orang Asli. *Parasit. Vectors* *6*, 40.
- Audebert, C., Even, G., Cian, A., Safadi, D.E., Certad, G., Delhaes, L., Pereira, B., Nourrisson, C., Poirier, P., Wawrzyniak, I., et al. (2016). Colonization with the enteric protozoa *Blastocystis* is associated with increased diversity of human gut bacterial microbiota. *Sci. Rep.* *6*, 25255.
- Baldursson, S., and Karanis, P. (2011). Waterborne transmission of protozoan parasites: Review of worldwide outbreaks – An update 2004–2010. *Water Res.* *45*, 6603–6614.

- Beatty, J., Akierman, S., Rioux, K., Beck, P., McKnight, W., Feener, T., Wallace, J., and Buret, A. (2013). Gut microbiota biofilm disruptions by *Giardia*: Pathology in human enterocytes and germ-free mice. *FASEB J.* 27, 131.1–131.1.
- Bevins, C.L., and Salzman, N.H. (2011). Paneth cells, antimicrobial peptides and maintenance of intestinal homeostasis. *Nat. Rev. Microbiol.* 9, 356–368.
- Beyhan, Y.E., Yilmaz, H., Cengiz, Z.T., and Ekici, A. (2015). Clinical significance and prevalence of *Blastocystis hominis* in Van, Turkey. *Saudi Med. J.* 36, 1118–1121.
- Brogden, K.A. (2005). Antimicrobial peptides: pore formers or metabolic inhibitors in bacteria? *Nat. Rev. Microbiol.* 3, 238–250.
- Bucki, R., Leszczyńska, K., Namiot, A., and Sokołowski, W. (2010). Cathelicidin LL-37: A Multitask Antimicrobial Peptide. *Arch. Immunol. Ther. Exp. (Warsz.)* 58, 15–25.
- Carryn, S., Schaefer, D.A., Imboden, M., Homan, E.J., Bremel, R.D., and Riggs, M.W. (2011). Phospholipases and Cationic Peptides Inhibit *Cryptosporidium parvum* Sporozoite Infectivity by Parasitocidal and Non-Parasitocidal Mechanisms. *J. Parasitol.* 98, 199–204.
- Casero, R.D., Mongi, F., Sánchez, A., and Ramírez, J.D. (2015). *Blastocystis* and urticaria: Examination of subtypes and morphotypes in an unusual clinical manifestation. *Acta Trop.* 148, 156–161.
- Cavalier-Smith, T. (1993). Kingdom protozoa and its 18 phyla. *Microbiol. Rev.* 57, 953–994.
- Cavalier-Smith, T. (1998). A revised six-kingdom system of life. *Biol. Rev.* 73, 203–266.
- Chandramathi, S., Suresh, K., Anita, Z.B., and Kuppusamy, U.R. (2012). Infections of *Blastocystis hominis* and microsporidia in cancer patients: are they opportunistic? *Trans. R. Soc. Trop. Med. Hyg.* 106, 267–269.
- Chen, X.Q., Singh, M., Ho, L.C., Tan, S.W., Ng, G.C., Moe, K.T., and Yap, E.H. (1997). Description of a *Blastocystis* species from *Rattus norvegicus*. *Parasitol. Res.* 83, 313–318.
- Chow, J.Y.C., Li, Z.J., Wu, W.K.K., and Cho, C.H. (2013). Cathelicidin a potential therapeutic peptide for gastrointestinal inflammation and cancer. *World J. Gastroenterol. WJG* 19, 2731–2735.
- Clark, C.G. (1997). Extensive genetic diversity in *Blastocystis hominis*. *Mol. Biochem. Parasitol.* 87, 79–83.
- Clark, C.G., van der Giezen, M., Alfellani, M.A., and Stensvold, C.R. (2013). Chapter One - Recent Developments in *Blastocystis* Research. In *Advances in Parasitology*, D. Rollinson, ed. (Academic Press), pp. 1–32.

- Cobo, E.R., He, C., Hirata, K., Hwang, G., Tran, U., Eckmann, L., Gallo, R.L., and Reed, S.L. (2012). *Entamoeba histolytica* Induces Intestinal Cathelicidins but Is Resistant to Cathelicidin-Mediated Killing. *Infect. Immun.* *80*, 143–149.
- Cole, J.N., and Nizet, V. (2016). Bacterial Evasion of Host Antimicrobial Peptide Defenses. *Microbiol. Spectr.* *4*.
- Collins, S.M. (2014). A role for the gut microbiota in IBS. *Nat. Rev. Gastroenterol. Hepatol.* *11*, 497–505.
- Coyle, C.M., Varughese, J., Weiss, L.M., and Tanowitz, H.B. (2012). *Blastocystis*: to treat or not to treat. *Clin. Infect. Dis. Off. Publ. Infect. Dis. Soc. Am.* *54*, 105–110.
- Das, R., Khalil, S., Mirdha, B.R., Makharia, G.K., Dattagupta, S., and Chaudhry, R. (2016). Molecular Characterization and Subtyping of *Blastocystis* Species in Irritable Bowel Syndrome Patients from North India: e0147055. *PLoS One* *11*.
- Elphick, D.A., and Mahida, Y.R. (2005). Paneth cells: their role in innate immunity and inflammatory disease. *Gut* *54*, 1802–1809.
- El Safadi, D., Gaayeb, L., Meloni, D., Cian, A., Poirier, P., Wawrzyniak, I., Delbac, F., Dabboussi, F., Delhaes, L., Seck, M., et al. (2014). Children of Senegal River Basin show the highest prevalence of *Blastocystis* sp. ever observed worldwide. *BMC Infect. Dis.* *14*.
- Engsbro, A.L., and Stensvold, C.R. (2012). *Blastocystis*: to treat or not to treat...but how? *Clin. Infect. Dis. Off. Publ. Infect. Dis. Soc. Am.* *55*, 1431–1432.
- Fabisiak, A., Murawska, N., and Fichna, J. (2016). LL-37: Cathelicidin-related antimicrobial peptide with pleiotropic activity. *Pharmacol. Rep.*
- Fjell, C.D., Hiss, J.A., Hancock, R.E.W., and Schneider, G. (2012). Designing antimicrobial peptides: form follows function. *Nat. Rev. Drug Discov.* *11*, 37–51.
- Flint, H.J., Scott, K.P., Louis, P., and Duncan, S.H. (2012). The role of the gut microbiota in nutrition and health. *Nat. Rev. Gastroenterol. Hepatol.* *9*, 577–589.
- Ganz, T. (2003). Defensins: antimicrobial peptides of innate immunity. *Nat. Rev. Immunol.* *3*, 710–720.
- Gordon, Y.J., Romanowski, E.G., and McDermott, A.M. (2005). A Review of Antimicrobial Peptides and Their Therapeutic Potential as Anti-Infective Drugs. *Curr. Eye Res.* *30*, 505–515.
- Govind, S.K., Khairul, A.A., and Smith, H.V. (2002). Multiple reproductive processes in *Blastocystis*. *Trends Parasitol.* *18*, 528.

- Govind, S.K., Anuar, K.A., and Smith, H.V. (2003). Response to Tan and Stenzel, and Windsor et al.: *Blastocystis* reproduction and morphology. *Trends Parasitol.* *19*, 291–292.
- Guo, C., Sinnott, B., Niu, B., Lowry, M.B., Fantacone, M.L., and Gombart, A.F. (2013). Synergistic induction of human cathelicidin antimicrobial peptide gene expression by vitamin D and stilbenoids. *Mol. Nutr. Food Res.* n/a – n/a.
- Hancock, R.E.W., and Sahl, H.-G. (2006). Antimicrobial and host-defense peptides as new anti-infective therapeutic strategies. *Nat. Biotechnol.* *24*, 1551–1557.
- Hase, K., Eckmann, L., Leopard, J.D., Varki, N., and Kagnoff, M.F. (2002). Cell Differentiation Is a Key Determinant of Cathelicidin LL-37/Human Cationic Antimicrobial Protein 18 Expression by Human Colon Epithelium. *Infect. Immun.* *70*, 953–963.
- Ho, L.C., Singh, M., Suresh, G., Ng, G.C., and Yap, E.H. (1993). Axenic culture of *Blastocystis hominis* in Iscove's modified Dulbecco's medium. *Parasitol. Res.* *79*, 614–616.
- Ho, S., Pothoulakis, C., and Koon, H.W. (2013). Antimicrobial Peptides and Colitis. *Curr. Pharm. Des.* *19*, 40–47.
- Hoover, D.M., Rajashankar, K.R., Blumenthal, R., Puri, A., Oppenheim, J.J., Chertov, O., and Lubkowski, J. (2000). The Structure of Human β -Defensin-2 Shows Evidence of Higher Order Oligomerization. *J. Biol. Chem.* *275*, 32911–32918.
- Hoover, D.M., Chertov, O., and Lubkowski, J. (2001). The structure of human beta-defensin-1: new insights into structural properties of beta-defensins. *J. Biol. Chem.* *276*, 39021–39026.
- Huang, C.M., Chen, H.C., and Zierdt, C.H. (1990). Magainin analogs effective against pathogenic protozoa. *Antimicrob. Agents Chemother.* *34*, 1824–1826.
- Huang, H.W., Chen, F.-Y., and Lee, M.-T. (2004). Molecular mechanism of Peptide-induced pores in membranes. *Phys. Rev. Lett.* *92*, 198304.
- Jäger, S., Stange, E.F., and Wehkamp, J. (2010). Antimicrobial peptides in gastrointestinal inflammation. *Int. J. Inflamm.* *2010*, 910283.
- Jäger, S., Stange, E.F., and Wehkamp, J. (2013). Antimicrobial Peptides and Inflammatory Bowel Disease. In *Antimicrobial Peptides and Innate Immunity*, P.S. Hiemstra, and S.A.J. Zaat, eds. (Springer Basel), pp. 255–273.
- Jeremiah, S., and Parija, S. (2013). *Blastocystis*: Taxonomy, biology and virulence. *Trop. Parasitol.* *3*, 17.
- Johansson, J., Gudmundsson, G.H., Rottenberg, M.E., Berndt, K.D., and Agerberth, B. (1998). Conformation-dependent Antibacterial Activity of the Naturally Occurring Human Peptide LL-37. *J. Biol. Chem.* *273*, 3718–3724.

- Kahlenberg, J.M., and Kaplan, M.J. (2013). Little Peptide, Big Effects: The Role of LL-37 in Inflammation and Autoimmune Disease. *J. Immunol.* *191*, 4895–4901.
- Kiani, H., Haghghi, A., Rostami, A., Azargashb, E., Tabaei, S.J.S., Solgi, A., and Zebardast, N. (2016). Prevalence, Risk Factors and Symptoms Associated to Intestinal Parasite Infections among Patients with Gastrointestinal Disorders in Nahavand, Western Iran. *Rev. Inst. Med. Trop. São Paulo* *58*.
- Kurt, Ö., Doğruman Al, F., and Tanyüksel, M. (2016). Eradication of *Blastocystis* in humans: Really necessary for all? *Parasitol. Int.*
- Lai, Y., and Gallo, R.L. (2009). AMPed up immunity: how antimicrobial peptides have multiple roles in immune defense. *Trends Immunol.* *30*, 131–141.
- Langhorst, J., Wieder, A., Michalsen, A., Musial, F., Dobos, G.J., and Rueffer, A. (2007). Activated innate immune system in irritable bowel syndrome? *Gut* *56*, 1325–1326.
- Lanuza, M.D., Carbajal, J.A., and Borrás, R. (1996). Identification of surface coat carbohydrates in *Blastocystis hominis* by lectin probes. *Int. J. Parasitol.* *26*, 527–532.
- LaRock, C.N., Döhrmann, S., Todd, J., Corriden, R., Olson, J., Johannssen, T., Lepenies, B., Gallo, R.L., Ghosh, P., and Nizet, V. (2015). Group A Streptococcal M1 Protein Sequesters Cathelicidin to Evade Innate Immune Killing. *Cell Host Microbe* *18*, 471–477.
- Lehrer, R.I., and Ganz, T. (1999). Antimicrobial peptides in mammalian and insect host defence. *Curr. Opin. Immunol.* *11*, 23–27.
- Lehrer, R.I., and Lu, W. (2012). α -Defensins in human innate immunity. *Immunol. Rev.* *245*, 84–112.
- Levine, N.D., Corliss, J.O., Cox, F.E.G., Deroux, G., Grain, J., Honigberg, B.M., Leedale, G.F., Loeblich, A.R., Lom, I.J., Lynn, D., et al. (1980). A Newly Revised Classification of the Protozoa*. *J. Eukaryot. Microbiol.* *27*, 37–58.
- Li, Y., Xiang, Q., Zhang, Q., Huang, Y., and Su, Z. (2012). Overview on the recent study of antimicrobial peptides: Origins, functions, relative mechanisms and application. *Peptides* *37*, 207–215.
- Lim, M.X., Png, C.W., Tay, C.Y.B., Teo, J.D.W., Jiao, H., Lehming, N., Tan, K.S.W., and Zhang, Y. (2014). Differential Regulation of Proinflammatory Cytokine Expression by Mitogen-Activated Protein Kinases in Macrophages in Response to Intestinal Parasite Infection. *Infect. Immun.* *82*, 4789–4801.
- Liu, P.T., Stenger, S., Tang, D.H., and Modlin, R.L. (2007). Cutting Edge: Vitamin D-Mediated Human Antimicrobial Activity against *Mycobacterium tuberculosis* Is Dependent on the Induction of Cathelicidin. *J. Immunol.* *179*, 2060–2063.

- Maçin, S., Kaya, F., Çağdaş, D., Hizarcioglu-Gulsen, H., Saltik-Temizel, I.N., Tezcan, İ., Demir, H., Ergüven, S., and Akyön, Y. (2016). Detection of parasites in children with chronic diarrhea. *Pediatr. Int.* *58*, 531–533.
- MacPherson, D.W., and MacQueen, W.M. (1994). Morphological diversity of *Blastocystis hominis* in sodium acetate-acetic acid-formalin-preserved stool samples stained with iron hematoxylin. *J. Clin. Microbiol.* *32*, 267–268.
- Mirza, H., Wu, Z., Kidwai, F., and Tan, K.S.W. (2011a). A Metronidazole-Resistant Isolate of *Blastocystis* spp. Is Susceptible to Nitric Oxide and Downregulates Intestinal Epithelial Inducible Nitric Oxide Synthase by a Novel Parasite Survival Mechanism. *Infect. Immun.* *79*, 5019–5026.
- Mirza, H., Teo, J.D.W., Upcroft, J., and Tan, K.S.W. (2011b). A Rapid, High-Throughput Viability Assay for *Blastocystis* spp. Reveals Metronidazole Resistance and Extensive Subtype-Dependent Variations in Drug Susceptibilities. *Antimicrob. Agents Chemother.* *55*, 637–648.
- Moal, V.L.-L., and Servin, A.L. (2006). The Front Line of Enteric Host Defense against Unwelcome Intrusion of Harmful Microorganisms: Mucins, Antimicrobial Peptides, and Microbiota. *Clin. Microbiol. Rev.* *19*, 315–337.
- Muniz, L.R., and Yeretssian, G. (2012). Intestinal antimicrobial peptides during homeostasis, infection, and disease. *Front. Chemoattractants* *3*, 310.
- Nagel, R., Cuttell, L., Stensvold, C.R., Mills, P.C., Bielefeldt-Ohmann, H., and Traub, R.J. (2012). *Blastocystis* subtypes in symptomatic and asymptomatic family members and pets and response to therapy. *Intern. Med. J.* *42*, 1187–1195.
- Nithyamathi, K., Chandramathi, S., and Kumar, S. (2016). Predominance of *Blastocystis* sp. Infection among School Children in Peninsular Malaysia. *PLOS ONE* *11*, e0136709.
- Noël, C., Dufernez, F., Gerbod, D., Edgcomb, V.P., Delgado-Viscogliosi, P., Ho, L.-C., Singh, M., Wintjens, R., Sogin, M.L., Capron, M., et al. (2005). Molecular Phylogenies of *Blastocystis* Isolates from Different Hosts: Implications for Genetic Diversity, Identification of Species, and Zoonosis. *J. Clin. Microbiol.* *43*, 348–355.
- Öhman, L., Törnblom, H., and Simrén, M. (2015). Crosstalk at the mucosal border: importance of the gut microenvironment in IBS. *Nat. Rev. Gastroenterol. Hepatol.* *12*, 36–49.
- Oppenheim, J.J., Biragyn, A., Kwak, L.W., and Yang, D. (2003). Roles of antimicrobial peptides such as defensins in innate and adaptive immunity. *Ann. Rheum. Dis.* *62*, ii17–ii21.
- Ordonez, S.R., Amarullah, I.H., Wubbolts, R.W., Veldhuizen, E.J.A., and Haagsman, H.P. (2014). Fungicidal mechanisms of Cathelicidins LL-37 and CATH-2 revealed by Live-cell Imaging. *Antimicrob. Agents Chemother.* 1670–13.

- Oren, Z., and Shai, Y. (1998). Mode of action of linear amphipathic alpha-helical antimicrobial peptides. *Biopolymers* 47, 451–463.
- Oren, Z., Lerman, J.C., Gudmundsson, G.H., Agerberth, B., and Shai, Y. (1999). Structure and organization of the human antimicrobial peptide LL-37 in phospholipid membranes: relevance to the molecular basis for its non-cell-selective activity. *Biochem. J.* 341, 501–513.
- Ostaff, M.J., Stange, E.F., and Wehkamp, J. (2013). Antimicrobial peptides and gut microbiota in homeostasis and pathology. *EMBO Mol. Med.* 5, 1465–1483.
- Park, K., Elias, P.M., Oda, Y., Mackenzie, D., Mauro, T., Holleran, W.M., and Uchida, Y. (2011). Regulation of Cathelicidin Antimicrobial Peptide Expression by an Endoplasmic Reticulum (ER) Stress Signaling, Vitamin D Receptor-independent Pathway. *J. Biol. Chem.* 286, 34121–34130.
- Park, K., Elias, P.M., Hupe, M., Borkowski, A.W., Gallo, R.L., Shin, K.-O., Lee, Y.-M., Holleran, W.M., and Uchida, Y. (2013). Resveratrol Stimulates Sphingosine-1-Phosphate Signaling of Cathelicidin Production. *J. Invest. Dermatol.*
- Peric, M., Koglin, S., Dombrowski, Y., Groß, K., Bradac, E., Ruzicka, T., and Schaubert, J. (2009). VDR and MEK-ERK dependent induction of the antimicrobial peptide cathelicidin in keratinocytes by lithocholic acid. *Mol. Immunol.* 46, 3183–3187.
- Peschel, A., and Sahl, H.-G. (2006). The co-evolution of host cationic antimicrobial peptides and microbial resistance. *Nat. Rev. Microbiol.* 4, 529–536.
- Peters, B.M., Shirtliff, M.E., and Jabra-Rizk, M.A. (2010). Antimicrobial peptides: primeval molecules or future drugs? *PLoS Pathog.* 6, e1001067.
- Poirier, P., Wawrzyniak, I., Vivarès, C.P., Delbac, F., and El Alaoui, H. (2012). New insights into *Blastocystis* spp.: a potential link with irritable bowel syndrome. *PLoS Pathog.* 8, e1002545.
- Poirier, P., Meloni, D., Nourrisson, C., Wawrzyniak, I., Viscogliosi, E., Livrelli, V., and Delbac, F. (2014). Molecular subtyping of *Blastocystis* spp. using a new rDNA marker from the mitochondria-like organelle genome. *Parasitology* 141, 670–681.
- Puthia, M.K., Vaithilingam, A., Lu, J., and Tan, K.S.W. (2005). Degradation of human secretory immunoglobulin A by *Blastocystis*. *Parasitol. Res.* 97, 386–389.
- Puthia, M.K., Lu, J., and Tan, K.S.W. (2008). *Blastocystis ratti* Contains Cysteine Proteases That Mediate Interleukin-8 Response from Human Intestinal Epithelial Cells in an NF- κ B-Dependent Manner. *Eukaryot. Cell* 7, 435–443.
- Rajamanikam, A., and Govind, S. (2013). Amoebic forms of *Blastocystis* spp. - evidence for a pathogenic role. *Parasit. Vectors* 6, 295.

- Ramírez, J.D., Sánchez, L.V., Bautista, D.C., Corredor, A.F., Flórez, A.C., and Stensvold, C.R. (2014). *Blastocystis* subtypes detected in humans and animals from Colombia. *Infect. Genet. Evol.* 22, 223–228.
- Ramírez, J.D., Sánchez, A., Hernández, C., Flórez, C., Bernal, M.C., Giraldo, J.C., Reyes, P., López, M.C., García, L., Cooper, P.J., et al. (2016). Geographic distribution of human *Blastocystis* subtypes in South America. *Infect. Genet. Evol.* 41, 32–35.
- Rangarajan, N., Bakshi, S., and Weisshaar, J.C. (2013). Localized permeabilization of *E. coli* membranes by the antimicrobial peptide Cecropin A. *Biochemistry (Mosc.)* 52, 6584–6594.
- Ras, R., Huynh, K., Desoky, E., Badawy, A., and Widmer, G. (2015). Perturbation of the intestinal microbiota of mice infected with *Cryptosporidium parvum*. *Int. J. Parasitol.* 45, 567–573.
- Rico-Mata, R., De Leon-Rodriguez, L.M., and Avila, E.E. (2013). Effect of antimicrobial peptides derived from human cathelicidin LL-37 on *Entamoeba histolytica* trophozoites. *Exp. Parasitol.* 133, 300–306.
- Rivas, L., Luque-Ortega, J.R., and Andreu, D. (2009). Amphibian antimicrobial peptides and Protozoa: Lessons from parasites. *Biochim. Biophys. Acta BBA - Biomembr.* 1788, 1570–1581.
- Rivas-Santiago, B., Hernandez-Pando, R., Carranza, C., Juarez, E., Contreras, J.L., Aguilar-Leon, D., Torres, M., and Sada, E. (2008). Expression of Cathelicidin LL-37 during Mycobacterium tuberculosis Infection in Human Alveolar Macrophages, Monocytes, Neutrophils, and Epithelial Cells. *Infect. Immun.* 76, 935–941.
- Roberts, T., Ellis, J., Harkness, J., Marriott, D., and Stark, D. (2014a). Treatment failure in patients with chronic *Blastocystis* infection. *J. Med. Microbiol.* 63, 252–257.
- Roberts, T., Stark, D., Harkness, J., and Ellis, J. (2014b). Update on the pathogenic potential and treatment options for *Blastocystis* sp. *Gut Pathog.* 6, 17.
- Safadi, D.E., Meloni, D., Poirier, P., Osman, M., Cian, A., Gaayeb, L., Wawrzyniak, I., Delbac, F., Alaoui, H.E., Delhaes, L., et al. (2013). Molecular Epidemiology of *Blastocystis* in Lebanon and Correlation between Subtype 1 and Gastrointestinal Symptoms. *Am. J. Trop. Med. Hyg.* 88, 1203–1206.
- Santos, H.J., and Rivera, W.L. (2013). Comparison of direct fecal smear microscopy, culture, and polymerase chain reaction for the detection of *Blastocystis* sp. in human stool samples. *Asian Pac. J. Trop. Med.* 6, 780–784.
- Scanlan, P.D., Stensvold, C.R., Rajilić-Stojanović, M., Heilig, H.G.H.J., De Vos, W.M., O’Toole, P.W., and Cotter, P.D. (2014). The microbial eukaryote *Blastocystis* is a prevalent and diverse member of the healthy human gut microbiota. *FEMS Microbiol. Ecol.* 90, 326–330.

- Schauber, J., and Gallo, R.L. (2008). The vitamin D pathway: a new target for control of the skin's immune response? *Exp. Dermatol.* *17*, 633–639.
- Schauber, J., Svanholm, C., Termén, S., Iffland, K., Menzel, T., Scheppach, W., Melcher, R., Agerberth, B., Lührs, H., and Gudmundsson, G.H. (2003). Expression of the cathelicidin LL-37 is modulated by short chain fatty acids in colonocytes: relevance of signalling pathways. *Gut* *52*, 735–741.
- Schmidtchen, A., Frick, I.-M., Andersson, E., Tapper, H., and Björck, L. (2002). Proteinases of common pathogenic bacteria degrade and inactivate the antibacterial peptide LL-37. *Mol. Microbiol.* *46*, 157–168.
- Scott, M.G., Davidson, D.J., Gold, M.R., Bowdish, D., and Hancock, R.E.W. (2002). The Human Antimicrobial Peptide LL-37 Is a Multifunctional Modulator of Innate Immune Responses. *J. Immunol.* *169*, 3883–3891.
- Sieprawska-Lupa, M., Mydel, P., Krawczyk, K., Wójcik, K., Puklo, M., Lupa, B., Suder, P., Silberring, J., Reed, M., Pohl, J., et al. (2004). Degradation of Human Antimicrobial Peptide LL-37 by *Staphylococcus aureus*-Derived Proteinases. *Antimicrob. Agents Chemother.* *48*, 4673–4679.
- Silberman, J.D., Sogin, M.L., Leipe, D.D., and Clark, C.G. (1996). Human parasite finds taxonomic home. *Nature* *380*, 398–398.
- Sio, S.W.S., Puthia, M.K., Lee, A.S.Y., Lu, J., and Tan, K.S.W. (2006). Protease activity of *Blastocystis hominis*. *Parasitol. Res.* *99*, 126–130.
- Sochacki, K.A., Barns, K.J., Bucki, R., and Weisshaar, J.C. (2011). Real-time attack on single *Escherichia coli* cells by the human antimicrobial peptide LL-37. *Proc. Natl. Acad. Sci.* *108*, E77–E81.
- Souppart, L., Moussa, H., Cian, A., Sanciu, G., Poirier, P., Alaoui, H.E., Delbac, F., Boorom, K., Delhaes, L., Dei-Cas, E., et al. (2010). Subtype analysis of *Blastocystis* isolates from symptomatic patients in Egypt. *Parasitol. Res.* *106*, 505–511.
- Srikanth, C.V., McCormick, B.A., Srikanth, C.V., and McCormick, B.A. (2008). Interactions of the Intestinal Epithelium with the Pathogen and the Indigenous Microbiota: A Three-Way Crosstalk, Interactions of the Intestinal Epithelium with the Pathogen and the Indigenous Microbiota: A Three-Way Crosstalk. *Interdiscip. Perspect. Infect. Dis. Interdiscip. Perspect. Infect. Dis.* *2008*, *2008*, e626827.
- Stensvold, C. (2013). *Blastocystis*: Genetic diversity and molecular methods for diagnosis and epidemiology. *Trop. Parasitol.* *3*, 26.
- Stensvold, C.R., Suresh, G.K., Tan, K.S.W., Thompson, R.C.A., Traub, R.J., Viscogliosi, E., Yoshikawa, H., and Clark, C.G. (2007). Terminology for *Blastocystis* subtypes--a consensus. *Trends Parasitol.* *23*, 93–96.

- Suresh, K., Howe, J., Ng, G.C., Ho, L.C., Ramachandran, N.P., Loh, A.K., Yap, E.H., and Singh, M. (1994). A multiple fission-like mode of asexual reproduction in *Blastocystis hominis*. *Parasitol. Res.* *80*, 523–527.
- Tan, K.S.W. (2004). *Blastocystis* in humans and animals: new insights using modern methodologies. *Vet. Parasitol.* *126*, 121–144.
- Tan, K.S.W. (2008). New Insights on Classification, Identification, and Clinical Relevance of *Blastocystis* spp. *Clin. Microbiol. Rev.* *21*, 639–665.
- Tan, K.S.W., and Stenzel, D.J. (2003). Multiple reproductive processes in *Blastocystis*: proceed with caution. *Trends Parasitol.* *19*, 290–291.
- Tan, K.S., Singh, M., and Yap, E.H. (2002). Recent advances in *Blastocystis hominis* research: hot spots in terra incognita. *Int. J. Parasitol.* *32*, 789–804.
- Teo, J.D.W., MacAry, P.A., and Tan, K.S.W. (2014). Pleiotropic Effects of *Blastocystis* spp. Subtypes 4 and 7 on Ligand-Specific Toll-Like Receptor Signaling and NF- κ B Activation in a Human Monocyte Cell Line. *PLoS ONE* *9*, e89036.
- Thompson, J.D., Higgins, D.G., and Gibson, T.J. (1994). CLUSTAL W: improving the sensitivity of progressive multiple sequence alignment through sequence weighting, position-specific gap penalties and weight matrix choice. *Nucleic Acids Res.* *22*, 4673–4680.
- Thwaite, J.E., Hibbs, S., Titball, R.W., and Atkins, T.P. (2006). Proteolytic Degradation of Human Antimicrobial Peptide LL-37 by *Bacillus anthracis* May Contribute to Virulence. *Antimicrob. Agents Chemother.* *50*, 2316–2322.
- Torrent, M., Pulido, D., Rivas, L., and Andreu, D. (2012). Antimicrobial Peptide Action on Parasites. *Curr. Drug Targets* *13*, 1138–1147.
- Vandamme, D., Landuyt, B., Luyten, W., and Schoofs, L. (2012). A comprehensive summary of LL-37, the factotum human cathelicidin peptide. *Cell. Immunol.* *280*, 22–35.
- Vdovenko, A.A. (2000). *Blastocystis hominis*: origin and significance of vacuolar and granular forms. *Parasitol. Res.* *86*, 8–10.
- Verdu, E.F., Galipeau, H.J., and Jabri, B. (2015). Novel players in coeliac disease pathogenesis: role of the gut microbiota. *Nat. Rev. Gastroenterol. Hepatol.* *12*, 497–506.
- Vizioli, J., and Salzet, M. (2002). Antimicrobial peptides versus parasitic infections? *Trends Parasitol.* *18*, 475–476.
- Wang, G. (2008). Structures of Human Host Defense Cathelicidin LL-37 and Its Smallest Antimicrobial Peptide KR-12 in Lipid Micelles. *J. Biol. Chem.* *283*, 32637–32643.

- Wang, G. (2014). Human Antimicrobial Peptides and Proteins. *Pharmaceuticals* 7, 545–594.
- Wang, G., Mishra, B., Lau, K., Lushnikova, T., Golla, R., and Wang, X. (2015). Antimicrobial Peptides in 2014. *Pharmaceuticals* 8, 123–150.
- Wawrzyniak, I., Texier, C., Poirier, P., Viscogliosi, E., Tan, K.S.W., Delbac, F., and El Alaoui, H. (2012). Characterization of two cysteine proteases secreted by *Blastocystis* ST7, a human intestinal parasite. *Parasitol. Int.* 61, 437–442.
- Wiesner, J., and Vilcinskas, A. (2010). Antimicrobial peptides: the ancient arm of the human immune system. *Virulence* 1, 440–464.
- Windsor, J.J., Stenzel, D.J., and Macfarlane, L. (2003). Multiple reproductive processes in *Blastocystis hominis*. *Trends Parasitol.* 19, 289–290.
- Wong, K.H.S., Ng, G.C., Lin, R.T.P., Yoshikawa, H., Taylor, M.B., and Tan, K.S.W. (2007). Predominance of subtype 3 among *Blastocystis* isolates from a major hospital in Singapore. *Parasitol. Res.* 102, 663–670.
- World Health Organization (2008). WHO | Guidelines for drinking-water quality - Volume 1: Recommendations.
- Wu, H., Zhang, G., Minton, J.E., Ross, C.R., and Blecha, F. (2000). Regulation of Cathelicidin Gene Expression: Induction by Lipopolysaccharide, Interleukin-6, Retinoic Acid, and *Salmonella enterica* Serovar Typhimurium Infection. *Infect. Immun.* 68, 5552.
- Wu, Z., Mirza, H., and Tan, K.S.W. (2014). Intra-Subtype Variation in Enteroadhesion Accounts for Differences in Epithelial Barrier Disruption and Is Associated with Metronidazole Resistance in *Blastocystis* Subtype-7. *PLoS Negl Trop Dis* 8, e2885.
- Yamada, M., and Yoshikawa, H. (2012). Morphology of Human and Animal *Blastocystis* Isolates with Special Reference to Reproductive Modes. In *Blastocystis: Pathogen or Passenger?*, H. Mehlhorn, K.S.W. Tan, and H. Yoshikawa, eds. (Springer Berlin Heidelberg), pp. 9–35.
- Yin, J., Howe, J., and Tan, K.S.W. (2010). Staurosporine-induced programmed cell death in *Blastocystis* occurs independently of caspases and cathepsins and is augmented by calpain inhibition. *Microbiology* 156, 1284–1293.
- Yin, L.M., Edwards, M.A., Li, J., Yip, C.M., and Deber, C.M. (2012). Roles of hydrophobicity and charge distribution of cationic antimicrobial peptides in peptide-membrane interactions. *J. Biol. Chem.* 287, 7738–7745.
- Yoshikawa, H., and Iwamasa, A. (2016). Human *Blastocystis* subtyping with subtype-specific primers developed from unique sequences of the SSU rRNA gene. *Parasitol. Int.*
- Yoshikawa, H., Koyama, Y., Tsuchiya, E., and Takami, K. (2016). *Blastocystis* phylogeny among various isolates from humans to insects. *Parasitol. Int.*

- Yu, G., Baeder, D.Y., Regoes, R.R., and Rolff, J. (2016). The More The Better? Combination Effects of Antimicrobial Peptides. *Antimicrob. Agents Chemother.* AAC.02434–15.
- Zaalouk, T.K., Bajaj-Elliott, M., George, J.T., and McDonald, V. (2004). Differential Regulation of β -Defensin Gene Expression during *Cryptosporidium parvum* Infection. *Infect. Immun.* 72, 2772–2779.
- Zaman, V., Howe, J., Ng, M., and Goh, T.K. (1999). Scanning electron microscopy of the surface coat of *Blastocystis hominis*. *Parasitol. Res.* 85, 974–976.
- Zasloff, M. (2002). Antimicrobial peptides of multicellular organisms. *Nature* 415, 389–395.
- Zasloff, M. (2016). Antimicrobial Peptides: Do They Have a Future as Therapeutics? In *Antimicrobial Peptides*, J. Harder, and J.-M. Schröder, eds. (Springer International Publishing), pp. 147–154.
- Zhang, X., Zhang, S., Qiao, J., Wu, X., Zhao, L., Liu, Y., and Fan, X. (2012). Ultrastructural insights into morphology and reproductive mode of *Blastocystis hominis*. *Parasitol. Res.* 110, 1165–1172.
- Zierdt, C.H. (1973). Studies of *Blastocystis hominis*. *J. Protozool.* 20, 114–121.
- Zierdt, C.H. (1991). *Blastocystis hominis*--past and future. *Clin. Microbiol. Rev.* 4, 61–79.

Blastocystis Isolate B Exhibits Multiple Modes of Resistance against Antimicrobial Peptide LL-37

John Anthony Yason, Sitara Swarna Rao Ajjampur, Kevin Shyong Wei Tan

Laboratory of Cellular and Molecular Parasitology, Department of Microbiology and Immunology, Yong Loo Lin School of Medicine, National University of Singapore, Singapore

Blastocystis is one of the most common eukaryotic organisms found in humans and many types of animals. Several reports have identified its role in gastrointestinal disorders, although its pathogenicity is yet to be clarified. *Blastocystis* is transmitted via the fecal-to-oral route and colonizes the large intestines. Epithelial cells lining the intestine secrete antimicrobial peptides (AMPs), including beta-defensins and cathelicidin, as a response to infection. This study explores the effects of host colonic antimicrobial peptides, particularly LL-37, a fragment of cathelicidin, on different *Blastocystis* subtypes. *Blastocystis* is composed of several subtypes that have genetic, metabolic, and biological differences. These subtypes also have various outcomes in terms of drug treatment and immune response. In this study, *Blastocystis* isolates from three different subtypes were found to induce intestinal epithelial cells to secrete LL-37. We also show that among the antimicrobial peptides tested, only LL-37 has broad activity on all the subtypes. LL-37 causes membrane disruption and causes *Blastocystis* to change shape. *Blastocystis* subtype 7 (ST7), however, showed relative resistance to LL-37. An isolate, ST7 isolate B (ST7-B), from this subtype releases proteases that can degrade the peptide. It also makes the environment acidic, which causes attenuation of LL-37 activity. The *Blastocystis* ST7-B isolate was also observed to have a thicker surface coat, which may protect the parasite from direct killing by LL-37. This study determined the effects of LL-37 on different *Blastocystis* isolates and indicates that AMPs have significant roles in *Blastocystis* infections.

Blastocystis is an intestinal protistan parasite commonly detected in humans and many types of animals (1, 2). This organism is classified under the stramenopiles, although it lacks chloroplasts or structures for locomotion, which are common features of many members of this group. *Blastocystis* is widely distributed throughout the world. Parasitological surveys usually place *Blastocystis* as the most common eukaryotic parasite detected (3, 4). This organism has a global distribution and has numerous animal hosts. There is little host specificity for this organism, and there are reports indicating the zoonotic potential of *Blastocystis* (5). This organism, in its cyst form, is transmitted via the fecal-to-oral route. It then colonizes the large intestine and is excysted to its various forms. These forms may appear vacuolar, multivacuolar, avacuolar, or granular under a light microscope. *Blastocystis* has been implicated in a number of intestinal disorders, although its pathogenesis is yet to be elucidated. There are few reports associating it with gastrointestinal disease, the most common symptoms of which are diarrhea, vomiting, nausea, and urticaria (1, 5–7). *Blastocystis* is a species complex that is comprised of up to 19 subtypes (STs), with ST1 to ST9 having been isolated from humans (8). Recently, a report found that ST12 and another possible novel ST also infect humans (9). *Blastocystis* STs may differ in size range, nuclear arrangement, growth rate, and morphology (8). There have been reports on the differences in host range, protease activity, and characteristics of the immune response triggered (10–12). There are also variations in drug sensitivities (13, 14). Some researchers have suggested that symptomatology is dictated by ST identity (15).

LL-37 is a 37-amino-acid fragment of human cathelicidin antimicrobial peptide (CAMP), which has a direct killing effect on prokaryotic and fungal organisms (16, 17). Because of its positive charge, it can bind to negatively charged surfaces, which is a feature of prokaryotic membranes (18). It can cause the formation of pores on the cell membrane and subsequently effect cell lysis.

LL-37 is also a modulator of downstream immune responses such as the recruitment of other immune cells and the release of cytokines (19). Cathelicidin is produced by epithelial cells, including those lining the small and large intestines. It is processed by proteases, which results in the LL-37 fragment. There is basal secretion of LL-37 in the intestinal lumen. During infection, LL-37 becomes highly expressed, along with other antimicrobial peptides (AMPs). This leads to other immune responses such as the recruitment of inflammatory cells and the production of cytokines (20).

In this study, we explore the possible interactions between *Blastocystis* and human intestinal AMPs, particularly LL-37. We determined if the parasite can induce intestinal epithelial cells to secrete LL-37 using *in vitro* cell culture and a mouse model. We also tested several isolates of *Blastocystis* from three STs for susceptibility to three colonic AMPs, including LL-37. AMPs had variable effects on *Blastocystis*, and their effects on different *Blastocystis* STs were also not uniform. We identified possible parasite factors by which *Blastocystis* can possibly attenuate LL-37 activity.

Received 25 April 2016 Accepted 14 May 2016

Accepted manuscript posted online 23 May 2016

Citation Yason JA, Ajjampur SSR, Tan KSW. 2016. *Blastocystis* isolate B exhibits multiple modes of resistance against antimicrobial peptide LL-37. Infect Immun 84:2220–2232. doi:10.1128/IAI.00339-16.

Editor: J. H. Adams, University of South Florida

Address correspondence to Kevin Shyong Wei Tan, kevin_tan@nuhs.edu.sg.

Supplemental material for this article may be found at <http://dx.doi.org/10.1128/IAI.00339-16>.

Copyright © 2016, American Society for Microbiology. All Rights Reserved.

MATERIALS AND METHODS

Parasite cultivation. Nine previously axenized *Blastocystis* isolates (21–23) representing 3 STs (ST1, ST4, and ST7) were used for this study. Culture medium consisted of 9 ml prereduced Iscove's modified Dulbecco's medium (IMDM) (Thermo Scientific) supplemented with 10% horse serum (Gibco). Culture tubes were maintained inside 2.5-liter sealed anaerobic jars with an anaerobic gas pack (Oxoid) at 37°C. Human *Blastocystis* isolates were acquired from patients at the Singapore General Hospital in the early 1990s, before the Institutional Review Board was established at the National University of Singapore (NUS). *Blastocystis* isolates B, C, E, G, and H are maintained at a microbial collection at the Department of Microbiology and Immunology of the NUS. NUH2 and NUH9 were isolated in 2007 from stool samples submitted for routine health screening. Permission from the National Healthcare Group Institutional Review Board was given before project commencement. All samples were anonymized. *Blastocystis* isolates WR1 and S1 were isolated from a Wistar rat and a Sprague–Dawley rat, respectively.

Subtyping of *Blastocystis* isolates. The isolates were previously genotyped by using primers in a PCR assay based on the organism's small-subunit (SSU) rRNA (23, 24) and mitochondrion-like organelle (MLO) (25) genes. Total DNAs were extracted from 1×10^6 cells by using a Qiagen DNA stool kit (Qiagen) according to the manufacturer's instructions. PCR was performed by using Q5 High-Fidelity 2 \times master mix (New England BioLabs) with 500 ng of DNA sample. All PCR runs were completed by using a Bio-Rad iQ5 thermocycler. PCR products were sequenced and compared to the National Center for Biotechnology Information (NCBI) (USA) nucleotide sequence database to confirm subtype identities.

AMP susceptibility screening. To determine the susceptibility of the 9 *Blastocystis* isolates to various human intestinal AMPs, a high-throughput viability assay developed previously by Mirza et al. (14) was applied. Briefly, flat-bottom 96-well plates (Greiner) were used, with each well containing 0.5×10^6 *Blastocystis* cells. The AMPs human beta-defensin 1 (hBD-1), hBD-2, and LL-37 were dissolved in complete medium at concentrations ranging between 0 and 50 μ M. After 24 h of incubation, resazurin dye (Sigma-Aldrich) at a 5% final dilution was added and incubated for another 3 h. Reading of fluorescence was done at 550-nm excitation and 570-nm emission wavelengths by using a Tecan Infinite F200 microplate reader. Half-maximal inhibitory concentration (IC₅₀) values were calculated by using GraphPad Prism software. Synthetic AMPs at 95% purity were obtained from Singapore Advanced Biologics.

Exposure of mouse intestinal explants to *Blastocystis*. C57BL/6 mice were obtained from the NUS and housed in an animal biosafety level 2 clean animal facility. Mice (7 to 9 weeks old) were euthanized by CO₂ inhalation. The intestinal tract was dissected and placed into 50-ml tubes with complete medium comprised of Dulbecco's modified Eagle's medium (DMEM) (HyClone) supplemented with 10% heat-inactivated fetal bovine serum (FBS) (Gibco), 1% each sodium pyruvate (Gibco) and non-essential amino acids (Gibco), and 2,000 U/ml penicillin-streptomycin (Gibco). The tissue was then dissected into segments of distal colon, proximal colon, cecum, and terminal ileum and opened along the mesenteric edge, and intestinal contents were removed. The segments were washed gently in cold penicillin-streptomycin and cut into bits measuring 1.5 cm by 1 cm. The explants were affixed onto 2% agarose layers in 6-well plates with the serosal surface facing down in prewarmed complete medium with penicillin-streptomycin (Gibco). Explants were incubated with 5×10^7 live *Blastocystis* ST7 isolate B (ST7-B) parasites for 1 h at 37°C. For all assays, more than one litter was used in order to avoid any litter-specific effects. After incubation, the explants were frozen in TRIzol (Invitrogen) at –80°C until further processing. The animal experiments were performed in accordance with Singapore National Advisory Committee for Laboratory Animal Research guidelines. The protocol (R13-5890) was reviewed and approved by the NUS Institutional Animal Care and Use Committee.

Coculture of *Blastocystis* with HT-29 intestinal epithelial cells. HT-29 epithelial cells were used to study whether *Blastocystis* parasites affect the expression of LL-37 in host cells. Cells were maintained in T-75 flasks (Corning) in a humidified incubator with 5% CO₂ at 37°C. Complete culture medium consisted of 10% heat-inactivated FBS (Gibco) and 1% each sodium pyruvate (Gibco), nonessential amino acids (Gibco), and penicillin-streptomycin in DMEM (Thermo Scientific). Cells were seeded onto 6-well plates (Greiner) by using complete medium. After reaching confluence, HT-29 cells were incubated for 48 h with serum-free medium supplemented with 3 mM sodium butyrate (Sigma-Aldrich). HT-29 cells were then cocultured with *Blastocystis* isolates NUH9 (ST1-NUH9), WR1 (ST4-WR1), and ST7-B at an MOI (multiplicity of infection) of 10 for 1 h. Culture supernatants were collected and set aside for determination of LL-37 secretion. The viability of HT-29 cells after coculture was determined by using a trypan blue exclusion assay.

Quantitative real-time PCR. Induction of cathelicidin-related antimicrobial peptide (CRAMP) gene expression on mouse intestinal explants and CAMP gene expression on HT-29 cells was determined after exposure to *Blastocystis*. Mouse explants in TRIzol were homogenized with zirconium oxide beads in a tissue homogenizer (WisBioMed), and RNA was extracted from homogenates by using the TRIzol method, followed by further purification with the NucleoSpin RNA kit (Macherey-Nagel). HT-29 cells were homogenized and lysed with RNazol (Molecular Research Center). Total RNA was extracted according to the manufacturer's protocol. Synthesis of cDNA was done by using an iScript cDNA synthesis kit (Bio-Rad) with 1 μ g of RNA sample in an iCycler thermocycler (Bio-Rad) according to the suggested protocol. Quantitative real-time PCR (qRT-PCR) was then performed by using an iTaq Universal SYBR green Supermix kit (Bio-Rad), 1 μ l of cDNA, and 500 nM (each) the following primers (Sigma-Aldrich): CRAMP-F (5'-TTT TGA CAT CAG CTG TAA CG-3') and CRAMP-R (5'-GCT TTT CAC CAA TCT TCT CC-3') for mouse samples and CAMP-F (5'-AGT GAA GGA GAC TGT ATG TG-3') and CAMP-R (5'-ATT TTC TTG AAC CGA AAG GG-3') for HT-29 samples. Mouse beta-actin (mBA-F [5'-GAT GTA TGA AGG CTT TGG TC-3'] and mBA-R [5'-TGT GCA CTT TTA TTG GTC TC-3']) and human glyceraldehyde-3-phosphate dehydrogenase (GAPDH) (hGAPDH-F [5'-CTT TTG CGT CGC CAG-3'] and hGAPDH-R [5'-TTG ATG GCA ACA ATA TCC AC-3']) genes were used as endogenous controls. Gene expression analysis was done by using iQ5 v2.1 software (Bio-Rad), which uses the $2^{-\Delta\Delta C_t}$ method.

LL-37 secretion assay. To quantitatively determine LL-37 secretion in HT-29 cells, supernatants (100 μ l) from cocultures with *Blastocystis* were used to coat flat-bottom 96-well MaxiSorp plates (Nunc) for 18 h at 4°C. The excess supernatant was disposed of, and the LL-37 peptide concentration was determined by using an enzyme-linked immunosorbent assay (ELISA). The plates were washed 3 times by using wash buffer containing 1 \times phosphate-buffered saline (PBS) with 0.05% Tween 20 (PBS-T) and blocked with 1% bovine serum albumin (BSA) (Santa Cruz Biotechnology) for 2 h at 25°C. LL-37 was probed with a 1:5,000 dilution of rabbit polyclonal anti-LL-37 human IgG antibody (Abcam) in blocking solution. After 1 h, the wells were washed 4 times with PBS-T. A 1:1,000 dilution of goat polyclonal secondary antibody to rabbit IgG horseradish peroxidase (HRP)-conjugated antibody (Abcam) in blocking solution was added, and the mixture was incubated at 25°C. After 1 h, the wells were washed 4 times with PBS-T. The wells were then incubated with the substrate 2,2'-azinobis(3-ethylbenzothiazoline-6-sulfonic acid) (ABTS) (Sigma-Aldrich) for 5 to 10 min. The absorbance was read at 492 nm by using a Tecan Infinite F200 microplate reader.

Fluorescence microscopy. To visualize the expression of LL-37 in HT-29 cells, a fluorescence microscopy assay was used. HT-29 cells were grown to confluence in 24-well cell culture plates (Greiner) with poly-L-lysine-treated glass coverslips. Complete medium was then replaced with 3 mM sodium butyrate in serum-free medium. After 48 h, cocultivation with *Blastocystis* isolates ST1-NUH9, ST4-WR1, and ST7-B at an MOI of 10 for 1 h was done. HT-29 cells were then washed with PBS and fixed with

absolute methanol for 15 min at -20°C . The cells were then washed with PBS and blocked with 5% normal goat serum in PBS for 2 h. LL-37 was probed by using a 1:500 dilution of rabbit polyclonal anti-LL-37 human IgG antibody (Abcam) in blocking solution overnight at 4°C . After the cells were washed 3 times with PBS-T for 5 min each, incubation was done with a 1:1,000 dilution of goat polyclonal secondary antibody to rabbit IgG fluorescein isothiocyanate (FITC)-conjugated antibody (Abcam) in blocking solution for 1 h at 25°C . The cells were then washed 3 times. The glass coverslips were then mounted by using Vectashield mounting medium and examined by using an Olympus BX60 fluorescence microscope. Total cell fluorescence was quantified by using ImageJ software version 1.48 (NIH).

Viability staining and flow cytometry. Propidium iodide (PI) (Bio-Vision) was used to stain *Blastocystis* cells to assess viability after LL-37 treatment. *Blastocystis* isolates ST1-NUH9, ST4-WR1, and ST7-B (1×10^7 cells/ml) were treated with LL-37 at concentrations of 0, 10, and 100 $\mu\text{g/ml}$ for 1 h. A necrotic control was added as a positive control. This was achieved by heating the cells at 95°C for 15 min. PI was then added to the cell suspension according to the manufacturer's instructions. Cells were then analyzed by using an LSRFortessa instrument (BD Biosciences). Data analysis was done by using Summit software version 4.3 (Dako).

Scanning electron microscopy. The effects of the LL-37 peptide on the *Blastocystis* membrane and surface coat were visualized by using a scanning electron microscope. *Blastocystis* cells with and without LL-37 treatment were fixed overnight with 4% glutaraldehyde in PBS. The cells were then washed and attached to 0.1% poly-L-lysine-treated coverslips for 30 min. The cells were dehydrated with increasing concentrations of ethanol. The coverslips with attached cells were placed into a critical-point drier (CPD 030; Balzers) for carbon dioxide infiltration. After drying, the coverslips were coated with 5- to 10-nm gold particles with a sputter coater. The cells were visualized with a JEOL JSM-6701F scanning electron microscope.

Imaging flow cytometry. Morphological changes of *Blastocystis* cells caused by LL-37 were observed by using an imaging flow cytometer. *Blastocystis* cultures were harvested and washed twice with PBS. Cell suspensions with 1×10^7 cells/ml were stained with 1 $\mu\text{g/ml}$ PI (BioVision), 5 μM carboxyfluorescein succinimidyl ester (CFSE) (Life Technologies), and 1 $\mu\text{g/ml}$ Hoechst 33342 (Life Technologies) for 15 min. The stained cells were analyzed by using an Amnis ImageStream MkII imaging flow cytometer (Merck Millipore) with a 4-laser attachment (375, 488, 561, and 642 nm). At least 2,000 events per run were acquired at low flow speed and a $\times 60$ magnification. The gating strategy included selection for focused cells and then single cells. Histograms based on circularity indices were generated. Data analysis was done by using IDEAS software version 6.1.

LL-37 bound to the surfaces of *Blastocystis* cells was also visualized by using imaging flow cytometry. Before the samples were run, 1×10^7 cells were treated with 50 $\mu\text{g/ml}$ LL-37 at room temperature. PI was added, and the cells were fixed by using 4% formaldehyde for 30 min. The cells were washed twice and suspended in PBS. LL-37 bound to the *Blastocystis* cell surface was probed with a 1:1,000 dilution of rabbit polyclonal anti-LL-37 human IgG antibody (Abcam) for 30 min. Goat polyclonal secondary antibody to rabbit IgG FITC-conjugated antibody (Abcam) at a 1:500 concentration was then added, and the mixture was incubated for 30 min. All the reactions were done at 25°C .

LL-37 degradation and viability assays. *Blastocystis* ST7-B and ST4-WR1 excretory-secretory products (ESPs) were harvested from cultures grown for 24 h. The cultures were washed twice in serum-free IMDM. The cells were then incubated for 2 h in prerduced IMDM at 37°C under anaerobic conditions at 1×10^8 cells per ml of IMDM. Culture supernatants were then collected by centrifugation at $1,000 \times g$ for 10 min and filtered twice by using 0.2- μm -pore-size filters (Millipore). *Blastocystis* secreted products were stored at -80°C until use. The effect of *Blastocystis* ESPs on peptide integrity was quantitatively determined by an enzyme-linked immunosorbent assay (ELISA). Briefly, each well of flat-bottom

TABLE 1 IC_{50} s of hBD-1, hBD-2, and LL-37 for *Blastocystis* STs

Subtype	Isolate	IC_{50} (μM)		
		HBD-1	HBD-2	LL-37
ST1	NUH2	>50	>50	6.0
	NUH9	>50	>50	4.7
ST4	WR1	>50	11.4	3.2
	S1	>50	5.0	5.4
ST7	B	>50	>50	42.6
	C	>50	>50	23.4
	E	>50	>50	23.2
	G	>50	>50	27.7
	H	>50	>50	28.7

96-well Nunc MaxiSorp plates was coated with 50 μl of LL-37 at a concentration of 2 $\mu\text{g/ml}$ for 18 h at 4°C . Plates coated with LL-37 were exposed for 2 h to *Blastocystis* ESPs alone or ESPs previously incubated for 6 h with $1 \times$ Halt protease inhibitor cocktail (Bio-Rad) at 37°C . The wells were then washed with PBS, and the concentration of intact LL-37 was determined by using an ELISA as outlined above. LL-37 peptide solutions previously incubated with *Blastocystis* ESPs were also used for the treatment of *Blastocystis* cultures. Viability was determined by using flow cytometry and PI staining after treatment. Denatured ESPs were also used in this assay, which entailed heating of the ESPs for 15 min at 95°C .

Transmission electron microscopy (TEM). Cultures of *Blastocystis* cells (1×10^7 cells) grown for 24 h were harvested, washed, and treated with 100 $\mu\text{g/ml}$ cationized ferritin (Sigma-Aldrich) for 2 h. Cationized ferritin binds to negatively charged surfaces (26). We found that it was useful to visualize the surface coat of *Blastocystis* by providing better contrast and maintaining its integrity during the preparation of cells for electron microscopy. The cells were then fixed overnight at 4°C with 8% glutaraldehyde. The cells were then washed 3 times with PBS. Postfixation included incubation of cells with 1% osmium tetroxide and 1% potassium ferrocyanide in PBS for 2 h. The cells were then washed 3 times. The cells were dehydrated with absolute ethanol 5 times. Embedding was done for 48 h by using London resin white. The solidified blocks were sectioned, mounted, and viewed by using a transmission electron microscope (JEM-1010; JEOL).

Statistical analysis. Tests for significant differences were done by using analysis of variance (ANOVA) and Student's *t* test. Error bars represent standard errors from at least 3 independent experiments. Calculations and generation of graphs were done with GraphPad Prism 5.0.

RESULTS

***Blastocystis* STs are inhibited by LL-37.** Nine *Blastocystis* isolates representing 3 STs were tested for susceptibility to AMP treatment (Table 1). All isolates from the three subtypes were considered susceptible to LL-37, although ST7 isolates showed higher IC_{50} s. Only ST4 isolates were susceptible to hBD-2, while treatment of all isolates with hBD-1 did not cause a loss of *Blastocystis* viability.

Blastocystis induces cathelicidin expression in mouse intestinal explants and human intestinal epithelial cells. Mouse intestinal samples were sectioned into terminal ileum, cecum, proximal colon, and distal colon sections and subsequently inoculated with *Blastocystis* ST7-B cells. qRT-PCR analysis showed that mouse distal colon explants showed a net upregulation of the CRAMP gene when exposed to the parasite (Fig. 1A). HT-29 cells also showed an upregulation of cathelicidin gene expression when coincubated with the *Blastocystis* ST1-NUH9, ST4-WR1, and ST7-B isolates (Fig. 1B). ELISA results showed an increase in the cathelicidin

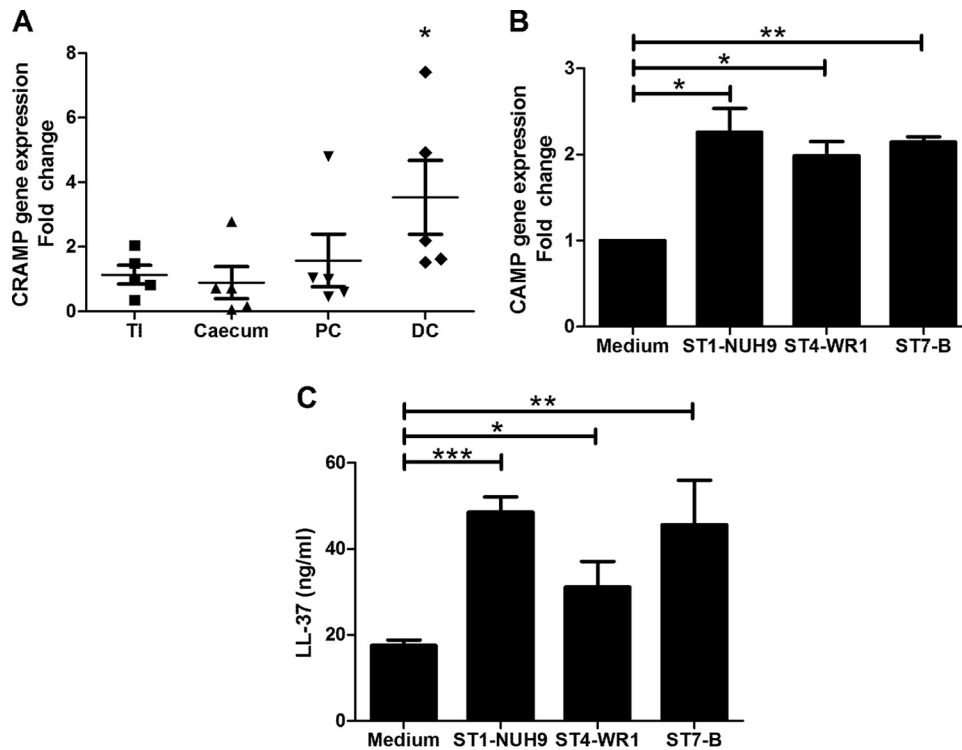


FIG 1 *Blastocystis* induces LL-37 expression in mouse distal colon explants and HT-29 colonic epithelial cells. (A) Intestines from five mice were externalized and partitioned into terminal ileum (TI), cecum, proximal colon (PC), and distal colon (DC). These segments were exposed to *Blastocystis* ST7-B cells for 1 h. CRAMP gene expression was determined by using qRT-PCR. Distal colon explants show significant upregulation of the CRAMP gene. (B) Three *Blastocystis* isolates (NUH9, WR1, and B) representing three STs (ST1, -4, and -7, respectively) also induced CAMP gene expression in confluent HT-29 cells after 30 min of coinubation at an MOI of 10. (C) The supernatant from the coculture shows a significant increase in the LL-37 content after 1 h of coinubation, as determined by an ELISA. *, $P < 0.05$; **, $P < 0.001$; ***, $P < 0.0001$.

concentration in the HT-29 culture supernatant when incubated with *Blastocystis* (Fig. 1C). At equal MOIs, ST1-NUH9 showed the highest level of induction, followed by the ST7-B and ST4-WR1 isolates. HT-29 cells showed 95% viability in all the wells, and no significant difference in viability was found between cells with parasites and those without (see Fig. S1 in the supplemental material). Fluorescence microscopy also showed an increase in FITC staining of HT-29 cells incubated with *Blastocystis* (Fig. 2).

LL-37 disrupts the *Blastocystis* cell membrane. Three isolates (ST1-NUH9, ST4-WR1, and ST7-B), each representing a particular subtype, were incubated with 0, 10, and 100 $\mu\text{g/ml}$ LL-37 for 1 h, and membrane disruption was analyzed by staining with PI. The proportion of cells with PI staining was determined by flow cytometry. All three isolates showed increases in the proportions of permeabilized cells as the concentration of LL-37 increased. At 100 $\mu\text{g/ml}$ LL-37, >50% of ST1-NUH9 and ST4-WR1 cells had PI staining, while only 36% of ST7-B cells showed PI staining (Fig. 3). Time-lapse micrographs show that by as early as 5 min of incubation of the *Blastocystis* ST7-B isolate with the peptide, smaller cells were already undergoing lysis. Larger cells were observed being lysed after 20 min. Before complete lysis, vesicles were seen forming in a few sections of the cell membrane (Fig. 4A). The cells appeared to flatten as well. In addition, the membrane-disruptive effect of LL-37 on a “resistant” isolate (ST7-B) was slower than that on a “sensitive” isolate (ST4-WR1). Flow cytometry analysis showed that >30% of ST4-WR1 cells had PI staining after 15 min of treatment with LL-37, while it took 30 min of treatment for ST7-B cells to reach this proportion (Fig. 4B).

LL-37 causes morphological changes in *Blastocystis*. An imaging flow cytometer was used to analyze the effect of LL-37 on the morphology of parasites (Fig. 5A). On average, *Blastocystis* cells appear round, with the cytoplasm being pushed to the edge by a large central vacuole. Irregularly shaped cells in culture are an indication of poor viability. All three of the isolates studied showed a decrease in the proportion of round cells when LL-37 was added to the cultures. At 10 $\mu\text{g/ml}$ LL-37, the change in the percentage of round cells was minimal. At 100 $\mu\text{g/ml}$ LL-37, the proportion of round cells is lower by at least half than for untreated cultures in all the ST populations (Fig. 5B). Scanning electron microscopy analysis showed the possible phenotypic features of affected *Blastocystis* cells. LL-37-treated cells exhibited membrane pores and compressed cells, which may be due to cytoplasmic leakage. ST4-WR1 cells also showed fragmentation when treated with LL-37 (Fig. 5C).

Blastocystis ST7-B, but not ST4-WR1, secretes proteases that can degrade LL-37. A modified ELISA was used to determine if *Blastocystis* ESPs can degrade LL-37. We used ESPs from ST7-B and ST4-WR1 cultures to represent LL-37-resistant and LL-37-susceptible isolates, respectively. The absorbance of wells after incubation with ESPs of the ST7-B isolate was lower than that of wells after incubation with ESPs of ST4-WR1 (Fig. 6A). This indicates that ST7-B isolates produce proteases that can degrade LL-37. This degradation was inhibited when ESPs were incubated with a protease cocktail inhibitor prior to the degradation assay. In addition, PI staining was also used to determine the viability of *Blastocystis* cells after treatment with LL-37 previously incubated

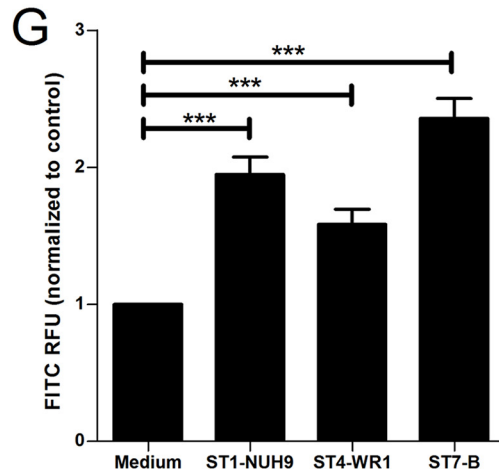
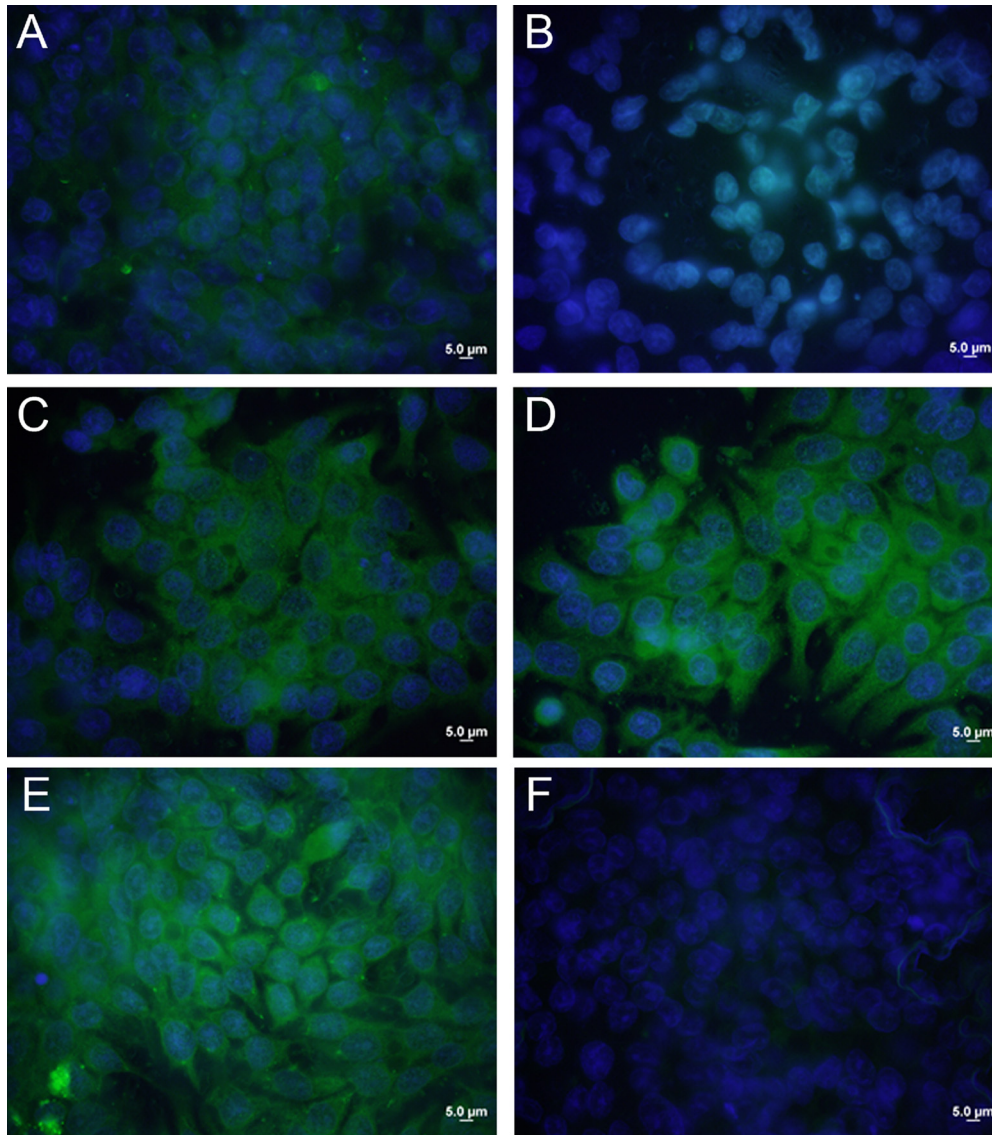


FIG 2 Confluent HT-29 cells in monolayers increase the production of cathelicidin after incubation with *Blastocystis*. (A and B) Immunofluorescence assay images show a basal level of cathelicidin production in differentiated HT-29 cells (A), which was absent in undifferentiated cells (B). (B to E) Differentiated HT-29 cells incubated with *Blastocystis* ST1-NUH9 (C), ST4-WR1 (D), and ST7-B (E) show brighter fluorescence after 1 h of coinoculation at an MOI of 10. (F) Negative control. (G) Total fluorescence units were quantified by using ImageJ software. RFU, relative fluorescence units. ***, $P < 0.0001$.

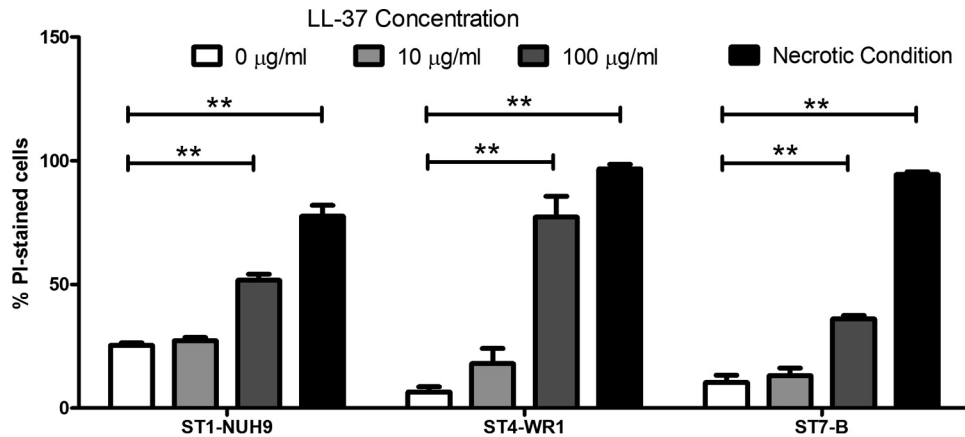


FIG 3 LL-37 causes disruption of the *Blastocystis* cell membrane. PI staining and flow cytometry were used to detect cells with permeabilized membranes. Graphs show proportions of PI-stained cells in ST1-NUH9, ST4-WR1, and ST7-B populations after incubation with 0, 10, and 100 µg/ml LL-37 for 1 h. Necrotic conditions were used as a positive control for PI staining. This was attained by heating *Blastocystis* cells for 15 min at 80°C. There is an increase in the proportion of permeabilized *Blastocystis* cells at higher concentrations of LL-37. The ST-B isolate showed relative resistance to LL-37 compared to both the ST1-NUH9 and ST4-WR1 isolates. **, $P < 0.001$.

with the ST7-B ESPs (Fig. 6B). The secreted proteases in the ST7-B ESPs inactivated LL-37 activity on *Blastocystis* cells. This, however, was reversed when ESPs were previously heat denatured before incubation with LL-37.

The *Blastocystis* ST7-B isolate decreases the pH in culture and attenuates LL-37 activity. The pH of complete medium for *Blastocystis* was adjusted and used to determine if it has an effect on the activity of LL-37 on *Blastocystis*. At pH 6.6, LL-37 had a minimal effect on the *Blastocystis* ST7-B and ST4-WR1 isolates, with cell counts at 90% and 88%, respectively, compared to that with untreated cultures. At pH 7.1, the relative resistance of ST7-B was observed and compared to that of ST4-WR1. Cell counts at this

pH with LL-37 were 76% and 41% for the ST7-B and ST4-WR1 isolates, respectively, compared to untreated cultures. At pH 8.0, ST7-B and ST4-WR1 cell counts were 44% and 38%, respectively, of those of untreated cultures. At this pH, the highest level of activity of LL-37 was observed, which negated the relative resistance of the ST7-B isolate (Fig. 7A). We also determined the pH of *Blastocystis* culture medium after 24 h. The average pH of the *Blastocystis* ST7-B culture was 6.8, while that of the ST-WR1 culture was 7.0 (Fig. 7B).

The *Blastocystis* ST7-B isolate has a thick surface coat compared to that of ST4-WR1. India ink was used as negative stain to visualize the surface coat of *Blastocystis* cells. Most cells from

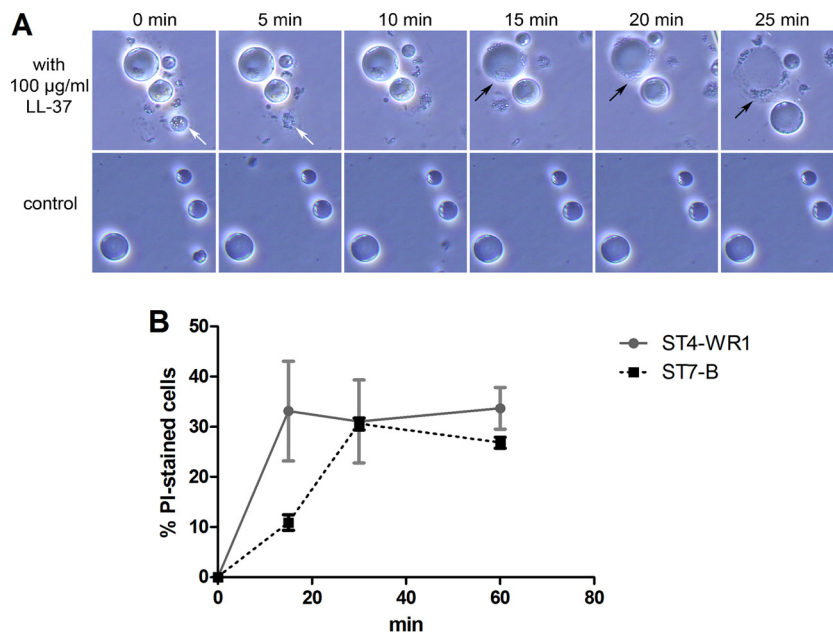


FIG 4 (A) Time lapse images of *Blastocystis* ST7-B cells treated with 100 µg/ml LL-37 (top) and controls (bottom). Images were taken every 5 min. Arrows point to cells undergoing lysis. Cells are lysed as early as 5 min after the addition of LL-37 (white arrow). (B) Time course lysis experiments using PI staining and flow cytometry were also done. Graphs show that the membrane-disrupting effect of LL-37 is faster among ST4-WR1 than among ST7-B cells.

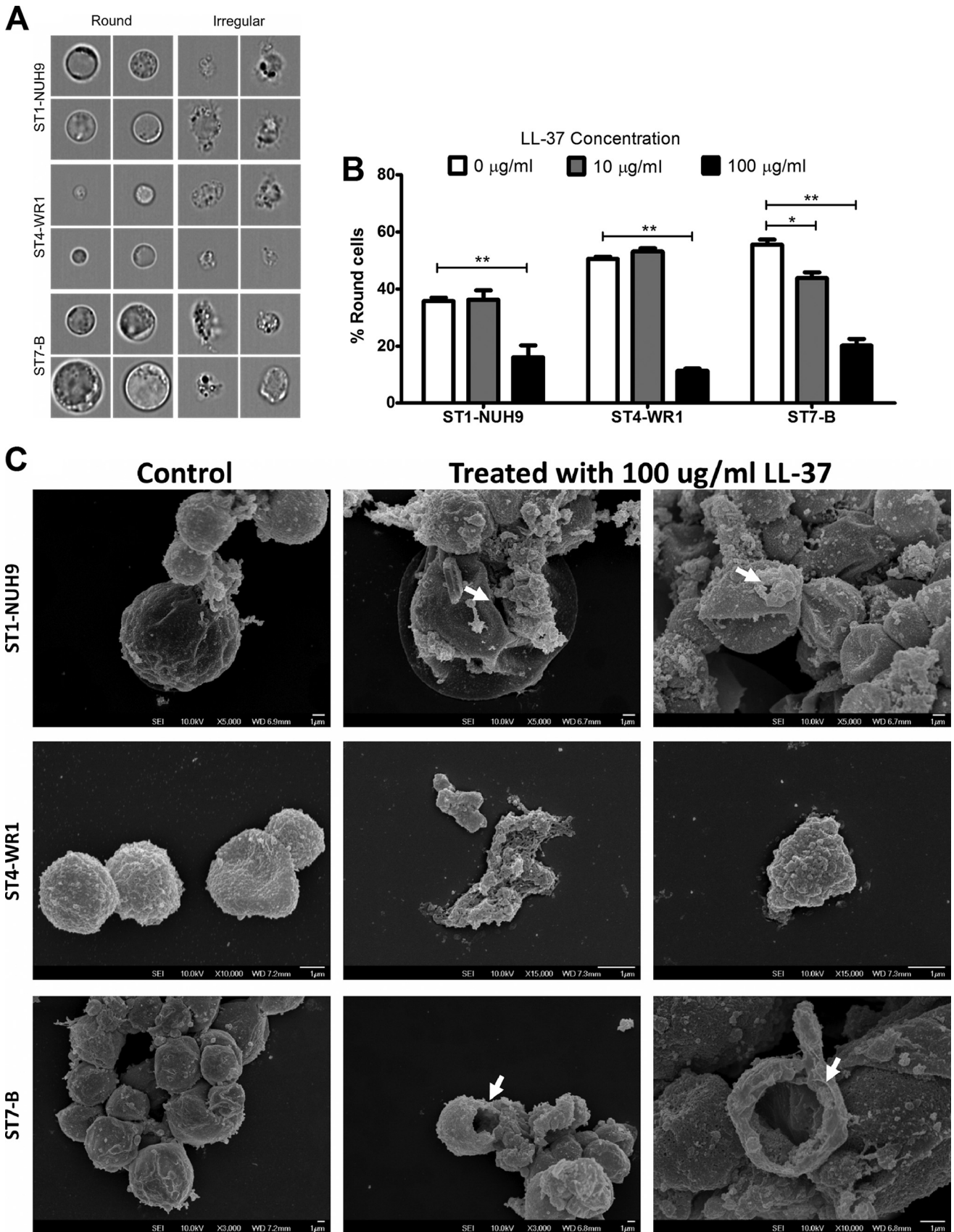


FIG 5 LL-37 causes morphological changes in *Blastocystis* isolates. *Blastocystis* cells were incubated with LL-37 for 1 h and analyzed by using an imaging flow cytometer. (A) Images show round and irregular cells, as determined by the circularity index generated by the software. (B) Bar graphs show that treatment of *Blastocystis* STs with LL-37 decreases the proportion of round cells. (C) Scanning electron micrographs also show that these cells have irregular shapes when treated with LL-37. The white arrows point to possible large membrane pores that could lead to cytoplasmic leakage. LL-37-treated *Blastocystis* ST4-WR1 cells also became highly fragmented. *, $P < 0.05$; **, $P < 0.001$.

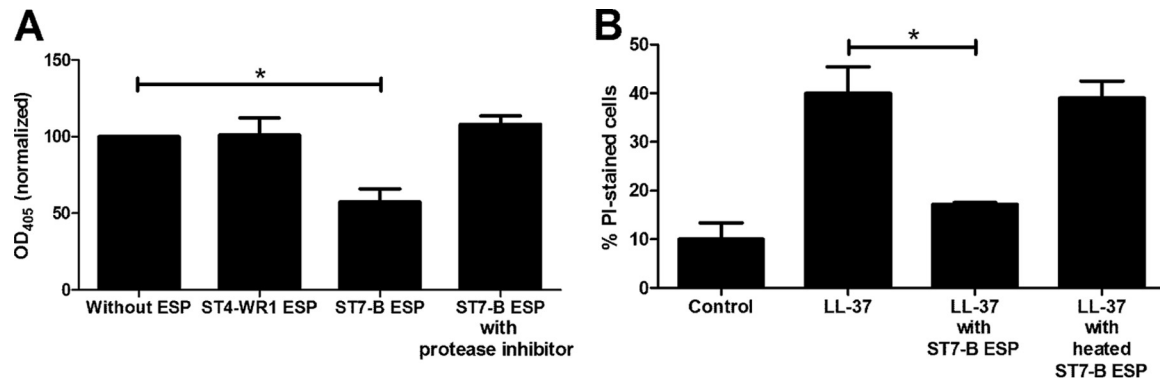


FIG 6 (A) *Blastocystis* isolate ST7-B (but not ST4-WR1) excreted-secreted products (ESPs) degrade LL-37, as shown by ELISA results. ELISA plates were coated with the LL-37 peptide, and the plates were incubated with *Blastocystis* ESPs for 2 h. Degradation was prevented when ST7-B ESPs were incubated with a protease inhibitor cocktail prior to incubation with the peptide. OD₄₀₅, optical density at 405 nm. (B) Viability experiments were also done by using LL-37 previously incubated with ST7-B ESPs. The graph shows that ST7-B ESPs attenuated LL-37 activity. This was reversed when the ESP was first heated to denature proteins. *, $P < 0.05$.

ST7-B cultures showed thicker surface coats (Fig. 8A and B). To observe the surface closely, we used transmission electron microscopy (TEM). Cationized ferritin was used to label negatively charged elements on the cell surface. Again, TEM showed a thicker surface coat for ST7-B cells than for ST4-WR1 cells (Fig. 8C to F). The coat's thickness in ST7-B cells was almost three times that of the coats in ST4-WR1 cells (Fig. 8G). Furthermore, ST7-B surface coats also appeared to be denser.

LL-37 binds more to *Blastocystis* ST4-WR1 cell surfaces than to ST7-B cell surfaces. Flow cytometry imaging was used to visualize LL-37 bound to *Blastocystis* cells (Fig. 9A). The proportion of cells with bound LL-37 was higher for ST4-WR1 than for ST7-B (Fig. 9B). Gating out for those cells with bound LL-37, we found that a high percentage of ST7-B cells was viable compared to the percentage of viable ST4-WR1 cells (Fig. 9C). The specificity of the primary antibody used was demonstrated by using LL-37-treated and untreated *Blastocystis* cells with or without the primary or secondary antibody.

DISCUSSION

Blastocystis causes large-bowel infections among humans, where it may cause diarrhea, abdominal pain, nausea, and other related symptoms. The organism is transmitted by the fecal-oral route by the means of the cyst form. Upon reaching the large intestine, it transforms into its various vegetative forms. Pathogenic events

include epithelial barrier disruption, adhesion, modulation, and evasion of host immune responses (5). Since most infections are self-limiting, it may be presumed that in these cases, *Blastocystis* is eradicated before it can colonize and penetrate the intestinal barrier. Events surrounding the removal of this parasite need to be elucidated. AMPs may be involved in these events, and therefore their possible roles in limiting *Blastocystis*-related pathologies need to be determined.

Host AMPs are important elements of innate immunity. AMP activities include membrane pore formation, which may cause cell death directly or allow other molecules to pass through the membrane and bind to intracellular targets (27). Some of these molecules are expressed by epithelial cells and provide an initial defense against invading pathogens. In this study, we explored the role of these peptides in human *Blastocystis* infections. We focused on the activity of LL-37 on *Blastocystis* after determining that this peptide has broad activity against all the *Blastocystis* STs that we tested using a screening assay (Table 1). There have been numerous studies showing the effectiveness of AMPs against bacterial, fungal, and even viral pathogens. There are, however, few studies on the action of AMPs on protistan parasites. A review (17) on the effect of AMPs on two parasites that cause the tropical diseases leishmaniasis and malaria outlined both positive and negative aspects of the use of AMPs against protists. Studies have shown that AMPs can also disrupt cellular processes in parasites (17). This makes AMPs promising candidates for drug development. Regarding the use of AMPs in human *Blastocystis* infections, one study found that analogs of an anuran skin peptide called magainin were effective against *Blastocystis hominis*, *Trypanosoma cruzi*, and *Entamoeba histolytica* (28). This 2-decade-old study showed that these AMPs can disrupt the cell membrane, leading to leakage of cell contents and, eventually, death.

Blastocystis is an enteric parasite, and it is expected to stimulate host epithelial cells to mount immune responses. For example, *Blastocystis* was found to induce nitric oxide production in epithelial cells as part of the host defense (14). In addition, *Blastocystis* could also induce epithelial cells to express antimicrobial peptides as part of the host's innate immune response. This is seen in other gastrointestinal infections by protistan parasites such as *Entamoeba* (29) and *Cryptosporidium* (30). In this study, we have also

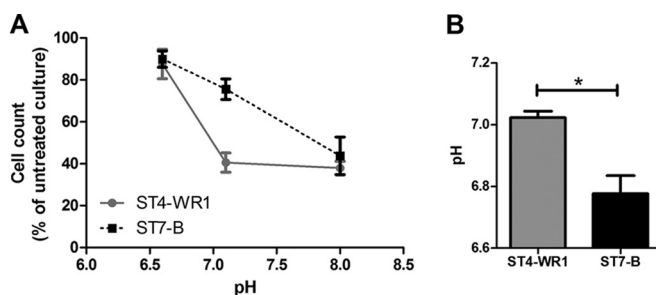


FIG 7 pH affects the activity of LL-37 on *Blastocystis*. (A) At acidic pH, LL-37 does not inhibit *Blastocystis*, while at neutral and alkaline pHs, both ST4-WR1 and ST7-B are inhibited by the AMP. (B) *Blastocystis* ST7-B (but not ST4-WR1) cultures cause the medium to be acidic after 24 h. *, $P < 0.05$.

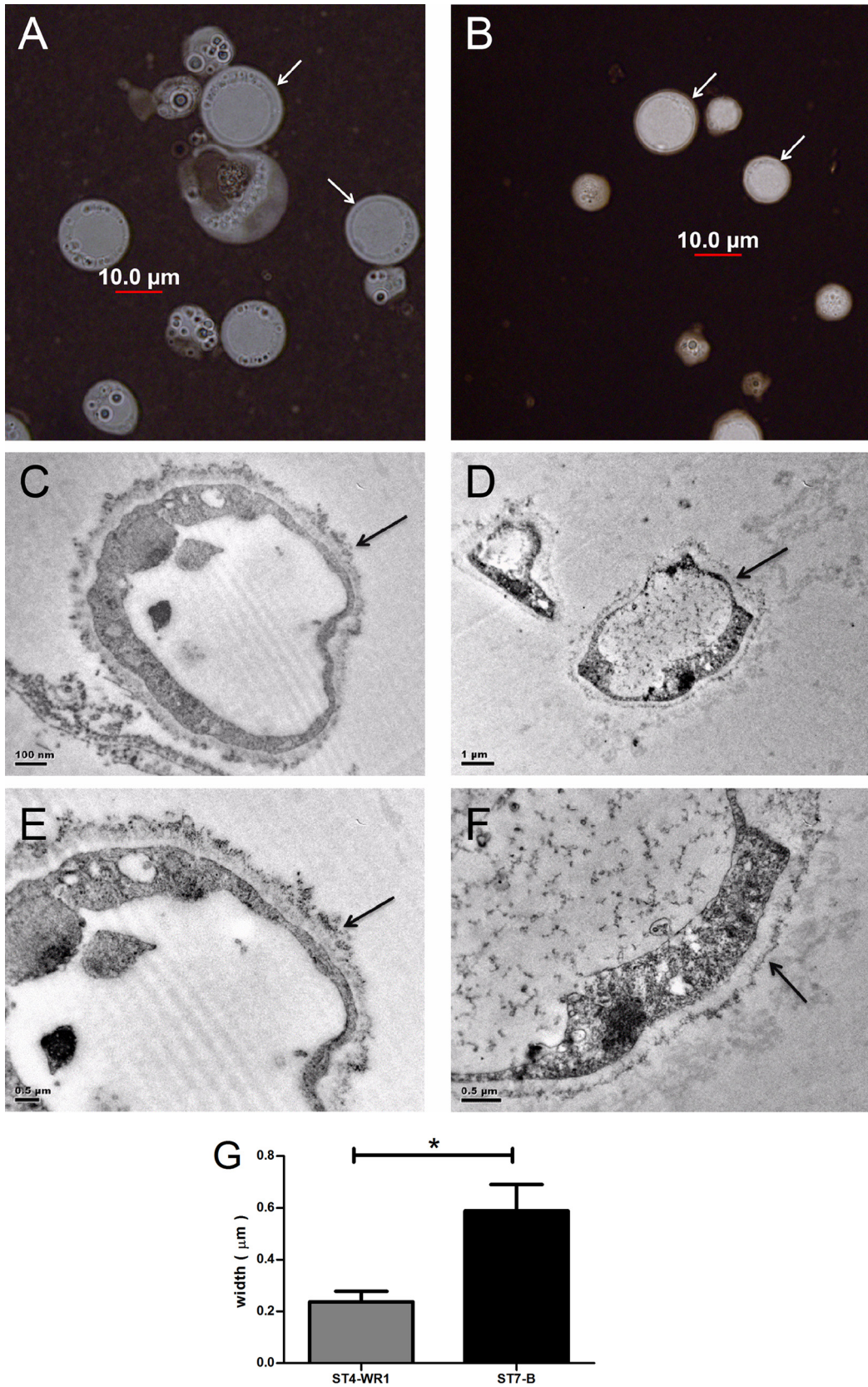


FIG 8 *Blastocystis* ST7-B cells (A, C, and E) have thicker and denser surface coats (arrows) than do ST4-WR1 cells (B, D, and F), as shown by using India ink as a negative stain for bright microscopy (A and B) and transmission electron microscopy (C, D, E, and F). (G) Images from TEM were used to measure the thickness of the surface coat. The surface coat of the ST7-B isolate is more than double the thickness of that of the ST4-WR1 isolate. *, $P < 0.05$.

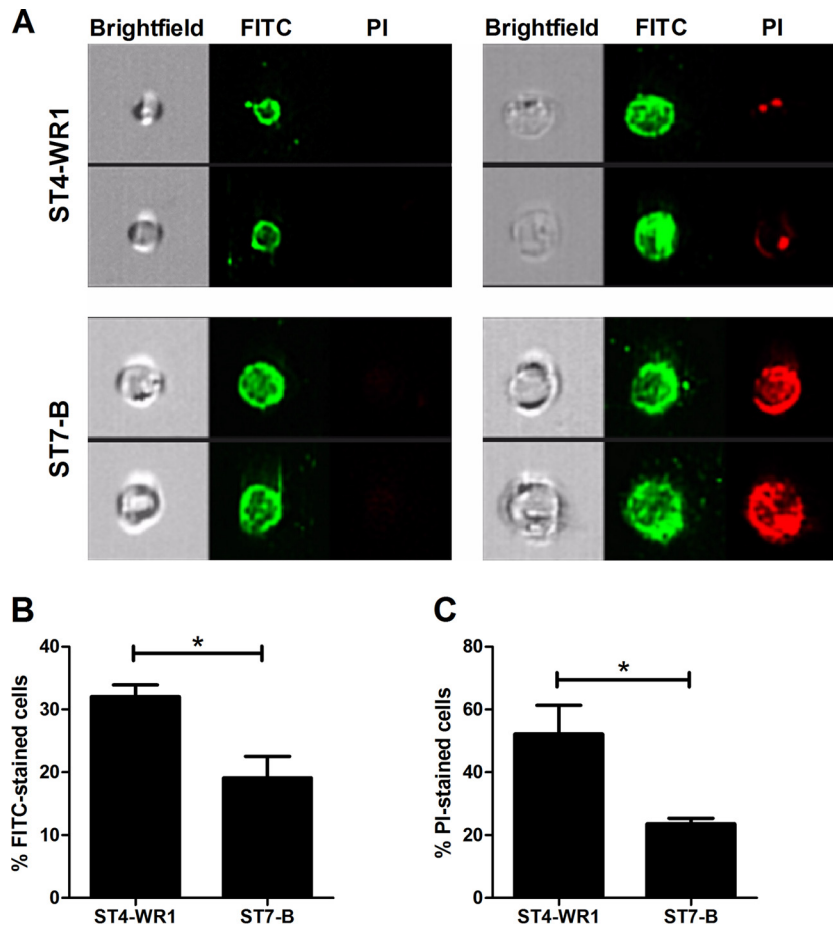


FIG 9 LL-37 binds to the cell surface of *Blastocystis*. (A) Images from the bright-field, FITC, and PI channels are displayed, showing both viable and nonviable cells with bound LL-37. LL-37 was detected by using FITC-conjugated antibodies. Viability was determined by using PI staining. (B) *Blastocystis* ST4-WR1 had a higher proportion of cells with bound LL-37 peptide. (C) Among the cells with bound LL-37, *Blastocystis* ST4-WR1 had a lower level of viability. *, $P < 0.05$.

found that all 3 represented *Blastocystis* STs are capable of inducing the expression and secretion of LL-37 by intestinal epithelial cells (Fig. 1B and C and Fig. 2). *Blastocystis* ST7-B was also able to induce LL-37 gene expression in mouse distal colon explants (Fig. 1A). This could indicate that LL-37 plays a role when *Blastocystis* tries to colonize the intestine. It is possible that LL-37 is among the first host defense peptides that are secreted in order to prevent parasite colonization and invasion. Furthermore, the differences in the abilities of the STs to induce the expression of LL-37 could also be relevant. *Blastocystis* ST1-NUH9 is relatively sensitive to LL-37 and was found to induce the highest level of secretion of LL-37 in HT-29 cells. This suggests that the pathogenic potential of ST1-NUH9 would be weaker than that of the ST7-B isolate.

As with AMP studies done on other protistan parasites, *Blastocystis* is likely to be susceptible to the direct killing effect of AMPs. As mentioned above, *Blastocystis* is composed of many subtypes showing various biological properties, and it is probable that a few STs will be resistant. Not all AMPs, however, may be effective against *Blastocystis*, although its mechanism of resistance may be different from that of prokaryotic organisms. For example, the membrane surface of *Blastocystis*, a eukaryotic organism, has a structure different from that of prokaryotes, and elements of this parasite's membrane may shield the negative charges. This differ-

ence may be a factor in the relative resistance of the parasite to antimicrobial peptide treatment. Some bacteria produce proteases that can inactivate AMPs (31–33). This may also be the case in *Blastocystis*.

In this study, resazurin-based viability assays showed that among the intestinal AMPs, only hBD-2 and LL-37 can inhibit *Blastocystis*. The effectiveness of hBD-2, however, is limited only to ST4. hBD-1 is constitutively expressed in colonic epithelial cells. It was found to kill a number of bacterial species, whether Gram negative or Gram positive (34). We did not find any inhibition when this peptide was added to *Blastocystis* cultures. hBD-1 and hBD-2 share very similar structures. A difference is found only on the tri-/disulfide motifs (35). Both motifs have been found to kill *Staphylococcus aureus* and *Escherichia coli*. It is interesting to note, therefore, that only hBD-2 can inhibit *Blastocystis*.

On the other hand, LL-37 has been found to be effective against all *Blastocystis* STs. Cathelicidins are characterized by a conserved N-terminal domain that is proteolytically cleaved to generate the mature, active peptide contained within the C terminus (36). These molecules are expressed in various immune cells, in salivary glands, and in epithelia of respiratory, digestive, and reproductive tracts, while keratinocytes and intestinal cells can be induced to enhance expression. Its main effect is pore formation in bacterial

membranes. It was also found to be capable of modulating toxic effects due to bacterial infection (37). LL-37's other activities include a chemotactic effect on blood cells, activation of histamine release from mast cells, or induction of angiogenesis (38). The absence of LL-37 has been associated with chronic periodontal disease (36). The only cathelicidin identified in humans is termed LL-37, indicating the 37-amino-acid sequence. It has been found to inhibit a number of Gram-positive, Gram-negative, and Gram-indeterminate bacterial species (39). It has also been found to cause membrane disruption with vacuolar enlargement in *Candida albicans* within 5 min (40). We have found the same effect on all representative isolates of *Blastocystis* ST1, ST4, and ST7. LL-37 causes a decrease in viability (Table 1) and membrane permeabilization, as observed by using PI staining (Fig. 5). We also observed the rapidity of LL-37 action. *Blastocystis* cells were lysed within 5 min of treatment with LL-37 (Fig. 4). The change in the morphology of cells from round to irregular was also observed by using imaging flow cytometry as well as scanning electron microscopy (Fig. 5). Our previous observation has been that irregularly shaped *Blastocystis* cells are an indication of poor health (41). LL-37, as it causes pore formation, may be responsible for the shape change in *Blastocystis* cells.

However, as determined by viability assays, the effects of LL-37 are not similar for all the isolates tested, as ST7 isolates have higher IC₅₀s (Table 1). PI staining (Fig. 3) and observed morphological changes (Fig. 5) also confirm this finding. The various effects of LL-37 on different *Blastocystis* STs suggest that its effectiveness is subtype dependent. *Blastocystis* ST7 isolates showed relative resistance compared to ST4 and ST1 isolates. We therefore attempted to identify the factors in *Blastocystis* ST7 isolates that may be responsible for their relative resistance to LL-37.

Blastocystis is known to release proteases (42, 43). Some of these proteases have been found to directly protect the parasite, such as those that can degrade antibodies (43). In this study, we have observed that the excretory-secretory products of *Blastocystis* contain proteases that can degrade LL-37. This effect was seen only in an ST7 isolate. In a sensitive strain such as ST4-WR1, this finding was not observed (Fig. 6). A study on the effect of LL-37 on an intestinal parasite, *Entamoeba histolytica*, also revealed the same outcome (29). The resistance of *E. histolytica* to LL-37 was partly due to its ability to release cysteine proteases that could degrade LL-37.

The attenuation of LL-37 by pH has been reported in previous bacterial studies. An acidic pH decreased the ability of LL-37 to kill *Staphylococcus aureus* and *Pseudomonas aeruginosa* (44). That study found that decreasing the pH from 8.0 to 6.8 can attenuate LL-37 activity. In this study, we also observed that at pH 6.5, both *Blastocystis* ST4-WR1 and ST7-B were not affected by LL-37. However, at alkaline pH (pH 8.0), both isolates became susceptible to LL-37 killing (Fig. 7A). Furthermore, we have determined that the *Blastocystis* ST7-B isolate is able to cause a change in the pH after 24 h. We have observed that the pH adjustment can go as low as pH 6.5 (Fig. 7B). This is enough to decrease the activity of LL-37 and protect the parasite from direct killing. In contrast, this pH adjustment was not seen in ST4-WR1 cultures and therefore may be a reason why this isolate is more susceptible to LL-37 attack.

Blastocystis cells feature an outer surface coat (45, 46) that has been proposed to confer protection to the parasite (5). We have observed that the characteristics of this surface can vary from one

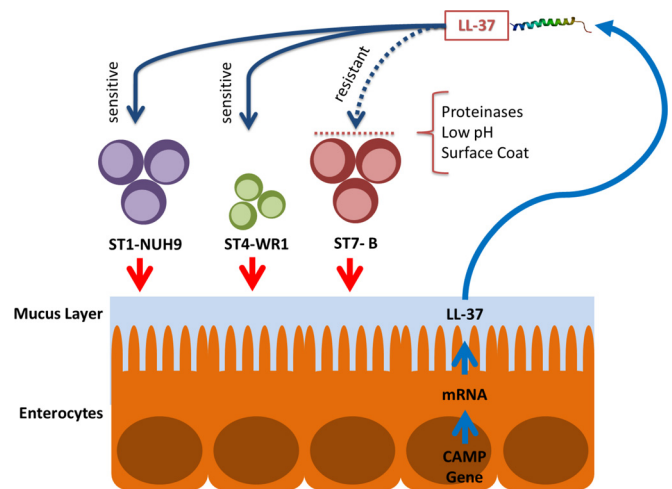


FIG 10 Interactions between *Blastocystis* subtypes and LL-37. *Blastocystis* STs induce epithelial cells to secrete LL-37. ST1 and ST4 are susceptible to LL-37 attack, while ST7 is relatively resistant. An isolate of ST7 (B isolate) is found to secrete proteases that degrade LL-37. It also decreases the pH, which decreases LL-37 activity. It also has a thicker surface coat that could possibly protect the parasite against LL-37 binding. (The LL-37 structure was obtained from RCSB Protein Data Bank [PDB] accession number 2K6O [50].)

isolate to another. Using a negative stain (India ink), we observed that the thickness of the surface coat is greater in *Blastocystis* ST7-B than in *Blastocystis* ST4-WR1 cells (Fig. 8A and B). Using transmission electron microscopy, the former also showed a denser structure than the latter (Fig. 8C to F). Recently, a study found LL-37 sequestration by a membrane-associated protein in a virulent bacterium (47). This protects the bacterium by neutralizing the activity of LL-37. It is also possible that some elements in the *Blastocystis* surface coat have the same function. LL-37 was seen to bind to the surface of the cell in the two isolates tested (ST7-B and ST4-WR1), but isolate ST7-B was less affected than ST4-WR1, as observed from the proportion of PI-stained cells (Fig. 9). It is possible that due to the thickness and density of the surface coat of the ST7-B isolate, LL-37 molecules may become trapped and may not have access to the parasite's cell membrane. This would then protect the cell from lysis.

Blastocystis ST1, along with ST3, is the most frequently detected ST in parasitological surveys in the world (8). ST4 is commonly detected in Europe. These particular STs are highly sensitive to LL-37 (Table 1 and Fig. 3 and 5). This could be one of the reasons why most *Blastocystis* infections are asymptomatic and self-limiting, as reported previously (5, 13). On the other hand, ST7-B is relatively resistant to LL-37 and is also rare in terms of being detected in human populations. This ST is also resistant to a number of drugs, including metronidazole (13, 48), and is capable of downregulating the expression of nitric oxide synthase (14), which is an essential element in the innate immune response. Isolates of ST7 have also been found to cause epithelial barrier disruption and have more adhesive properties in cell cultures (49), thereby making this ST potentially more pathogenic than the rest of the STs. Increases in prevalence rates of *Blastocystis* ST7 isolates therefore would pose greater risks to the population.

In conclusion, this study explored the interactions between *Blastocystis* and the antimicrobial peptide LL-37 (Fig. 10). This is the first study to determine the effects of an important element in

innate immunity to *Blastocystis*, a common eukaryote found in the human colon. Our *ex vivo* and *in vitro* culture experiments indicate that LL-37 is a significant molecule secreted by the host during *Blastocystis* infections. We have also shown for the first time that *Blastocystis* isolates are susceptible to the effects of LL-37. The ST7-B isolate is able to alleviate the detrimental effects of this AMP by various modes: first by the secretion of proteases that degrade LL-37 and second by making its environment acidic, which is enough to attenuate LL-37 activity. We also speculate on the protective function of the parasite's surface coat against AMPs. This study further differentiates the subtypes of *Blastocystis*, particularly regarding host immune responses and the parasite's ability to evade these responses.

ACKNOWLEDGMENTS

We are grateful to Geok Choo Ng, Josephine Howe, Zhaona Wu, and Wan Ni Chia for technical assistance.

J.A.Y. acknowledges the generous Graduate Research Scholarship grant from the National University of Singapore.

FUNDING INFORMATION

This work, including the efforts of John Anthony Yason, Sitara Swarna Rao Ajampur, and Kevin Shyong Wei Tan, was funded by MOH | National Medical Research Council (NMRC).

REFERENCES

- Clark CG, van der Giezen M, Alfellani MA, Stensvold CR. 2013. Recent developments in *Blastocystis* research. *Adv Parasitol* 82:1–32. <http://dx.doi.org/10.1016/B978-0-12-407706-5.00001-0>.
- Scanlan PD, Stensvold CR, Rajilić-Stojanović M, Heilig HGJ, De Vos WM, O'Toole PW, Cotter PD. 2014. The microbial eukaryote *Blastocystis* is a prevalent and diverse member of the healthy human gut microbiota. *FEMS Microbiol Ecol* 90:326–330. <http://dx.doi.org/10.1111/1574-6941.12396>.
- Bart A, Wentink-Bonnema EM, Gilis H, Verhaar N, Wassenaar CJ, van Vugt M, Goorhuis A, van Gool T. 2013. Diagnosis and subtype analysis of *Blastocystis* sp. in 442 patients in a hospital setting in the Netherlands. *BMC Infect Dis* 13:389. <http://dx.doi.org/10.1186/1471-2334-13-389>.
- Stensvold CR, Suresh GK, Tan KSW, Thompson RCA, Traub RJ, Viscogliosi E, Yoshikawa H, Clark CG. 2007. Terminology for *Blastocystis* subtypes—a consensus. *Trends Parasitol* 23:93–96. <http://dx.doi.org/10.1016/j.pt.2007.01.004>.
- Tan KSW. 2008. New insights on classification, identification, and clinical relevance of *Blastocystis* spp. *Clin Microbiol Rev* 21:639–665. <http://dx.doi.org/10.1128/CMR.00022-08>.
- Coyle CM, Varughese J, Weiss LM, Tanowitz HB. 2012. *Blastocystis*: to treat or not to treat. *Clin Infect Dis* 54:105–110. <http://dx.doi.org/10.1093/cid/cir810>.
- Poirier P, Wawrzyniak I, Vivarès CP, Delbac F, El Alaoui H. 2012. New insights into *Blastocystis* spp.: a potential link with irritable bowel syndrome. *PLoS Pathog* 8:e1002545. <http://dx.doi.org/10.1371/journal.ppat.1002545>.
- Alfellani MA, Stensvold CR, Vidal-Lapiedra A, Onuoha ESU, Fagbenro-Beyioku AF, Clark CG. 2013. Variable geographic distribution of *Blastocystis* subtypes and its potential implications. *Acta Trop* 126:11–18. <http://dx.doi.org/10.1016/j.actatropica.2012.12.011>.
- Ramírez JD, Sánchez A, Hernández C, Flórez C, Bernal MC, Giraldo JC, Reyes P, López MC, García L, Cooper PJ, Vicuña Y, Mongi F, Casero RD. 2016. Geographic distribution of human *Blastocystis* subtypes in South America. *Infect Genet Evol* 41:32–35. <http://dx.doi.org/10.1016/j.meegid.2016.03.017>.
- Mirza H, Tan KSW. 2009. *Blastocystis* exhibits inter- and intra-subtype variation in cysteine protease activity. *Parasitol Res* 104:355–361. <http://dx.doi.org/10.1007/s00436-008-1203-1>.
- Ramírez JD, Sánchez LV, Bautista DC, Corredor AF, Flórez AC, Stensvold CR. 2014. *Blastocystis* subtypes detected in humans and animals from Colombia. *Infect Genet Evol* 22:223–228. <http://dx.doi.org/10.1016/j.meegid.2013.07.020>.
- Roberts T, Stark D, Harkness J, Ellis J. 2013. Subtype distribution of *Blastocystis* isolates from a variety of animals from New South Wales, Australia. *Vet Parasitol* 196:85–89. <http://dx.doi.org/10.1016/j.vetpar.2013.01.011>.
- Roberts T, Stark D, Harkness J, Ellis J. 2014. Update on the pathogenic potential and treatment options for *Blastocystis* sp. *Gut Pathog* 6:17. <http://dx.doi.org/10.1186/1757-4749-6-17>.
- Mirza H, Wu Z, Kidwai F, Tan KSW. 2011. A metronidazole-resistant isolate of *Blastocystis* spp. is susceptible to nitric oxide and downregulates intestinal epithelial inducible nitric oxide synthase by a novel parasite survival mechanism. *Infect Immun* 79:5019–5026. <http://dx.doi.org/10.1128/IAI.05632-11>.
- Safadi DE, Meloni D, Poirier P, Osman M, Cian A, Gaayeb L, Wawrzyniak I, Delbac F, Alaoui HE, Delhaes L, Dei-Cas E, Mallat H, Daboussi F, Hamze M, Viscogliosi E. 2013. Molecular epidemiology of *Blastocystis* in Lebanon and correlation between subtype 1 and gastrointestinal symptoms. *Am J Trop Med Hyg* 88:1203–1206. <http://dx.doi.org/10.4269/ajtmh.12-0777>.
- Zanetti M. 2004. Cathelicidins, multifunctional peptides of the innate immunity. *J Leukoc Biol* 75:39–48.
- Torrent M, Pulido D, Rivas L, Andreu D. 2012. Antimicrobial peptide action on parasites. *Curr Drug Targets* 13:1138–1147. <http://dx.doi.org/10.2174/138945012802002393>.
- Yin LM, Edwards MA, Li J, Yip CM, Deber CM. 2012. Roles of hydrophobicity and charge distribution of cationic antimicrobial peptides in peptide-membrane interactions. *J Biol Chem* 287:7738–7745. <http://dx.doi.org/10.1074/jbc.M111.303602>.
- Kahlenberg JM, Kaplan MJ. 2013. Little peptide, big effects: the role of LL-37 in inflammation and autoimmune disease. *J Immunol* 191:4895–4901. <http://dx.doi.org/10.4049/jimmunol.1302005>.
- Bevens CL, Salzman NH. 2011. Paneth cells, antimicrobial peptides and maintenance of intestinal homeostasis. *Nat Rev Microbiol* 9:356–368. <http://dx.doi.org/10.1038/nrmicro2546>.
- Chen XQ, Singh M, Ho LC, Tan SW, Ng GC, Moe KT, Yap EH. 1997. Description of a *Blastocystis* species from *Rattus norvegicus*. *Parasitol Res* 83:313–318. <http://dx.doi.org/10.1007/s004360050255>.
- Ho LC, Singh M, Suresh G, Ng GC, Yap EH. 1993. Axenic culture of *Blastocystis hominis* in Iscove's modified Dulbecco's medium. *Parasitol Res* 79:614–616. <http://dx.doi.org/10.1007/BF00932249>.
- Wong KHS, Ng GC, Lin RTP, Yoshikawa H, Taylor MB, Tan KSW. 2008. Predominance of subtype 3 among *Blastocystis* isolates from a major hospital in Singapore. *Parasitol Res* 102:663–670. <http://dx.doi.org/10.1007/s00436-007-0808-0>.
- Noël C, Dufernez F, Gerbod D, Edgcomb VP, Delgado-Viscogliosi P, Ho L-C, Singh M, Wintjens R, Sogin ML, Capron M, Pierce R, Zenner L, Viscogliosi E. 2005. Molecular phylogenies of *Blastocystis* isolates from different hosts: implications for genetic diversity, identification of species, and zoonosis. *J Clin Microbiol* 43:348–355. <http://dx.doi.org/10.1128/JCM.43.1.348-355.2005>.
- Poirier P, Meloni D, Nourrisson C, Wawrzyniak I, Viscogliosi E, Livrelli V, Delbac F. 2014. Molecular subtyping of *Blastocystis* spp. using a new rDNA marker from the mitochondria-like organelle genome. *Parasitology* 141:670–681. <http://dx.doi.org/10.1017/S0031182013001996>.
- Souza WD, Arguello C, Martínez-Palomo A, Trissl D, González-Robles A, Chiari E. 1977. Surface charge of *Trypanosoma cruzi*. Binding of cationized ferritin and measurement of cellular electrophoretic mobility. *J Eukaryot Microbiol* 24:411–415.
- Peters BM, Shirliff ME, Jabra-Rizk MA. 2010. Antimicrobial peptides: primeval molecules or future drugs? *PLoS Pathog* 6:e1001067. <http://dx.doi.org/10.1371/journal.ppat.1001067>.
- Huang CM, Chen HC, Zierdt CH. 1990. Magainin analogs effective against pathogenic protozoa. *Antimicrob Agents Chemother* 34:1824–1826. <http://dx.doi.org/10.1128/AAC.34.9.1824>.
- Cobo ER, He C, Hirata K, Hwang G, Tran U, Eckmann L, Gallo RL, Reed SL. 2012. *Entamoeba histolytica* induces intestinal cathelicidins but is resistant to cathelicidin-mediated killing. *Infect Immun* 80:143–149. <http://dx.doi.org/10.1128/IAI.05029-11>.
- Giacometti A, Cirioni O, Del Prete MS, Skerlavaj B, Circo R, Zanetti M, Scalise G. 2003. In vitro effect on *Cryptosporidium parvum* of short-term exposure to cathelicidin peptides. *J Antimicrob Chemother* 51:843–847. <http://dx.doi.org/10.1093/jac/dkg149>.
- Schmidtchen A, Frick I-M, Andersson E, Tapper H, Björck L. 2002. Proteinases of common pathogenic bacteria degrade and inactivate the

- antibacterial peptide LL-37. *Mol Microbiol* 46:157–168. <http://dx.doi.org/10.1046/j.1365-2958.2002.03146.x>.
32. Thwaite JE, Hibbs S, Titball RW, Atkins TP. 2006. Proteolytic degradation of human antimicrobial peptide LL-37 by *Bacillus anthracis* may contribute to virulence. *Antimicrob Agents Chemother* 50:2316–2322. <http://dx.doi.org/10.1128/AAC.01488-05>.
 33. Sieprawska-Lupa M, Mydel P, Krawczyk K, Wójcik K, Puklo M, Lupa B, Suder P, Silberring J, Reed M, Pohl J, Shafer W, McAleese F, Foster T, Travis J, Potempa J. 2004. Degradation of human antimicrobial peptide LL-37 by *Staphylococcus aureus*-derived proteinases. *Antimicrob Agents Chemother* 48:4673–4679. <http://dx.doi.org/10.1128/AAC.48.12.4673-4679.2004>.
 34. Ho S, Pothoulakis C, Koon HW. 2013. Antimicrobial peptides and colitis. *Curr Pharm Des* 19:40–47.
 35. Selsted ME, Tang YQ, Morris WL, McGuire PA, Novotny MJ, Smith W, Henschen AH, Cullor JS. 1993. Purification, primary structures, and antibacterial activities of beta-defensins, a new family of antimicrobial peptides from bovine neutrophils. *J Biol Chem* 268:6641–6648.
 36. Wiesner J, Vilcinskas A. 2010. Antimicrobial peptides: the ancient arm of the human immune system. *Virulence* 1:440–464. <http://dx.doi.org/10.4161/viru.1.5.12983>.
 37. Bucki R, Leszczyńska K, Namiot A, Sokołowski W. 2010. Cathelicidin LL-37: a multitask antimicrobial peptide. *Arch Immunol Ther Exp (Warsz)* 58:15–25. <http://dx.doi.org/10.1007/s00005-009-0057-2>.
 38. Jäger S, Stange EF, Wehkamp J. 2013. Antimicrobial peptides and inflammatory bowel disease, p 255–273. *In* Hiemstra PS, Zaai SAJ (ed), *Antimicrobial peptides and innate immunity*. Springer, Basel, Switzerland.
 39. Vandamme D, Landuyt B, Luyten W, Schoofs L. 2012. A comprehensive summary of LL-37, the factotum human cathelicidin peptide. *Cell Immunol* 280:22–35. <http://dx.doi.org/10.1016/j.cellimm.2012.11.009>.
 40. Ordóñez SR, Amarullah IH, Wubbolts RW, Veldhuizen EJA, Haagsman HP. 2014. Fungicidal mechanisms of cathelicidins LL-37 and CATH-2 revealed by live-cell imaging. *Antimicrob Agents Chemother* 58:2240–2248. <http://dx.doi.org/10.1128/AAC.01670-13>.
 41. Yason JA, Tan KSW. 2015. Seeing the whole elephant: imaging flow cytometry reveals extensive morphological diversity within *Blastocystis* isolates. *PLoS One* 10:e0143974. <http://dx.doi.org/10.1371/journal.pone.0143974>.
 42. Sio SWS, Puthia MK, Lee ASY, Lu J, Tan KSW. 2006. Protease activity of *Blastocystis hominis*. *Parasitol Res* 99:126–130. <http://dx.doi.org/10.1007/s00436-006-0131-1>.
 43. Puthia MK, Vaithilingam A, Lu J, Tan KSW. 2005. Degradation of human secretory immunoglobulin A by *Blastocystis*. *Parasitol Res* 97:386–389. <http://dx.doi.org/10.1007/s00436-005-1461-0>.
 44. Alaiwa MHA, Reznikov LR, Gansemer ND, Sheets KA, Horswill AR, Stoltz DA, Zabner J, Welsh MJ. 2014. pH modulates the activity and synergism of the airway surface liquid antimicrobials β-defensin-3 and LL-37. *Proc Natl Acad Sci U S A* 111:18703–18708. <http://dx.doi.org/10.1073/pnas.1422091112>.
 45. Zaman V, Howe J, Ng M, Goh TK. 1999. Scanning electron microscopy of the surface coat of *Blastocystis hominis*. *Parasitol Res* 85:974–976. <http://dx.doi.org/10.1007/s004360050668>.
 46. Lanuza MD, Carbajal JA, Borrás R. 1996. Identification of surface coat carbohydrates in *Blastocystis hominis* by lectin probes. *Int J Parasitol* 26:527–532. [http://dx.doi.org/10.1016/0020-7519\(96\)00010-0](http://dx.doi.org/10.1016/0020-7519(96)00010-0).
 47. LaRock CN, Döhrmann S, Todd J, Corriden R, Olson J, Johannessen T, Lepenies B, Gallo RL, Ghosh P, Nizet V. 2015. Group A streptococcal M1 protein sequesters cathelicidin to evade innate immune killing. *Cell Host Microbe* 18:471–477. <http://dx.doi.org/10.1016/j.chom.2015.09.004>.
 48. Mirza H, Teo JDW, Upcroft J, Tan KSW. 2011. A rapid, high-throughput viability assay for *Blastocystis* spp. reveals metronidazole resistance and extensive subtype-dependent variations in drug susceptibilities. *Antimicrob Agents Chemother* 55:637–648. <http://dx.doi.org/10.1128/AAC.00900-10>.
 49. Wu Z, Mirza H, Tan KSW. 2014. Intra-subtype variation in enteroadhesion accounts for differences in epithelial barrier disruption and is associated with metronidazole resistance in *Blastocystis* subtype-7. *PLoS Negl Trop Dis* 8:e2885. <http://dx.doi.org/10.1371/journal.pntd.0002885>.
 50. Wang G. 2008. Structures of human host defense cathelicidin LL-37 and its smallest antimicrobial peptide KR-12 in lipid micelles. *J Biol Chem* 283:32637–32643. <http://dx.doi.org/10.1074/jbc.M805533200>.

RESEARCH ARTICLE

Seeing the Whole Elephant: Imaging Flow Cytometry Reveals Extensive Morphological Diversity within *Blastocystis* Isolates

John Anthony Yason, Kevin Shyong Wei Tan*

Department of Microbiology, Yong Loo Lin School of Medicine, National University of Singapore, Singapore, Singapore

* kevin_tan@nuhs.edu.sg



CrossMark
click for updates

OPEN ACCESS

Citation: Yason JA, Tan KSW (2015) Seeing the Whole Elephant: Imaging Flow Cytometry Reveals Extensive Morphological Diversity within *Blastocystis* Isolates. PLoS ONE 10(11): e0143974. doi:10.1371/journal.pone.0143974

Editor: Nikolas Nikolaidis, California State University Fullerton, UNITED STATES

Received: August 11, 2015

Accepted: November 11, 2015

Published: November 30, 2015

Copyright: © 2015 Yason, Tan. This is an open access article distributed under the terms of the [Creative Commons Attribution License](https://creativecommons.org/licenses/by/4.0/), which permits unrestricted use, distribution, and reproduction in any medium, provided the original author and source are credited.

Data Availability Statement: Data are from the Blastocystis ImageStream study may be assessed at: <http://dx.doi.org/10.5281/zenodo.32605>.

Funding: The work was generously funded by a grant from the National University of Singapore (R-182-000-710-733). The funders had no role in study design, data collection and analysis, decision to publish, or preparation of the manuscript. JAY acknowledges the generous research scholarship from the National University of Singapore.

Competing Interests: The authors have declared that no competing interests exist.

Abstract

Blastocystis is a common protist isolated in humans and many animals. The parasite is a species complex composed of 19 subtypes, 9 of which have been found in humans. There are biological and molecular differences between *Blastocystis* subtypes although microscopy alone is unable to distinguish between these subtypes. *Blastocystis* isolates also display various morphological forms. Several of these forms, however, have not been properly evaluated on whether or not these play significant functions in the organism's biology. In this study, we used imaging flow cytometry to analyze morphological features of *Blastocystis* isolates representing 3 subtypes (ST1, ST4 and ST7). We also employed fluorescence dyes to discover new cellular features. The profiles from each of the subtypes exhibit considerable differences with the others in terms of shape, size and granularity. We confirmed that the classical vacuolar form comprises the majority in all three subtypes. We have also evaluated other morphotypes on whether these represent distinct life stages in the parasite. Irregularly-shaped cells were identified but all of them were found to be dying cells in one isolate. Granular forms were present as a continuum in both viable and non-viable populations, with non-viable forms displaying higher granularity. By analyzing the images, rare morphotypes such as multinucleated cells could be easily observed and quantified. These cells had low granularity and lower DNA content. Small structures containing nucleic acid were also identified. We discuss the possible biological implications of these unusual forms.

Introduction

Blastocystis spp. are protistan parasites found in humans and many types of animals. It is the most commonly isolated eukaryote in humans [1,2]. *Blastocystis* is a species complex comprising 19 subtypes (STs). ST1-9 have been found in humans and, with the exception of ST9, in other animal hosts as well. *Blastocystis* ST1 and ST3 are most frequently isolated, but there is geographical diversity in global distribution. For example, ST4 is common in Europe but not in the rest of the world [3]. ST2 and ST6 had a higher occurrence than ST3 in a study in Colombia

[4] and ST4 has not been detected at all. This was also the case in a study in Argentina [5]. ST9 had the lowest occurrence and was only found in Denmark and Japan [3]. Subtypes of *Blastocystis* can be determined by genetic analyses, but STs also exhibit differences in size, morphology, growth in culture, host range, drug resistance, host immune response, adhesion to host cells and protease activities [6–10]. Studies have also indicated that ST identity may determine symptomatology and pathogenic potential [5,11]. While its pathogenicity is still yet to be elucidated, *Blastocystis* has been associated with gastrointestinal diseases [11]. It has also been implicated in waterborne disease outbreaks [12,13]. Due to its ubiquity and numerous animal hosts, it has the potential to be a threat in public health.

The conventional method for detection of *Blastocystis* is by microscopic observation in clinical (mainly fecal specimens) and environmental samples. This method, however, is not adequate to differentiate *Blastocystis* STs [6,14,15]. Under the microscope, *Blastocystis* appear round with a prominent central vacuole. The cytoplasm is usually located at the edges where the nucleus (or several nuclei) and other organelles can be found. Granular forms can also be observed and some multi-vacuolar forms have been reported [6,16]. Irregularly-shaped cells are also seen and these have been labelled as amoeboid forms in some studies [6,16,17].

There have been controversies on the life cycle of *Blastocystis* [18–21]. This is partly due to the unknown status of several morphological forms observed both in culture and clinical samples. For example, multivacuolar forms have been thought as *Blastocystis* undergoing multiple fission or schizogony similar to what happens in other protistan parasites [18]. There are also suggestions that amoeboid forms may undergo plasmotomy [22]. Whether or not granular forms have specific biological functions is still yet to be discovered [16]. There was also a report on granular amoeboid forms expelling small granules in xenic cultures [16]. The authors however did not investigate further if these granules represent reproductive stages. Currently, only binary fission has been accepted as the type of reproduction in *Blastocystis* since only this mode has been observed. Other investigators also suggest that other forms may be artefacts and do not represent reproductive stages [1,6,23]. There is, however, an interest on looking for alternative modes of reproduction. For some, binary fission alone could not explain the high number of cells in cultures and in fecal specimens [18]. Just like the parable of the blind men and the elephant, various groups have reported on distinct forms without taking into consideration the morphological complexity of the parasite. This often leads to biases and confusion in the *Blastocystis* field. There is therefore a need to evaluate morphological forms exhibited by *Blastocystis* in terms of their biological importance.

In this study, we used an imaging flow cytometer to survey the morphological characteristics of 3 *Blastocystis* subtypes (ST1, ST4 and ST7). The Amnis ImageStream Mark II is capable of acquiring thousands of images in a sample. These images can then be analyzed based on specific characteristics such as size, aspect ratio, fluorescence staining intensity, etc. We applied this technique to characterize morphological features such as shape, size, granularity and location of nuclei that can differentiate one subtype from the others. We also used fluorescence dyes to visualize cellular structures such as vacuoles and nuclei. We then calculated for the proportions of cells showing these features. This study is the first to provide a comprehensive and unbiased overview of the various morphological forms of *Blastocystis* in culture and sheds new light on the roles of certain forms of the parasite.

Methods

Parasite Axenic Cultivation

Blastocystis NUH9, WR1 and B isolates were maintained in 9ml Hyclone Iscove's Modified Dulbecco Medium (IMDM) (GE Healthcare Life Sciences, Logan, UT) supplemented with 10%

horse serum (Life Technologies, Grand Island, NY). These isolates were previously axenized [24–26]. NUH9 was isolated during a health screening from an asymptomatic patient [26]; WR1 from Wistar rat [24]; and B from a patient complaining of diarrhea [25,27]. *Blastocystis* complete medium were pre-reduced for at least 12 hrs before use. Culture tubes were kept in 5-L anaerobic jars with anaerogen gas pack (Oxoid, Basingtoke, UK) at 37°C.

Ethics Statement

Blastocystis isolate B was obtained from an existing collection at the Department of Microbiology of the National University of Singapore (NUS). Human isolates were obtained from patients at the Singapore General Hospital in the early 1990s, before Institutional Review Board was established in NUS. NUH9 was isolated in 2007 from stool samples submitted for routine health screening and approval from the National Healthcare Group Institutional Review Board was obtained before project commencement. All samples were anonymized.

Subtyping of *Blastocystis* Isolates

The isolates were previously genotyped using primers based on the organism's small sub-unit ribosomal RNA (SSU rRNA) gene [26,28]. We also confirmed the isolates' subtypes using PCR protocol based on DNA from the parasite's mitochondria-like organelle (MLO) [29]. Total DNA were extracted from 1×10^6 cells using Qiagen DNA stool kit (Qiagen, Hilden, Germany) following the manufacturer's instructions. PCR was performed using Q5 High-Fidelity 2X Master Mix (New England BioLabs, Ipswich, MA) with 500 ng of DNA sample. All PCR runs were completed using BioRad iQ5 thermocycler (Hercules, CA). PCR products were sequenced and compared to National Center for Biotechnology Information (NCBI) (USA) nucleotide sequence database to confirm subtype identities.

Fluorescence Staining and Imaging Flow Cytometry

In order to analyze cultures at the same stage of growth, 2-day old cultures of *Blastocystis* isolates WR1 and B and 7-day old culture of isolate NUH9 were harvested. The cells were washed twice by centrifugation at $1,000 \times g$ using warm PBS. 2×10^7 cells in 200 μ L PBS were collected into 1.5 μ L microtubes. The cell suspensions were then stained with 1 μ g/mL propidium iodide (PI) (BioVision, Mountain View, CA), 5 μ M carboxyfluorescein succinimidyl ester (CFSE) (Life Technologies, Eugene, OR) and 1 μ g/mL Hoechst 33342 (Life Technologies, Eugene, OR) for 15 mins. PI stain was used to select for viable and non-viable cells. Cells will only take up PI when there is membrane disruption. CFSE is used in proliferation studies and is found to stain vacuolar compartments of *Blastocystis* [8]. Hoechst stains the DNA and is useful for cell-cycle analyses. Actively dividing cells will have higher emission while dying cells undergoing DNA fragmentation will have lower fluorescence readings. The cells were then washed to remove excess stains and fixed in 2% formaldehyde. Single stained cells were also prepared and used to create a compensation matrix. *Blastocystis* cell suspension heated to 80°C for 15 mins was used as positive control for PI-staining. We used Amnis ImageStream MarkII (Merck Millipore, Seattle, WA) with 4-laser attachment (375, 488, 561 and 642) to acquire *Blastocystis* cell images. 2,000 events were obtained with low flow speed at 60x magnification. Images at extended depth of field (EDF) setting were also acquired. EDF involves deconvolution to obtain highly focused images. Gating strategy involved selecting for focused cells using RMS gradient values, then for single cells using brightfield aspect ratio (Fig 1). Viable *Blastocystis* cells were identified as those without PI-staining. Cell shapes were characterized using aspect ratios from brightfield and CFSE staining. Acquisition was done using 3 different batches of cultures. Analysis of images was performed using IDEAS software version 6.1.

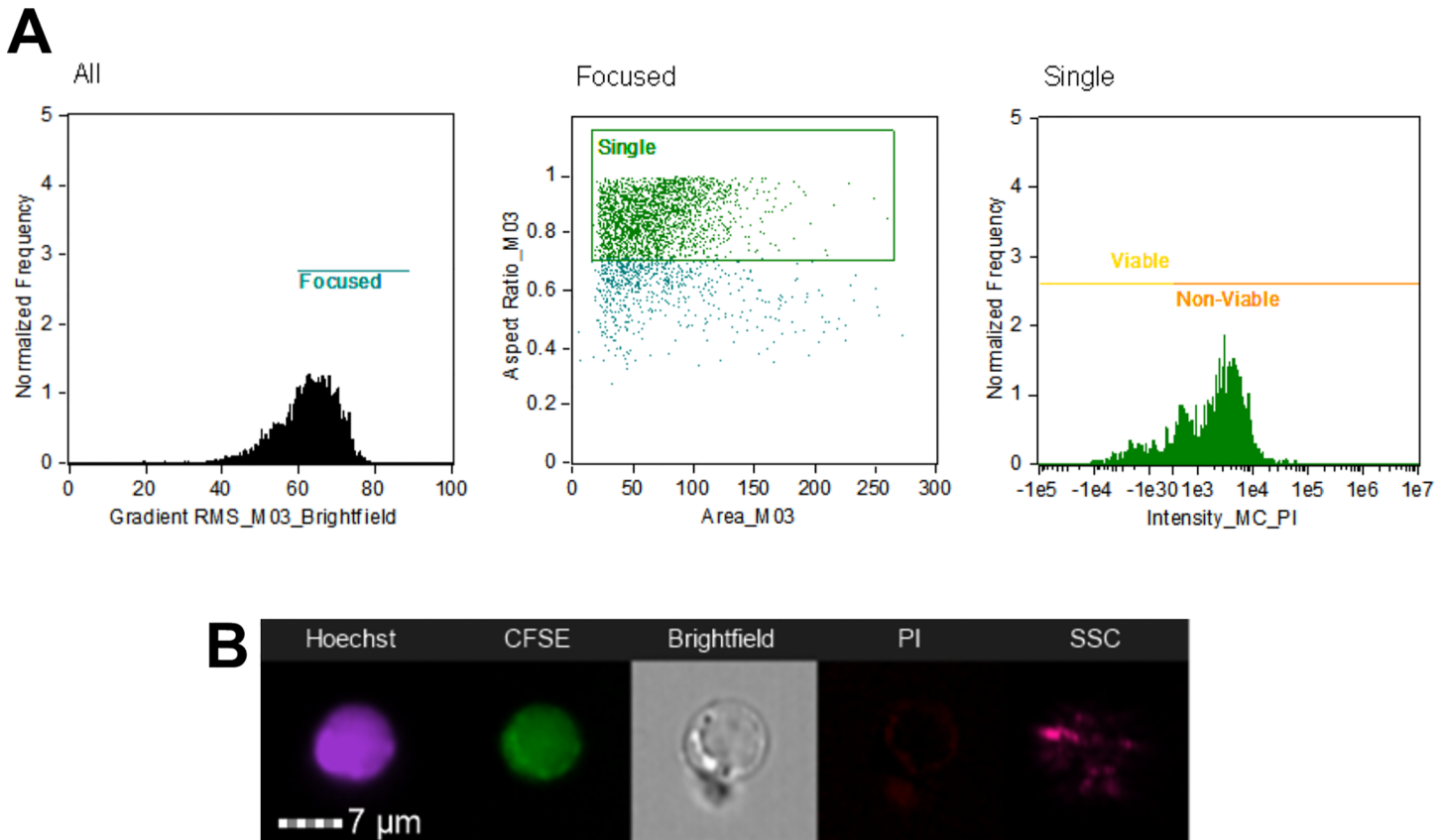


Fig 1. Initial gating strategy to analyze *Blastocystis* cells. Cells were gated for focused cells using brightfield channel, then selection of single cells using aspect ratio and area units, and finally to classify viable and non-viable cells using PI-staining characteristics. The above graphs shows the analysis for *Blastocystis* ST1-NUH9 isolate (A). Subsequent analyses made use of features arising from Hoechst and CFSE staining characteristics as well as features from brightfield and side-scatter channels (B).

doi:10.1371/journal.pone.0143974.g001

Statistical Analyses

The proportion of populations based on shape and granularity were analysed for significant differences using Student's two-tailed T-test. Hoechst-staining differences between groups based on circularity were analysed for significance using ANOVA. Statistical analyses were done using GraphPad Prism 5.0

Results and Discussion

Blastocystis cultures of NUH9, WR1 and B isolates were harvested at the log phase of their corresponding growth curves. NUH9 has the slowest growth rate and cultures from this isolate were harvested after 7 days. Two-day old WR1 and B cultures were collected and used in the experiment. Subtyping of the isolates using MLO-based primers confirmed the identities of the isolates used: NUH9 is ST1, WR1 is ST4 and B is ST7. This step also made certain that each culture contain only one isolate/ST and was not contaminated by others.

Using imaging flow cytometry, both round and irregular shapes were found in all *Blastocystis* isolates (Figs 2A and 3). The proportion of these shapes however differs from one subtype to another. Viable *Blastocystis* ST1-NUH9 is exclusively round, but only 76% round (the rest are irregular) in non-viable cells. Viable *Blastocystis* ST4-WR1 and ST7-B isolates are 83% and

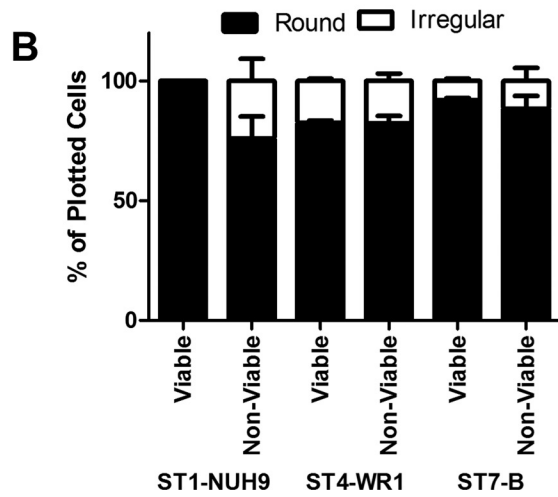
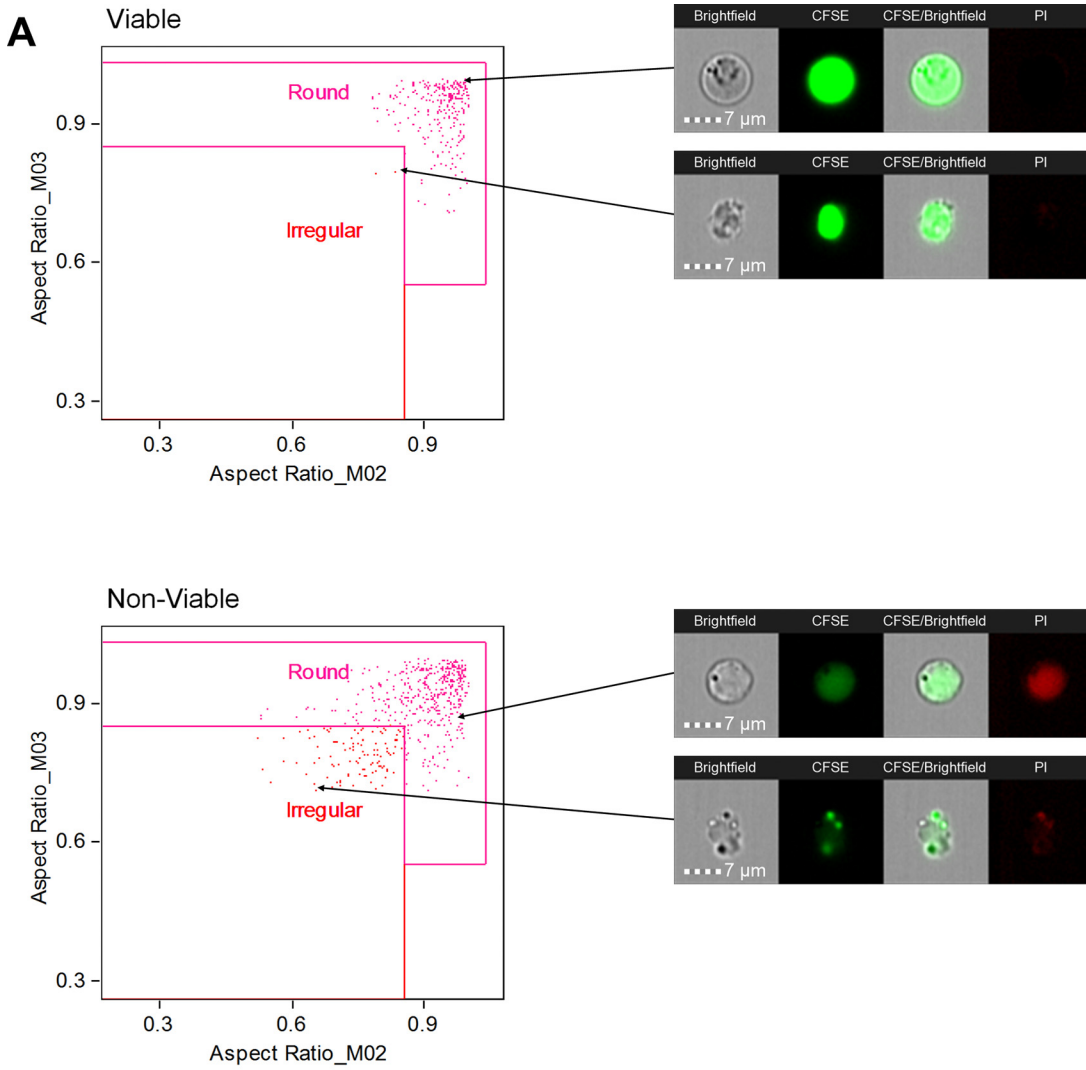


Fig 2. Gating for round and irregular shapes of *Blastocystis*. The shapes of *Blastocystis* were selected based on aspect ratios from the brightfield channel (M03) and CFSE staining (M02). Viable and non-viable cells were plotted separately. The above graphs shows the gating for *Blastocystis* ST1-NUH9 isolate (A). The average proportion of round and irregular shapes found in cultures of *Blastocystis* ST1-NUH9, ST4-WR1 and ST7-B were then plotted in a graph (B). These are based on three separate batches of cultures and independent runs in ImageStream. Error bars signify standard error values. *p*-values comparing the proportion of round cells between viable and non-viable populations are 0.06, 0.47 and 0.31 for ST1-NUH9, ST4-WR1 and ST7-B isolates, respectively.

doi:10.1371/journal.pone.0143974.g002

92% round-shaped, respectively. These proportions are slightly lower (82% for ST4-WR1 and 88% for ST7-B) in non-viable cells (Fig 2B).

Several studies have attached significance to amoeboid forms in terms of reproduction and pathogenicity and these appear as irregularly-shaped cells [13,20]. These reports however did not identify the subtype of *Blastocystis* they have observed. Past studies also did not take into account the viability of the cells being observed. In this study, we were able to analyze morphological features of *Blastocystis* while determining their viability using PI-staining. We found that irregularly-shaped cells in ST1 are non-viable and therefore may not have any biological significance in this particular *Blastocystis* subtype. ST4 and ST7 isolates, on the other hand, have viable irregularly-shaped cells. This irregularity are due either to the cells' elongated shape or due to amoeboid features such as pseudopod-like structures (Fig 3). In our analyses, these amoeboid forms are rare among viable populations as most irregularly-shaped cells (especially in ST4) are elongated (Fig 3). In ST1 and ST4, these forms are more numerous but all are non-viable. Analysis of cells from viable ST7 isolates showed only one cell (out of ~1000 cells) that could be characterized as amoeboid (Fig 3). Experiments using different ages of cultures may be done in the future to determine the consistency of these rare cells in the population. Likewise, xenic cultures can also be investigated as suggested [30] noting that amoeboid forms may be more numerous in this type of culture condition.

Analysis of single Hoechst-staining was also done to further correlate *Blastocystis* shape and reproductive status. Hoechst-staining is used for cell-cycle analysis. Actively dividing cells register higher fluorescence compared to inert cells. In all the isolates studied, round-shaped cells had higher average Hoechst-staining (Fig 4). This finding links well with the observation using PI-staining that most irregularly-shaped may not have biological or reproductive roles at all.

Aside from the round vacuolar forms, round granular forms are also commonly observed in clinical samples and in cultures [6,16]. Vdovenko [23] observed that these forms can naturally arise from vacuolar forms possibly by environmental exposure or fixation artefact. A more recent study has also mentioned this phenomenon [16]. In this study, we used the side-scatter channel to measure granularity of the cells. The average intensity coming from the channel in all STs in non-viable cells are higher compared to viable cells. Cells that are more granular can be found mostly among non-viable cells (Fig 5A). Non-viable cells have wider range in terms of granularity in contrast to viable cells where these tend to have lower side-scatter channel intensity. These findings are consistent among the 3 STs studied (Fig 5B). Nevertheless, cells that are more granular can also be found among viable cells. Our data suggests that there exists two populations of granular cells: true granular cells and those that are degenerating (Fig 5C) as reported previously [1,23]. We also add that granularity of these dying cells may be due more to environmental exposure rather than caused by fixation since we have observed the same proportion of granular forms in both fixed and unfixed samples (data not shown). We also used the Hoechst staining intensity of viable granular cells to find their biological significance. We have observe that these cells have higher DNA content compared to granular ones (Fig 6) These cells may therefore be in a more active reproductive state compared to less granular ones. We also analysed the granularity of multinucleated cells.

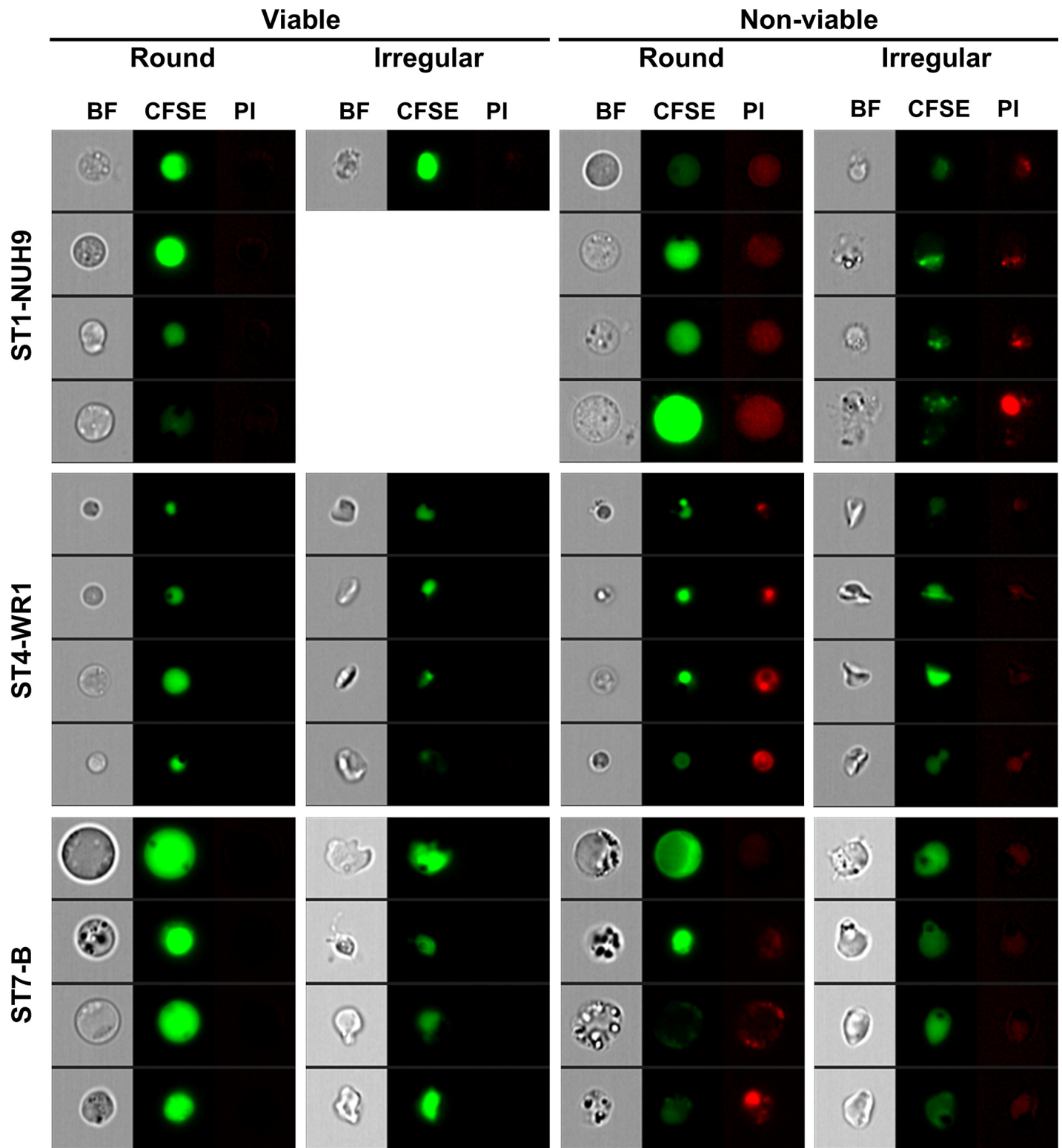


Fig 3. *Blastocystis* STs display various shapes from both viable and non-viable populations. Image gallery of *Blastocystis* cells showing round and irregular shapes from viable and non-viable populations. Each cell shown in the brightfield (BF) view has corresponding images which display CFSE and PI staining. The latter was used to determine viability. Irregular-shaped cells show elongated cells and amoeboid forms. Amoeboid forms with prominent pseudopodia and filamentous attachments are restricted to non-viable forms ST1-NUH9 and ST4-WR1. There are rare (0.1%) cells in viable ST7-B population that show an amoeboid-like morphology.

doi:10.1371/journal.pone.0143974.g003

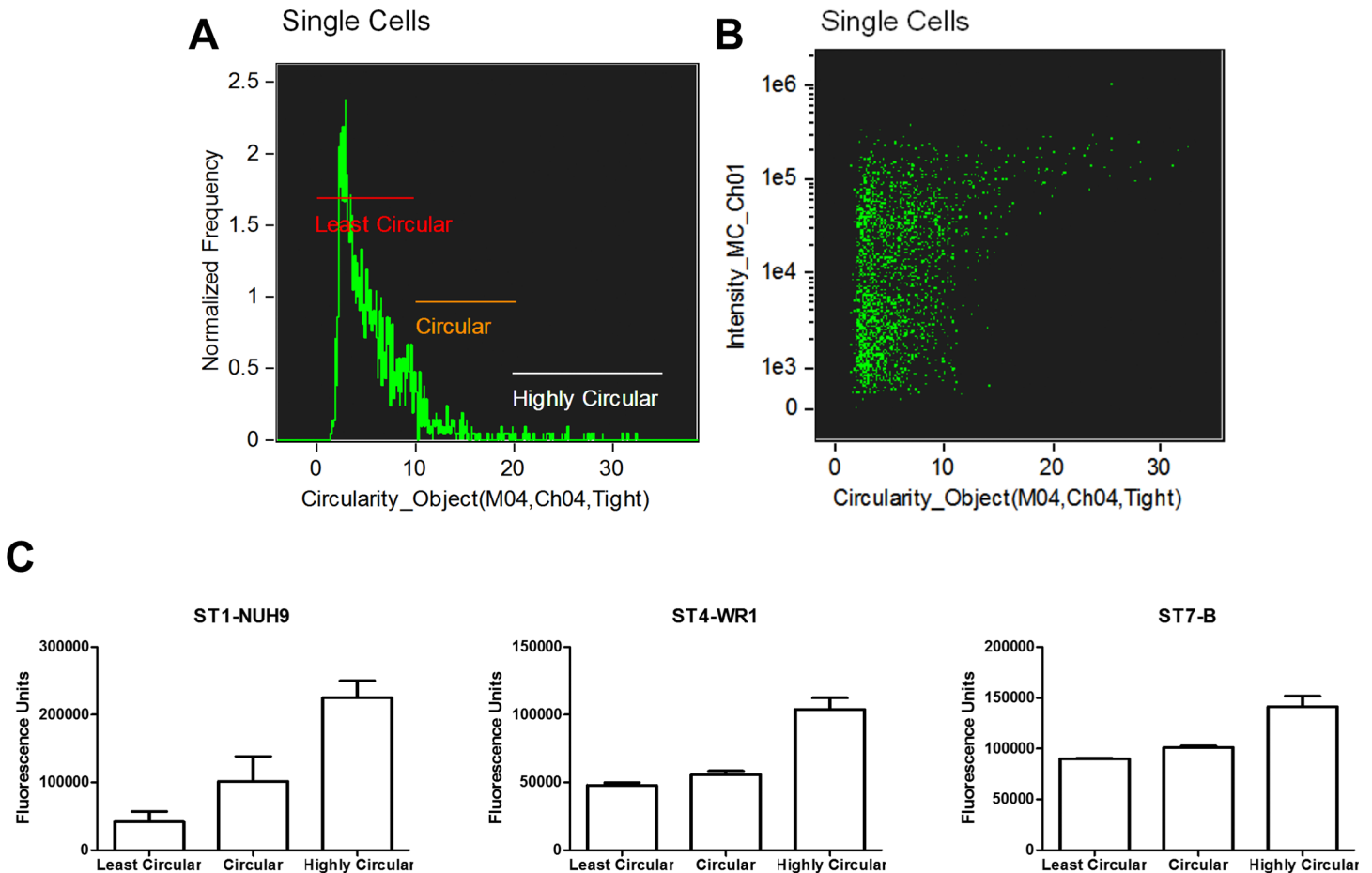


Fig 4. Round *Blastocystis* have higher DNA content. *Blastocystis* cells were plotted according to circularity using the software's shape wizard. The population of cells was then divided into three groups: low, mid and high circularity (A). A dot-plot was generated to analyze the relationship between circularity and DNA content indicated by Hoechst staining of *Blastocystis* cells (B). The dot-plot shows that some highly circular cells have the highest DNA content while the least circular cells have the lowest DNA content. Bar graphs show the average Hoechst-staining of the three groups of *Blastocystis* cells based on circularity (C). Differences between groups based on circularity in each ST were found to be significant ($p < 0.05$) using ANOVA.

doi:10.1371/journal.pone.0143974.g004

The diameter of *Blastocystis* vacuolar forms have been estimated to be between 2 and 200 μm [6]. A study MacPherson and MacQueen [31] indicated that the diameter of 80.8% of the *Blastocystis* they observed fell between 5 and 15 μm . This paper, however, was published before the genotyping era and so the particular ST of the isolate is unknown. In this study, we determined the size ranges of viable cells in each of the three subtypes. ST1-NUH9 and ST7-B isolates are bigger compared to ST4-WR1 isolates (Table 1). Furthermore, more than half (51.7%) of ST1-NUH9 cells have diameter of greater than or equal to 5 μm while only 37.3% of ST7-B cells have this size. ST4-WR1 cells are generally small with diameter of less than 5 μm in 98.3% of the population. Mirza et al. have previously reported differences in sizes between ST4 and ST7 isolates using flow cytometry [32]. In that study, the diameter of majority of *Blastocystis* cells after 48 hours of culture were 6 to 10 μm and 3 to 6 μm for ST7 and ST4 isolates, respectively. The calculations made for ST4 in this study mirrors that of the previous report. However, the measurement in this study for ST7 is smaller. The previous study has determined the sizes indirectly using known-sized beads and set them as standards for the forward scatter channel values in flow cytometry. This study however makes use of actual images of the cells and converting the pixel measurements to micrometers. We were also able to exclude doublets

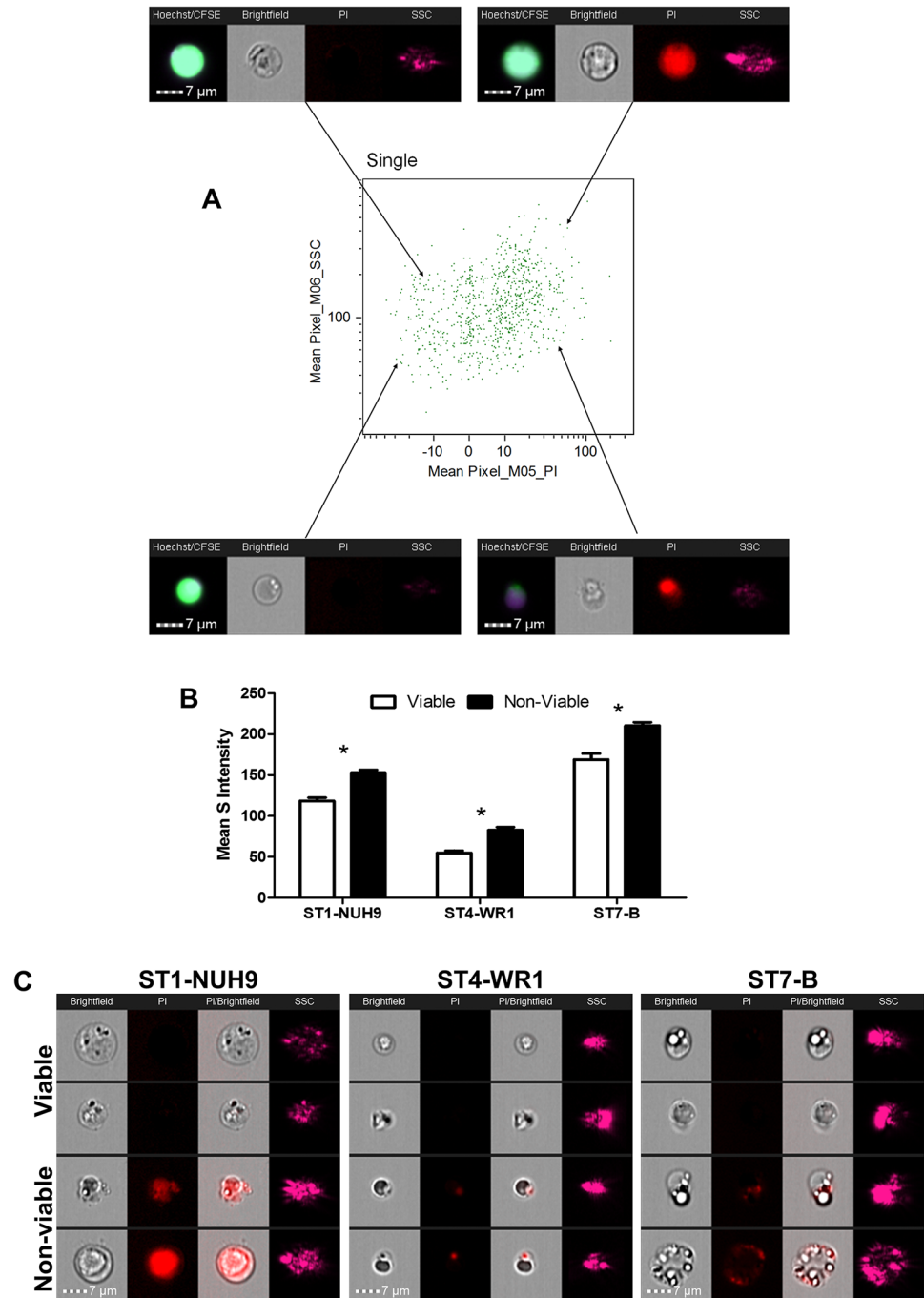


Fig 5. Analysis of *Blastocystis* based on granularity. *Blastocystis* populations were plotted according to mean pixel intensities of both side scatter channel and PI staining to determine the cells' granularity and viability, respectively (A). Cells with higher PI staining have more granularity compared to cells with lower PI staining. This observation is common to all subtypes used in this study as shown in a graph (B); *, $p < 0.05$. Sample images showing cells with high granularity among viable and non-viable populations (C). These cells may represent true granular cells and degenerating cells, respectively.

doi:10.1371/journal.pone.0143974.g005

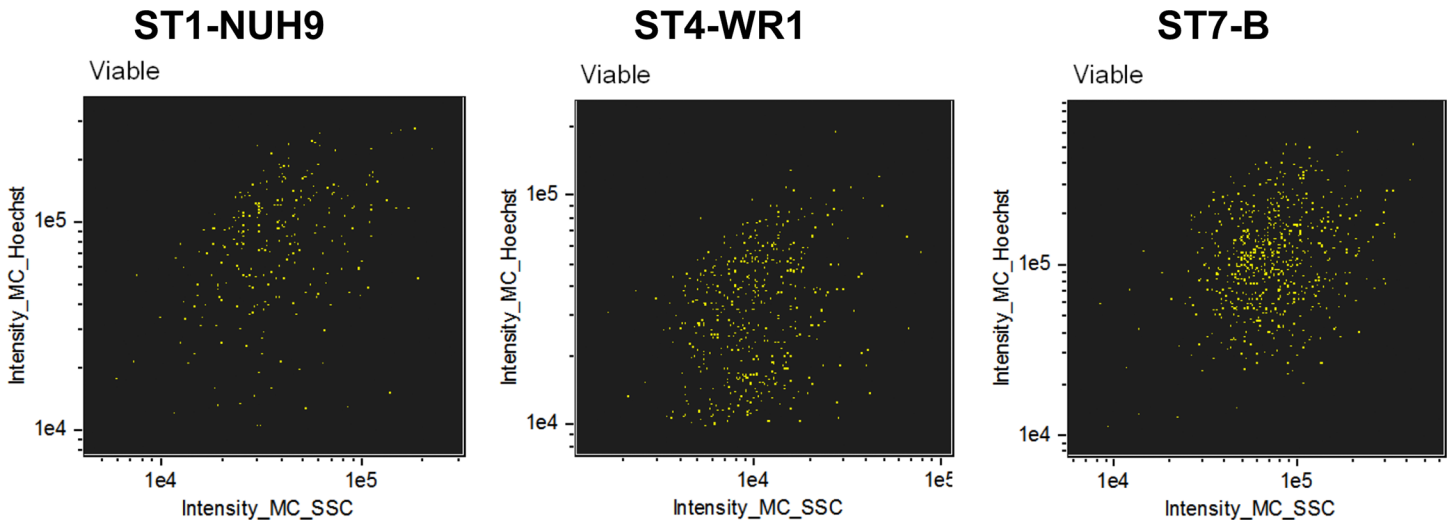


Fig 6. Viable *Blastocystis* cells with high granularity have higher DNA content. Dot-plot shows the populations of *Blastocystis* cells plotted according to circularity and Hoechst staining.

doi:10.1371/journal.pone.0143974.g006

in measurement. There might be bigger-sized cells depending on the type and age of samples as well the amount of initial inoculum. Our analyses highlight the importance of taking into account the subtype used in any morphological studies. Our data suggest that the size range of *Blastocystis* is not as wide as between 2 and 200 μm, but narrower when ST identity is established. We also specifically measured viable cells only as the non-viable cells may feature degenerating cells and assume irregular shapes (Table 1).

We used Hoechst staining and the EDF setting of the imaging flow cytometer to analyze nuclear arrangement of viable *Blastocystis* cells. More than 80% of the population from the three subtypes studied featured 1–2 nuclei (Fig 7) located at the edge of the cells. ST4-WR1 isolates all feature one or two nuclei (and not more). This reflects the previous observation [31] whereby 98.4% of the cells have a similar arrangement. This study therefore supports the classical representation of *Blastocystis*. More infrequently, in the other STs (1–2% in ST1 and 2–8% in ST7), other nuclear features were observed. These cells either show more than 2 nuclei or that the nucleic acid stain covers a large area of the cell (Fig 8). The latter show an apparent nucleic acid condensation which may represent cells about to undergo binary fission. Surprisingly, we have observed multinucleation only in round cells in these two subtypes. We did not find evidence to support alternative modes of reproduction such as plasmotomy and budding in *Blastocystis* as suggested by others [16,18,22] since we did not observe multinucleation in irregularly-shaped viable cells. Some of the multinucleated cells show the nuclei located in the center of the cell with the size of the central vacuole diminished (as indicated by lower intensity of CFSE staining) (Fig 8A). If this is a reproductive stage, it may be an evidence of a multiple fission event in *Blastocystis* as suggested [33]. These, however, showed lower granularity

Table 1. Viable *Blastocystis* size profiles indicated by cell diameter range and average diameter.

Subtype-Isolate	Diameter Range (μm)	Average Diameter (μm)	Cells with diameter ≥ 5 μm (%)
ST1-NUH9	2.7–8.7	5.0 ± 0.8	51.7 ± 6.1
ST4-WR1	2.2–6.2	3.6 ± 0.6	1.7 ± 0.4
ST7-B	3.2–7.5	4.9 ± 0.7	37.3 ± 4.5

doi:10.1371/journal.pone.0143974.t001

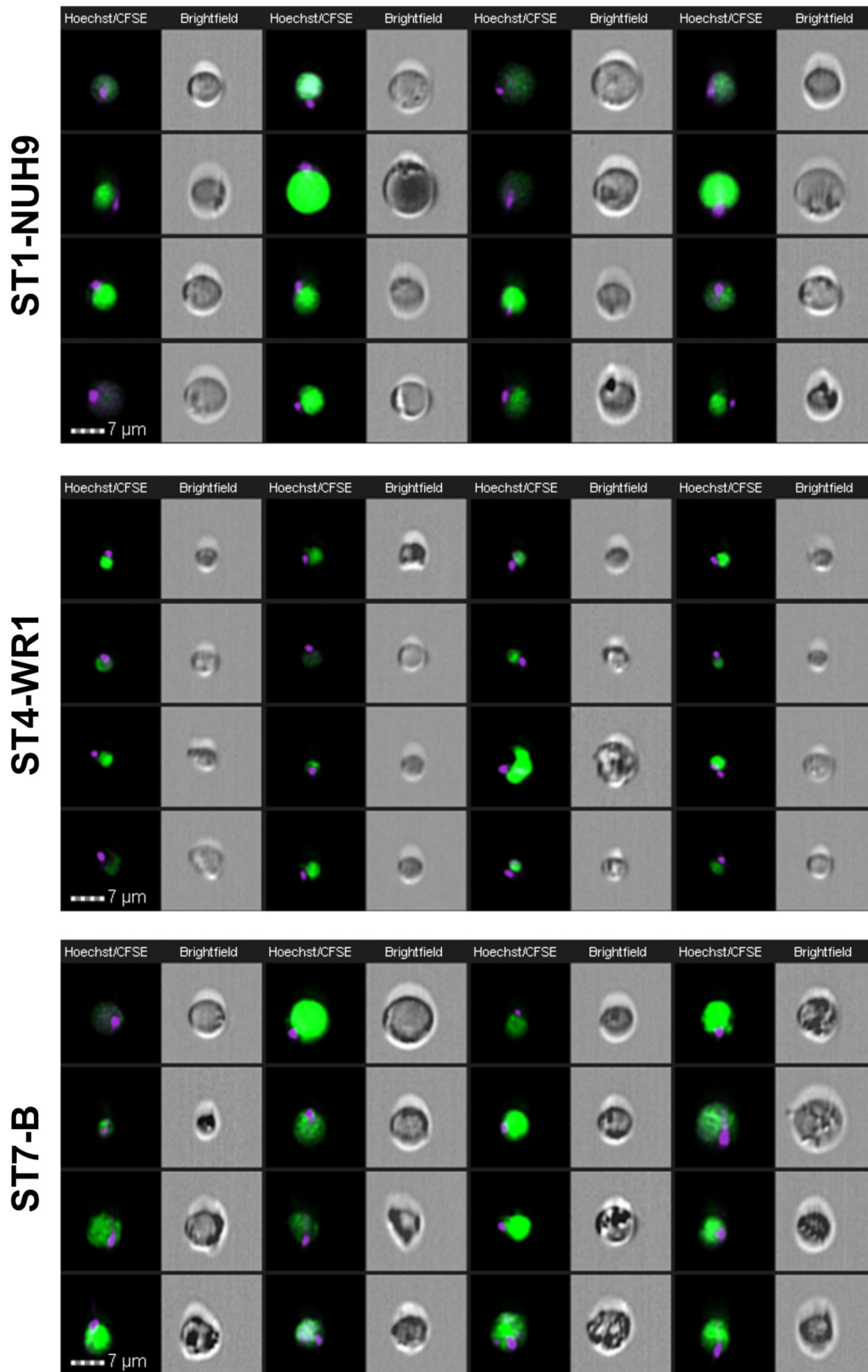


Fig 7. Image gallery of *Blastocystis* showing classical morphological forms at varying sizes in the viable populations. Images were acquired using EDF setting of the imaging flow cytometer. Each cell is represented by two images: Hoechst-CFSE-staining composite and brightfield image. The nuclei were stained with Hoechst and the vacuole with CFSE. These round forms show a single nuclei located at the edge of the cell. These forms comprise more than half of the population in all the subtypes studied.

doi:10.1371/journal.pone.0143974.g007

(Fig 9). Cells with single or two nuclei also showed higher DNA content. This is consistent with the data above (Fig 6) and these suggests that multinucleated cells may not be in active reproductive stage as compared to the other cells. We have also observed small structures containing nucleic acid (Fig 8B). These structures are rare (2–4% of viable cells). They also do not appear to have vacuoles as indicated by low CFSE staining but consist mainly of nucleic acid material in its compartment. Our experiments did not determine whether these structures originate from bigger and multinucleated cells. It may also be possible that these represent starving cells or a state where *Blastocystis* sheds off its vacuole.

Conclusions

In this study, we analyzed three STs of *Blastocystis* based on shape, size, granularity and nuclear arrangement using high content imaging flow cytometry. These features may be used to compare one *Blastocystis* ST to another. We have also identified rare multi-nuclear forms which are unlikely to represent an alternative mode of reproduction in the parasite. It would be interesting to investigate other isolates coming from the same or other STs so that

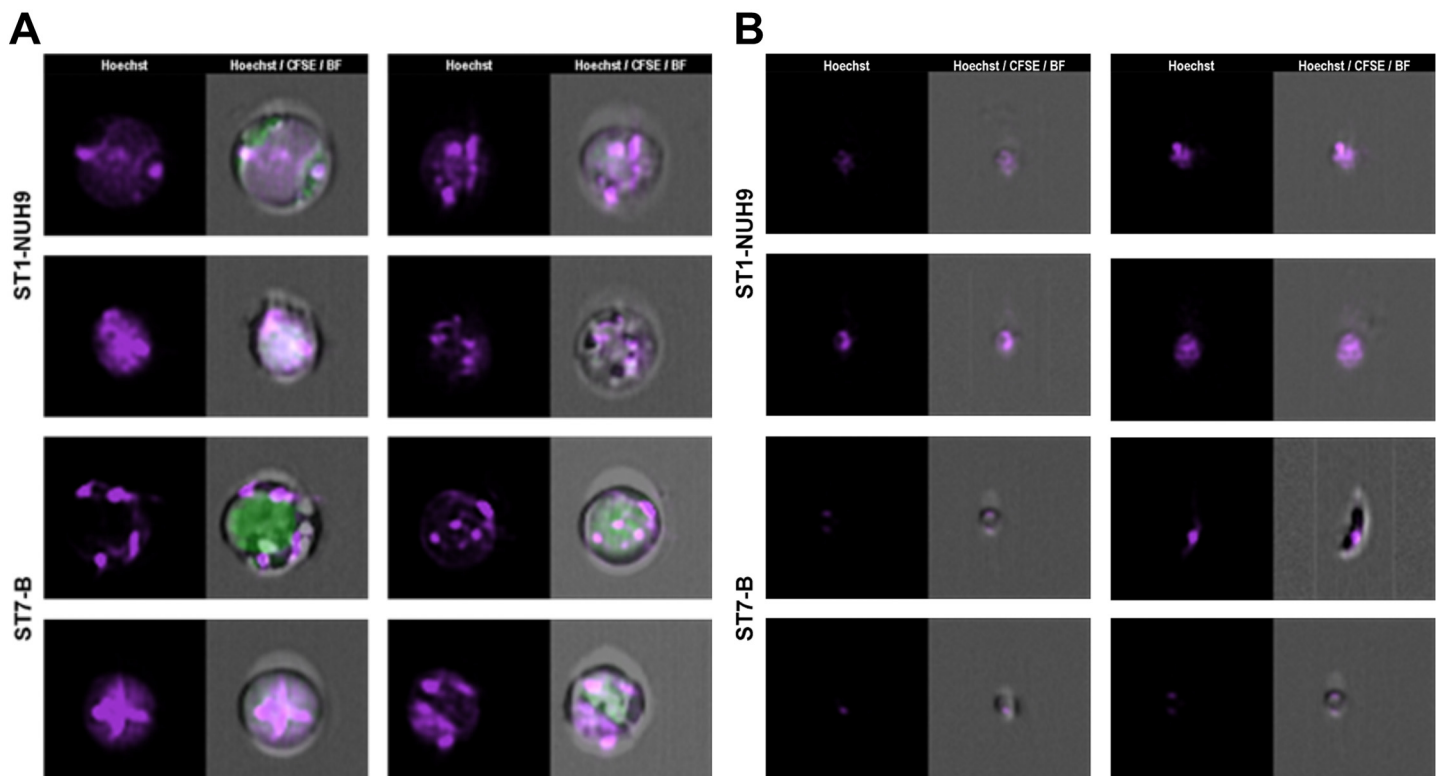


Fig 8. Image gallery of rare *Blastocystis* multinucleated cells. The nuclei is visualized by Hoechst staining. The nuclei number more than three and some appear to be concentrated in the center and not along the edges (A). Some of these cells also appear to show nuclear condensation. (B) Image gallery showing small structures which contains DNA.

doi:10.1371/journal.pone.0143974.g008

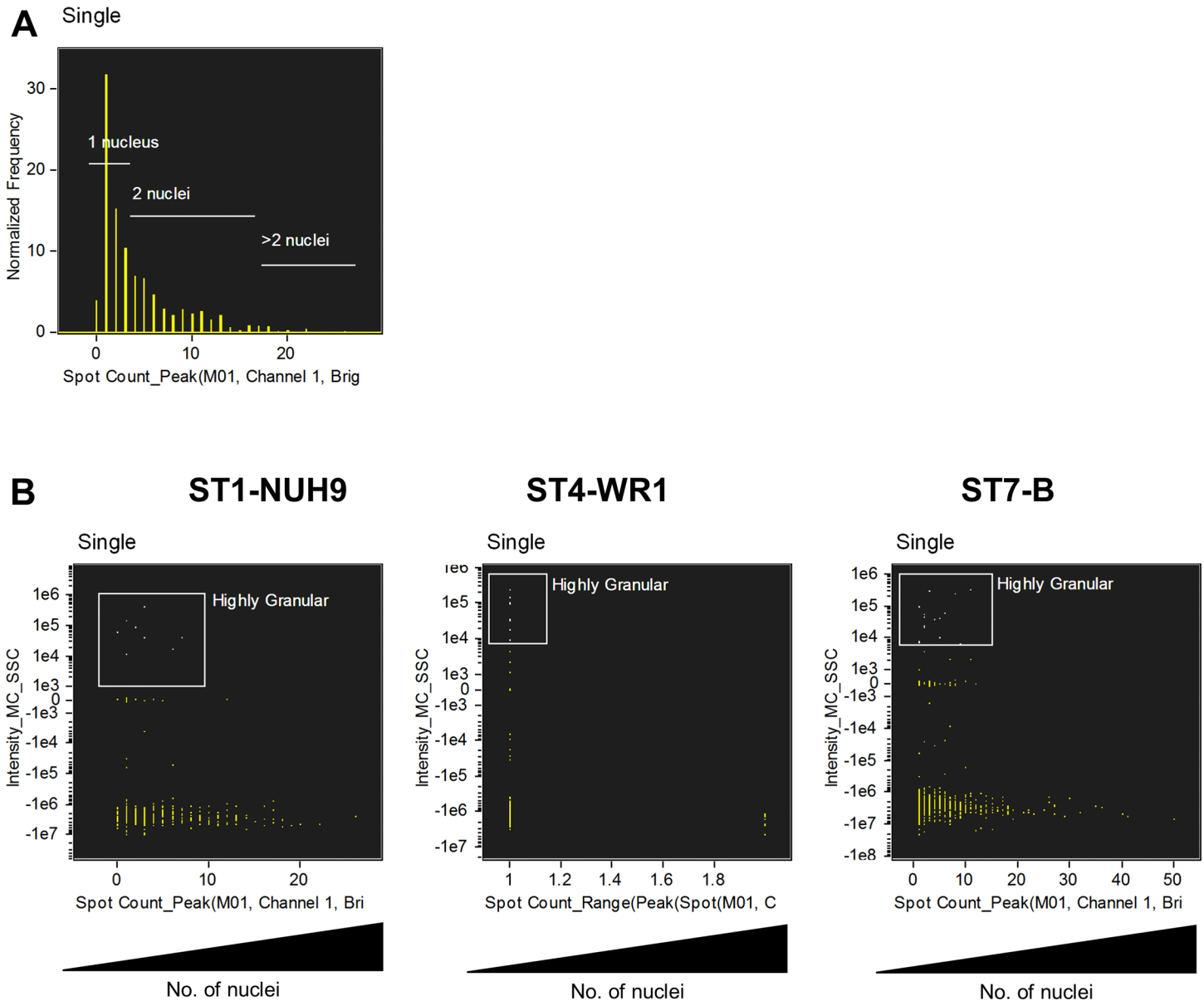


Fig 9. Multinucleated *Blastocystis* cells do not display higher granularity compared to uninucleated cells. The spot wizard of the IDEAS software was used to group cells based on number of nuclei. This was done by counting the ‘spots’ stained with Hoechst. The images were then visually analysed to determine the precise spot values that correspond to the number of nuclei (A). Dot-plots were generated for each ST to analyse granularity in multinucleated cells. These plots show that cells with high granularity are found in the populations of uninucleated cells.

doi:10.1371/journal.pone.0143974.g009

inter- and intra-subtype variations in morphology can be determined. We used axenic cultures of *Blastocystis* but it would also be attractive to investigate cells from xenic cultures or from fecal samples. The methods outlined in this study can also be used to detect changes in *Blastocystis* upon treatment of drugs or modification of culture conditions. Data from this study provides an important and useful reference on the morphological profile of *Blastocystis* STs.

Supporting Information

S1 Table. Summary of Proportions of viable *Blastocystis* morphological forms and range of granularity found in each population of the three STs studied.
(DOCX)

Author Contributions

Conceived and designed the experiments: KSWT JAY. Performed the experiments: JAY. Analyzed the data: JAY KSWT. Contributed reagents/materials/analysis tools: KSWT. Wrote the paper: JAY KSWT.

References

1. Clark CG, van der Giezen M, Alfellani MA, Stensvold CR. Chapter One—Recent Developments in *Blastocystis* Research. In: Rollinson D., editor. *Advances in Parasitology*. Academic Press; 2013. p. 1–32.
2. Scanlan PD, Stensvold CR, Rajilić-Stojanović M, Heilig HG, De Vos WM, O'Toole PW, et al. The microbial eukaryote *Blastocystis* is a prevalent and diverse member of the healthy human gut microbiota. *FEMS Microbiol Ecol*. 2014 Oct 1; 90(1):326–30. doi: [10.1111/1574-6941.12396](https://doi.org/10.1111/1574-6941.12396) PMID: [25077936](https://pubmed.ncbi.nlm.nih.gov/25077936/)
3. Alfellani MA, Stensvold CR, Vidal-Lapiedra A, Onuoha ESU, Fagbenro-Beyioku AF, Clark CG. Variable geographic distribution of *Blastocystis* subtypes and its potential implications. *Acta Trop*. 2013 Apr; 126(1):11–8. doi: [10.1016/j.actatropica.2012.12.011](https://doi.org/10.1016/j.actatropica.2012.12.011) PMID: [23290980](https://pubmed.ncbi.nlm.nih.gov/23290980/)
4. Ramírez JD, Sánchez LV, Bautista DC, Corredor AF, Flórez AC, Stensvold CR. Blastocystis subtypes detected in humans and animals from Colombia. *Infect Genet Evol*. 2014 Mar; 22:223–8. doi: [10.1016/j.meegid.2013.07.020](https://doi.org/10.1016/j.meegid.2013.07.020) PMID: [23886615](https://pubmed.ncbi.nlm.nih.gov/23886615/)
5. Casero RD, Mongi F, Sánchez A, Ramírez JD. *Blastocystis* and urticaria: Examination of subtypes and morphotypes in an unusual clinical manifestation. *Acta Trop*. 2015 Aug; 148:156–61. doi: [10.1016/j.actatropica.2015.05.004](https://doi.org/10.1016/j.actatropica.2015.05.004) PMID: [25976414](https://pubmed.ncbi.nlm.nih.gov/25976414/)
6. Tan KSW. New Insights on Classification, Identification, and Clinical Relevance of *Blastocystis* spp. *Clin Microbiol Rev*. 2008 Oct 1; 21(4):639–65. doi: [10.1128/CMR.00022-08](https://doi.org/10.1128/CMR.00022-08) PMID: [18854485](https://pubmed.ncbi.nlm.nih.gov/18854485/)
7. Mirza H, Wu Z, Kidwai F, Tan KSW. A Metronidazole-Resistant Isolate of *Blastocystis* spp. Is Susceptible to Nitric Oxide and Downregulates Intestinal Epithelial Inducible Nitric Oxide Synthase by a Novel Parasite Survival Mechanism. *Infect Immun*. 2011 Dec 1; 79(12):5019–26. doi: [10.1128/IAI.05632-11](https://doi.org/10.1128/IAI.05632-11) PMID: [21930763](https://pubmed.ncbi.nlm.nih.gov/21930763/)
8. Wu Z, Mirza H, Tan KSW. Intra-Subtype Variation in Enteroadhesion Accounts for Differences in Epithelial Barrier Disruption and Is Associated with Metronidazole Resistance in *Blastocystis* Subtype-7. *PLoS Negl Trop Dis*. 2014 May 22; 8(5):e2885. doi: [10.1371/journal.pntd.0002885](https://doi.org/10.1371/journal.pntd.0002885) PMID: [24851944](https://pubmed.ncbi.nlm.nih.gov/24851944/)
9. Teo JDW, MacAry PA, Tan KSW. Pleiotropic Effects of *Blastocystis* spp. Subtypes 4 and 7 on Ligand-Specific Toll-Like Receptor Signaling and NF- κ B Activation in a Human Monocyte Cell Line. *PLoS ONE*. 2014 Feb 14; 9(2):e89036. doi: [10.1371/journal.pone.0089036](https://doi.org/10.1371/journal.pone.0089036) PMID: [24551212](https://pubmed.ncbi.nlm.nih.gov/24551212/)
10. Roberts T, Ellis J, Harkness J, Marriott D, Stark D. Treatment failure in patients with chronic *Blastocystis* infection. *J Med Microbiol*. 2014 Feb 1; 63(Pt 2):252–7. doi: [10.1099/jmm.0.065508-0](https://doi.org/10.1099/jmm.0.065508-0) PMID: [24243286](https://pubmed.ncbi.nlm.nih.gov/24243286/)
11. Roberts T, Stark D, Harkness J, Ellis J. Update on the pathogenic potential and treatment options for *Blastocystis* sp. *Gut Pathog*. 2014 May 28; 6(1):17.
12. Anuar TS, Ghani MKA, Azreen SN, Salleh FM, Mokhtar N. *Blastocystis* infection in Malaysia: Evidence of waterborne and human-to-human transmissions among the Proto-Malay, Negrito and Senoi tribes of Orang Asli. *Parasit Vectors*. 2013 Feb 22; 6(1):40.
13. Baldursson S, Karanis P. Waterborne transmission of protozoan parasites: Review of worldwide outbreaks—An update 2004–2010. *Water Res*. 2011 Dec 15; 45(20):6603–14. doi: [10.1016/j.watres.2011.10.013](https://doi.org/10.1016/j.watres.2011.10.013) PMID: [22048017](https://pubmed.ncbi.nlm.nih.gov/22048017/)
14. Santos HJ, Rivera WL. Comparison of direct fecal smear microscopy, culture, and polymerase chain reaction for the detection of *Blastocystis* sp. in human stool samples. *Asian Pac J Trop Med*. 2013 Oct; 6(10):780–4. doi: [10.1016/S1995-7645\(13\)60138-8](https://doi.org/10.1016/S1995-7645(13)60138-8) PMID: [23870466](https://pubmed.ncbi.nlm.nih.gov/23870466/)
15. Stensvold C. *Blastocystis*: Genetic diversity and molecular methods for diagnosis and epidemiology. *Trop Parasitol*. 2013; 3(1):26. doi: [10.4103/2229-5070.113896](https://doi.org/10.4103/2229-5070.113896) PMID: [23961438](https://pubmed.ncbi.nlm.nih.gov/23961438/)

16. Zhang X, Zhang S, Qiao J, Wu X, Zhao L, Liu Y, et al. Ultrastructural insights into morphology and reproductive mode of *Blastocystis hominis*. *Parasitol Res.* 2012 Mar 1; 110(3):1165–72. doi: [10.1007/s00436-011-2607-x](https://doi.org/10.1007/s00436-011-2607-x) PMID: [21845408](https://pubmed.ncbi.nlm.nih.gov/21845408/)
17. Rajamanikam A, Govind S. Amoebic forms of *Blastocystis* spp.—evidence for a pathogenic role. *Parasit Vectors.* 2013; 6(1):295. doi: [10.1186/1756-3305-6-295](https://doi.org/10.1186/1756-3305-6-295) PMID: [24499467](https://pubmed.ncbi.nlm.nih.gov/24499467/)
18. Govind SK, Khairul AA, Smith HV. Multiple reproductive processes in *Blastocystis*. *Trends Parasitol.* 2002 Dec 1; 18(12):528.
19. Tan KSW, Stenzel DJ. Multiple reproductive processes in *Blastocystis*: proceed with caution. *Trends Parasitol.* 2003 Jul; 19(7):290–1. PMID: [12855376](https://pubmed.ncbi.nlm.nih.gov/12855376/)
20. Windsor JJ, Stenzel DJ, Macfarlane L. Multiple reproductive processes in *Blastocystis hominis*. *Trends Parasitol.* 2003 Jul; 19(7):289–90. PMID: [12855375](https://pubmed.ncbi.nlm.nih.gov/12855375/)
21. Govind SK, Anuar KA, Smith HV. Response to Tan and Stenzel, and Windsor et al.: *Blastocystis* reproduction and morphology. *Trends Parasitol.* 2003 Jul 1; 19(7):291–2.
22. Yamada M, Yoshikawa H. Morphology of Human and Animal Blastocystis Isolates with Special Reference to Reproductive Modes. In: Mehlhorn H, Tan KSW, Yoshikawa H, editors. *Blastocystis: Pathogen or Passenger?* Springer Berlin Heidelberg; 2012. p. 9–35.
23. Vdovenko AA. *Blastocystis hominis*: origin and significance of vacuolar and granular forms. *Parasitol Res.* 2000 Jan 1; 86(1):8–10. PMID: [10669129](https://pubmed.ncbi.nlm.nih.gov/10669129/)
24. Chen XQ, Singh M, Ho LC, Tan SW, Ng GC, Moe KT, et al. Description of a *Blastocystis* species from *Rattus norvegicus*. *Parasitol Res.* 1997 Apr 1; 83(4):313–8. PMID: [9134551](https://pubmed.ncbi.nlm.nih.gov/9134551/)
25. Ho LC, Singh M, Suresh G, Ng GC, Yap EH. Axenic culture of *Blastocystis hominis* in Iscove's modified Dulbecco's medium. *Parasitol Res.* 1993 Jul 1; 79(7):614–6. PMID: [8278347](https://pubmed.ncbi.nlm.nih.gov/8278347/)
26. Wong KHS, Ng GC, Lin RTP, Yoshikawa H, Taylor MB, Tan KSW. Predominance of subtype 3 among *Blastocystis* isolates from a major hospital in Singapore. *Parasitol Res.* 2007 Dec 7; 102(4):663–70. PMID: [18064490](https://pubmed.ncbi.nlm.nih.gov/18064490/)
27. Moe KT, Singh M, Howe J, Ho LC, Tan SW, Chen XQ, et al. Experimental *Blastocystis hominis* infection in laboratory mice. *Parasitol Res.* 1997 Apr; 83(4):319–25. PMID: [9134552](https://pubmed.ncbi.nlm.nih.gov/9134552/)
28. Noël C, Dufernez F, Gerbod D, Edgcomb VP, Delgado-Viscogliosi P, Ho L-C, et al. Molecular Phylogenies of *Blastocystis* Isolates from Different Hosts: Implications for Genetic Diversity, Identification of Species, and Zoonosis. *J Clin Microbiol.* 2005 Jan 1; 43(1):348–55. PMID: [15634993](https://pubmed.ncbi.nlm.nih.gov/15634993/)
29. Poirier P, Meloni D, Nourrisson C, Wawrzyniak I, Viscogliosi E, Livrelli V, et al. Molecular subtyping of *Blastocystis* spp. using a new rDNA marker from the mitochondria-like organelle genome. *Parasitology.* 2014; 141(05):670–81.
30. Tan TC, Suresh KG. Predominance of amoeboid forms of *Blastocystis hominis* in isolates from symptomatic patients. *Parasitol Res.* 2006 Feb 1; 98(3):189–93. PMID: [16323025](https://pubmed.ncbi.nlm.nih.gov/16323025/)
31. MacPherson DW, MacQueen WM. Morphological diversity of *Blastocystis hominis* in sodium acetate-acetic acid-formalin-preserved stool samples stained with iron hematoxylin. *J Clin Microbiol.* 1994 Jan 1; 32(1):267–8. PMID: [7510311](https://pubmed.ncbi.nlm.nih.gov/7510311/)
32. Mirza H, Tan KSW. *Blastocystis* exhibits inter- and intra-subtype variation in cysteine protease activity. *Parasitol Res.* 2008 Oct 10; 104(2):355–61. doi: [10.1007/s00436-008-1203-1](https://doi.org/10.1007/s00436-008-1203-1) PMID: [18846388](https://pubmed.ncbi.nlm.nih.gov/18846388/)
33. Suresh K, Howe J, Ng GC, Ho LC, Ramachandran NP, Loh AK, et al. A multiple fission-like mode of asexual reproduction in *Blastocystis hominis*. *Parasitol Res.* 1994 Jun 1; 80(6):523–7. PMID: [7809004](https://pubmed.ncbi.nlm.nih.gov/7809004/)